How do species other than mammals regenerate organs?

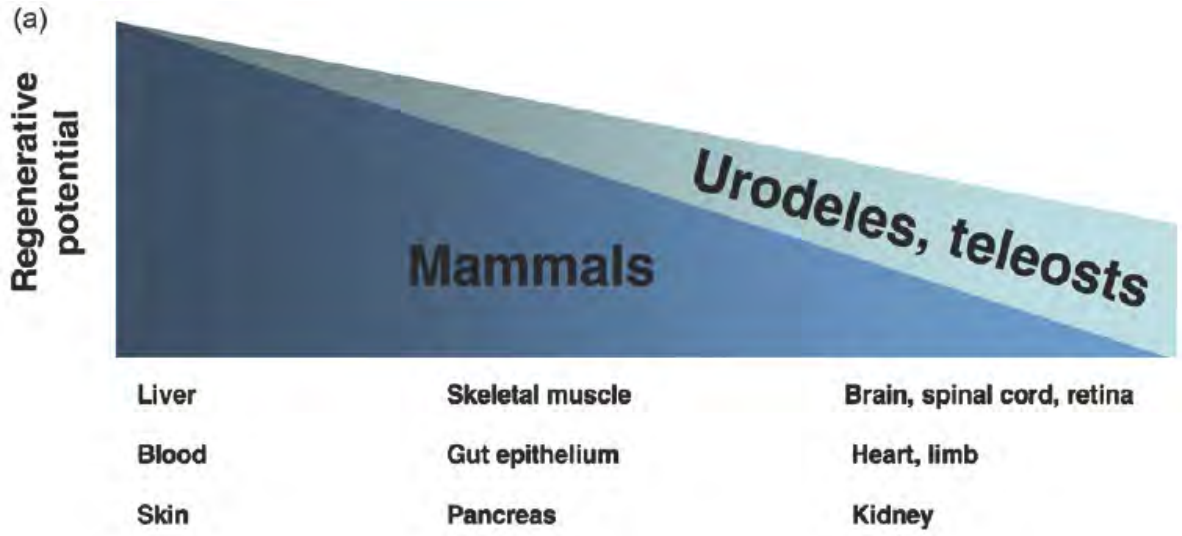

Species or group	Regenerative capabilities	Microarray	Transgenesis	Knockout/knock down	Genome sequenced
Invertebrates					
Hydra	All tissues and organs	No	Yes	RNAi	No
Planarians	All tissues (neurons, muscles, epithelia) and organs (brain, sensory organs, digestive system, musculature)	Yes	No	RNAi	Yes
Ascidians	All tissues and organs	Yes	Yes	Morpholinos	Yes
Vertebrates					
Newts	Limbs, tail, heart, lens, spinal cord, brain, jaw, retina, hair cells of the inner ear	Yes	Yes	Morpholinos	No
Axolotls	Limbs, tails, heart, spinal cord, brain	Yes	Yes	Morpholinos	No
Frogs	Pre-metamorphic limbs, tail, retina, lens, hair cells of the inner ear	Yes	Yes	Morpholinos	Yes
Zebrafish	Fins, tail, heart, liver, spinal cord, hair cells of inner ear, lateral line	Yes	Yes	Mutagenesis, morpholinos	Yes
Chicks	Hair cell of the inner ear	Yes	Yes	Morpholinos	Yes
Mice	Liver, digit tips	Yes	Yes	Mutagenesis, homologous recombination	Yes

Tissue heterogeneity and stem-cell functionality for homeostasis and repair

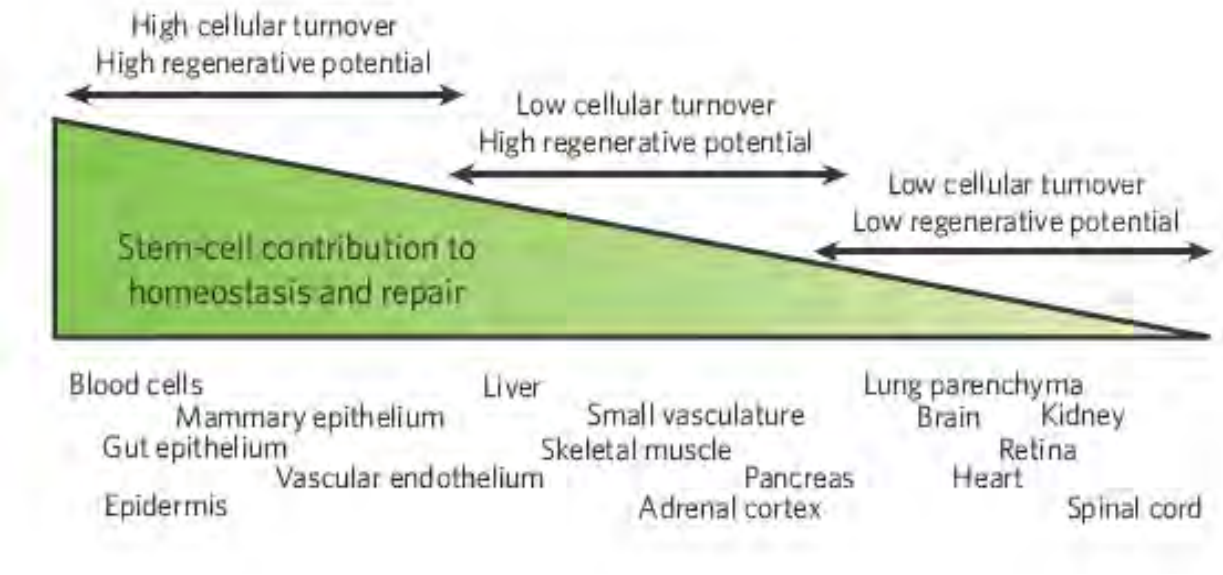

The extent to which the effects of ageing on the resident stem cells determine the phenotype of an aged tissue is likely to correlate with the extent to which stem cells are responsible for normal tissue homeostasis and repair. Along this spectrum, tissues generally fall into one of three categories.

1. Tissues with high turnover (such as blood, skin and gut) have a prominent stem-cell compartment and, by definition, have high regenerative capacity.
2. Tissues with low turnover but high regenerative potential might use different strategies to ensure effective repair in the setting of acute injury.
3. Tissues with low turnover and low regenerative potential might have stem cells that mediate only limited tissue repair. Although there has been much interest in harnessing the potential of stem cells in the brain and heart for therapeutic purposes, for example, there is limited endogenous repair capacity of these tissues following acute injuries.

In Urodeles Amphibians:

THE UNIVERSITY OF UTAH

ODELBERG LABORATORY

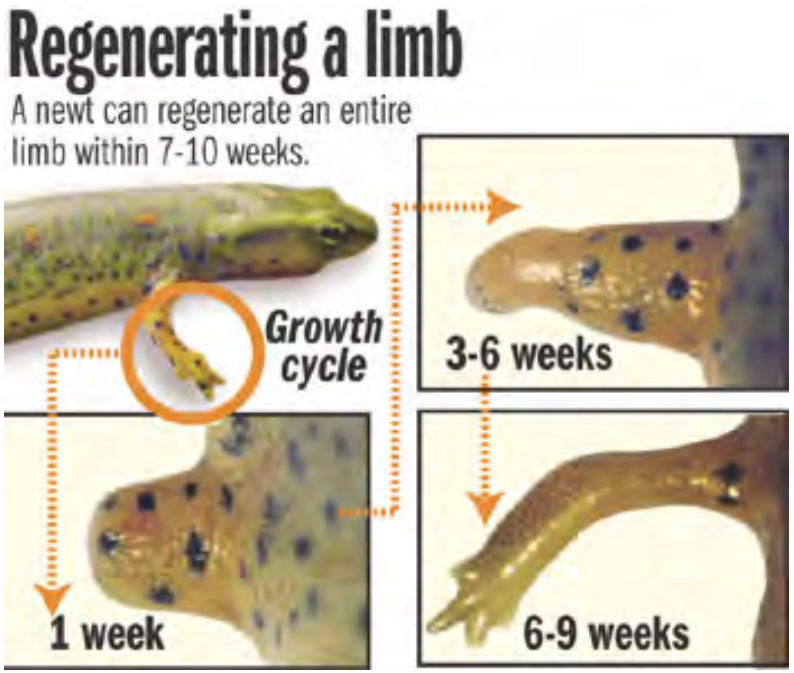

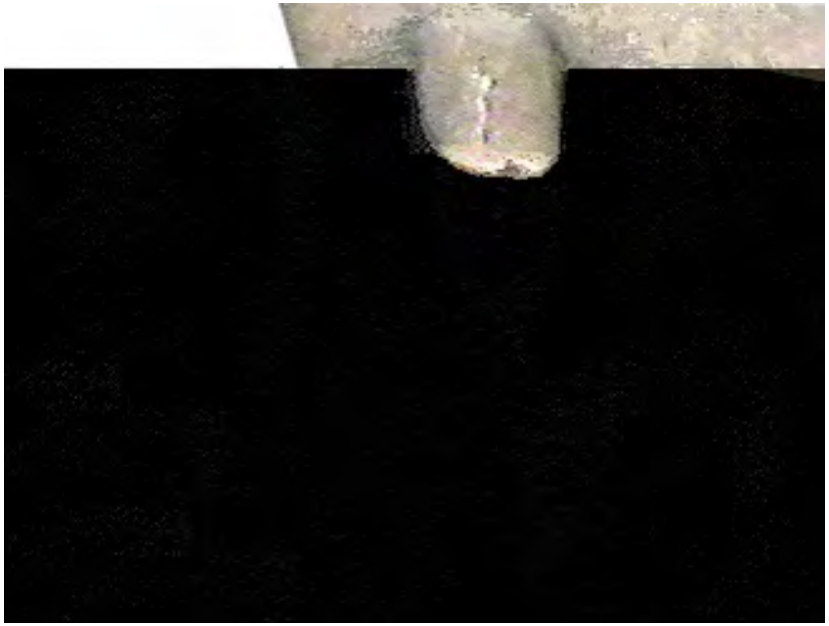

Basic steps in the formation of **blastema** in vertebrates and invertebrates.

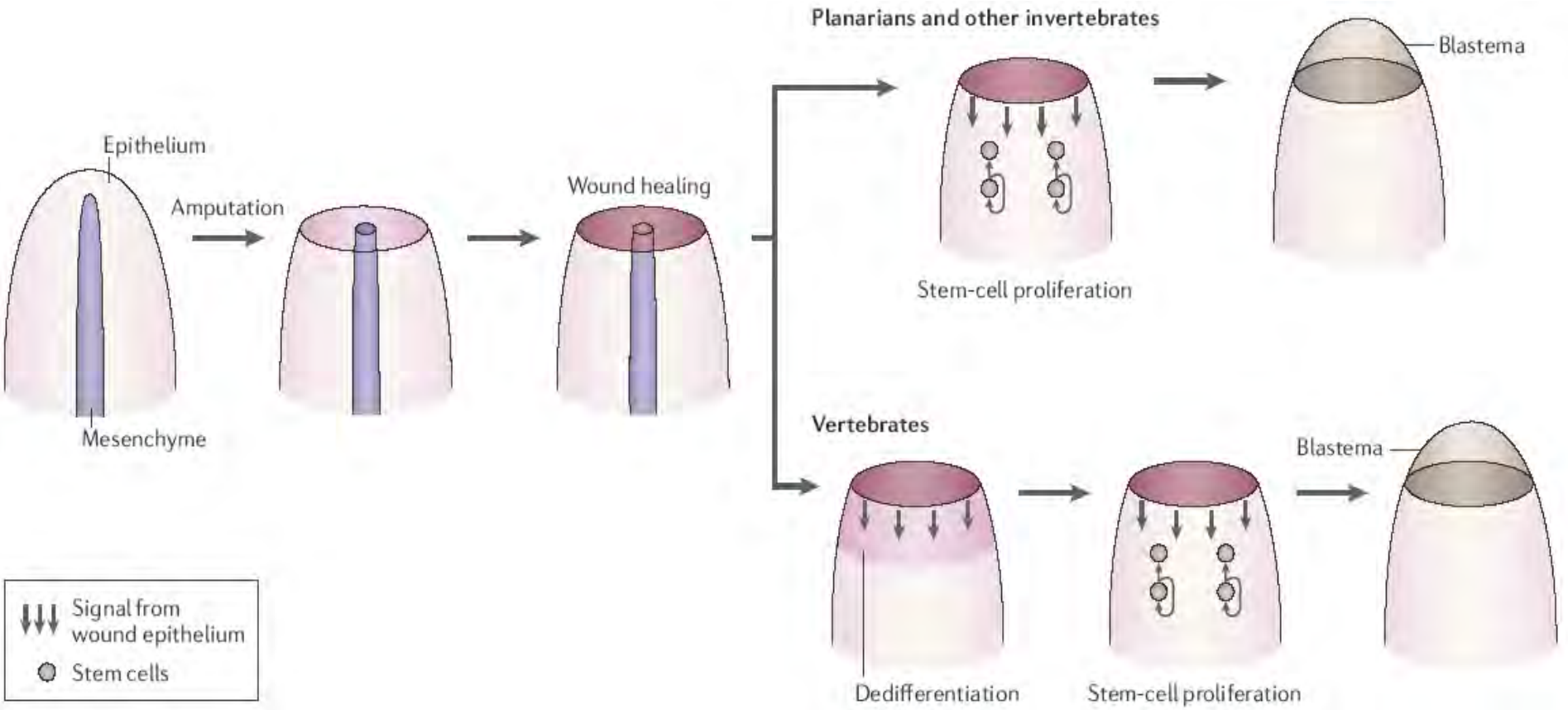

In **Vertebrates**, there is evidence that both stem cells and cell-dedifferentiation processes have a role in blastema-mediated regeneration.

In **Invertebrates** such as planarians, stem-cell proliferation seems to have a pivotal role.

Limb Regeneration: A New Development?

Eugen Nacu and Elly M. Tanaka

DFG-Center for Regenerative Therapies Dresden, Technische Universität Dresden, and Max Planck Institute of Molecular Cell Biology and Genetics, 01307 Dresden, Germany; email: eugeniu.nacu@crt-dresden.de, elly.tanaka@crt-dresden.de

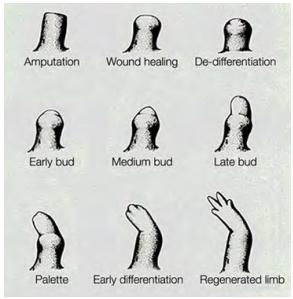

After amputation, cartilage, connective tissue and muscle cells loose their differentiated characteristics and form a blastema.

Blastema: a mesenchymal growth zone that undergo proliferation, differentiation and morphogenesis to regenerate the limb

Does blastema formation involve cellular dedifferentiation or activation of quiescent stem cells?

Cellular dedifferentiation does appear to occur during newt limb blastema formation together with stem cells proliferation.

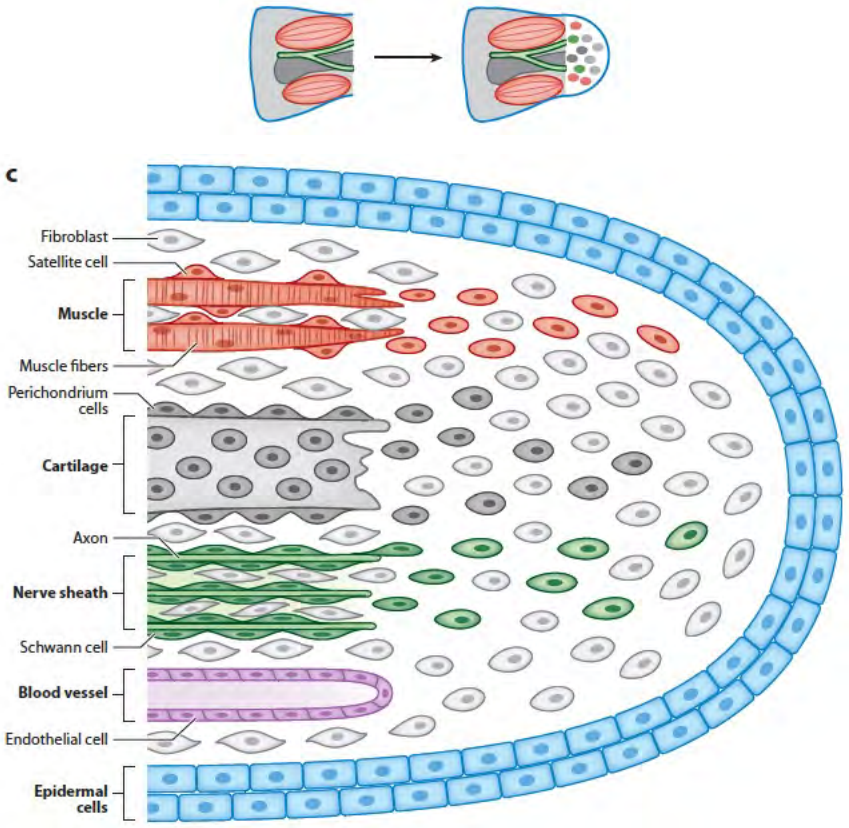

Regeneration genetics: *limb* regeneration in newts

Gene	**Function of the encoded protein**
wfgf	A signaling protein expressed in the wound epidermis shortly after injury
fgfr1	It is expressed in mesenchymal cells underlying the wound epidermis and required for blastema formation (a cell population immediately beneath the wound epidermis)
msx	Homeodomain transcription repressors expressed in mesenchymal cells that coalesce to form pluripotent regeneration cells of the distal blastema. Msx can induce cellular dedifferentiation
mps1	A mitotic checkpoint kinase critical for cell cycle progression in rapidly proliferating cells
sly1	An intracellular trafficking protein is encoded *Expression of both mps1 and sly1 is induced in, and restricted to, intensely proliferating, proximal blastema cells during regenerative outgrowth* *Loss of mps1 or sly1 function eliminates regenerative outgrowth*
wnt	A signaling molecules expressed in the epithelium adjacent to the blastema
sonic hedgehog	A signaling molecules expressed in the epithelium adjacent to the blastema

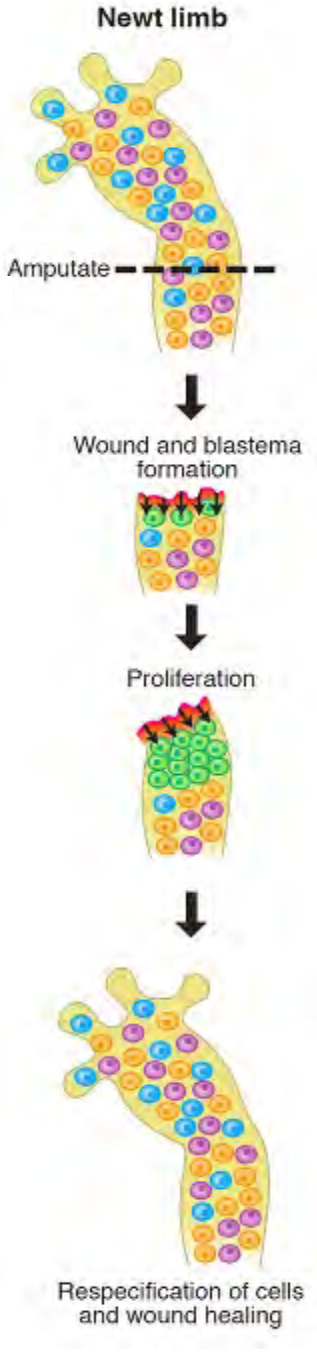

Common signaling pathways inducing regeneration

Planaria

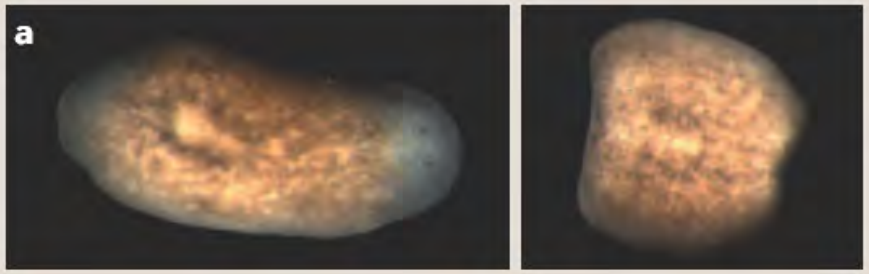

TGFB → TGFBR (?) → SMAD4 → Blastema formation

Cephalic and caudal regeneration in planarians is inhibited by the abrogation of the TGF-β pathway (silencing the expression of smad4)

Newt

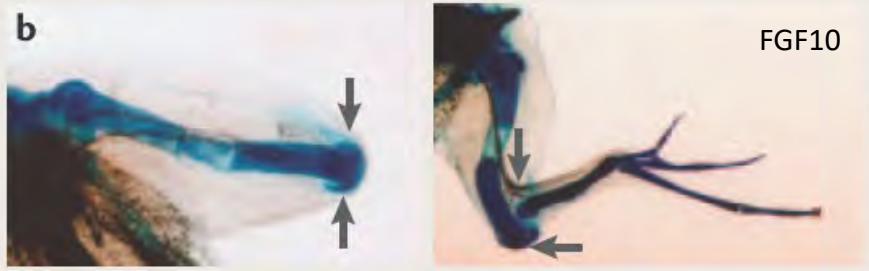

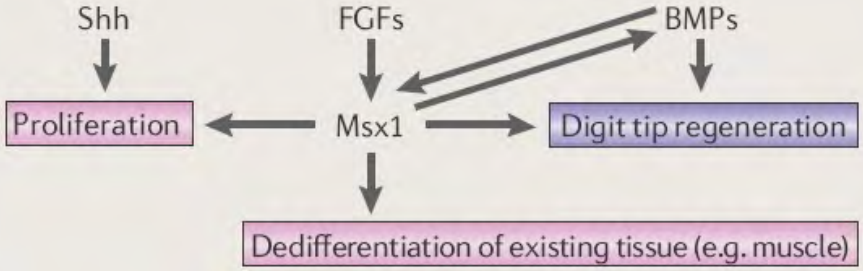

Zebrafish

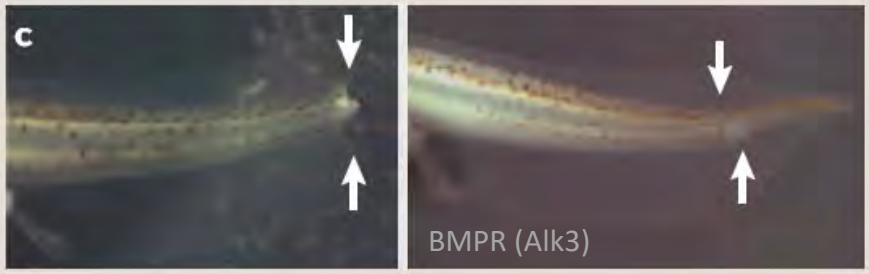

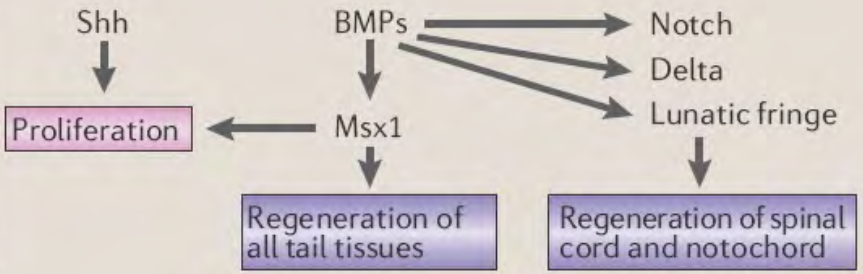

Received: 22 August 2016 | Revised: 9 September 2016 | Accepted: 12 September 2016
DOI: 10.1002/reg2.69

REVIEW

WILEY Regeneration Open Access

The cellular and molecular mechanisms of tissue repair and regeneration as revealed by studies in *Xenopus*

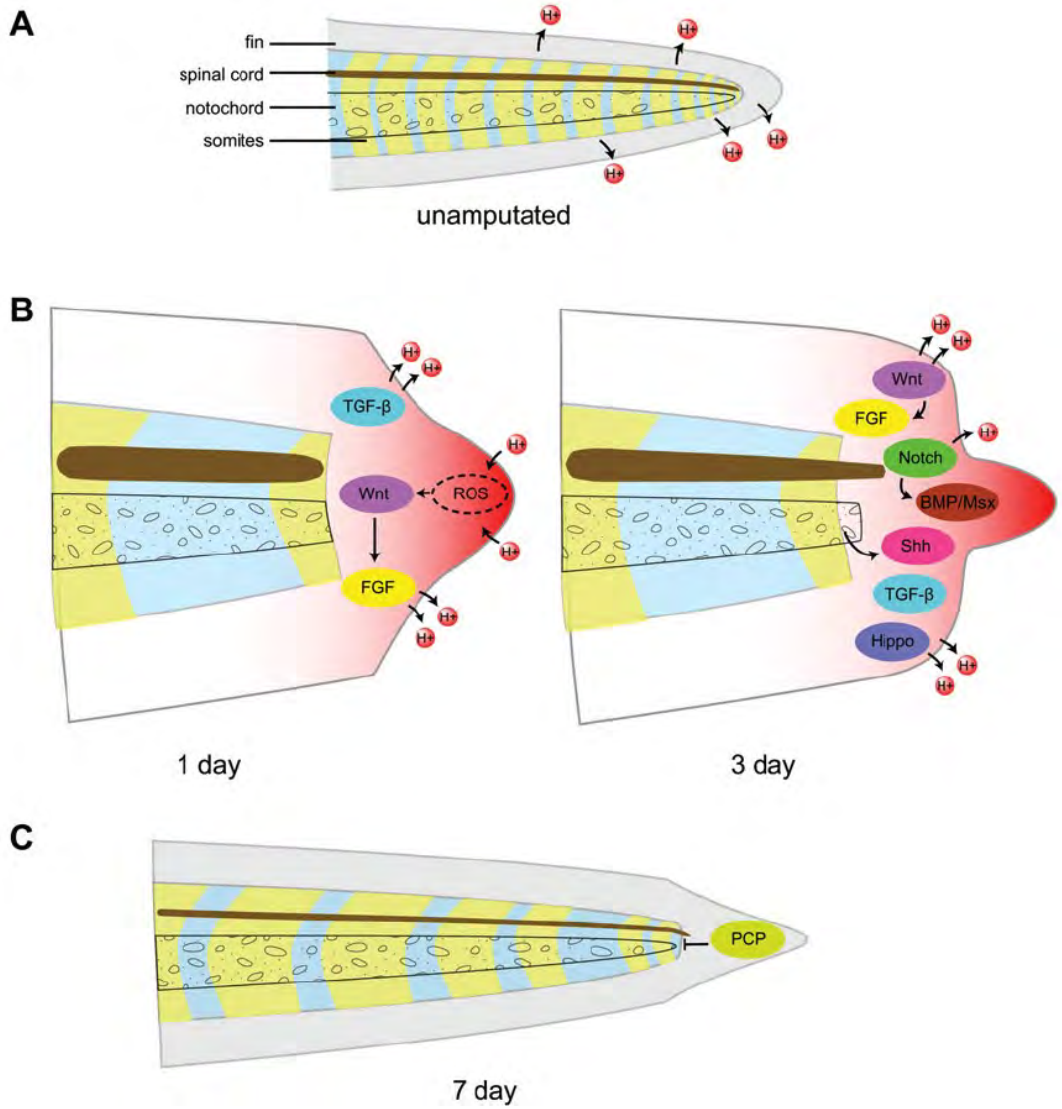

Stages of tadpole tail regeneration.

A *Xenopus* tadpole tail is composed of a number of axial structures including the spinal cord, notochord, and somites.

An unamputated tail is in a polarized state, sustained by V-ATPase pumps in the skin.
After amputation, wounded tail is depolarized and simultaneously reactive oxygen species (ROS) are produced at the amputation site.
Downstream targets of the ROS include Wnt, FGF, Shh, TGF-β, BMP, Notch, and Hippo pathways. V-ATPases are also upregulated at this stage to repolarize the skin.
A fully functional tail is regenerated 7 days after amputation.

Major signaling pathways involved in cellular differentiation are extensively conserved!

Signalling pathway	Species or group		
	Hydra magnipapillata	*Schmidtea mediterranea*	Vertebrates
TGFB	Yes	Yes	Yes
Notch	Yes	Yes	Yes
Wingless	Yes	Yes	Yes
Hedgehog	Yes	Yes	Yes
JAK/STAT	Unknown	Yes	Yes
EGF receptor	Yes	Yes	Yes
FGF receptor	Yes	Yes	Yes
Toll/NFκB	Unknown	Yes	Yes

Cell, Vol. 103, 1099–1109, December 22, 2000, Copyright ©2000 by Cell Press

Dedifferentiation of Mammalian Myotubes Induced by msx1

Shannon J. Odelberg,*§‖ Angela Kollhoff,† and Mark T. Keating*†‡‖#
*Division of Cardiology, Department of Internal Medicine

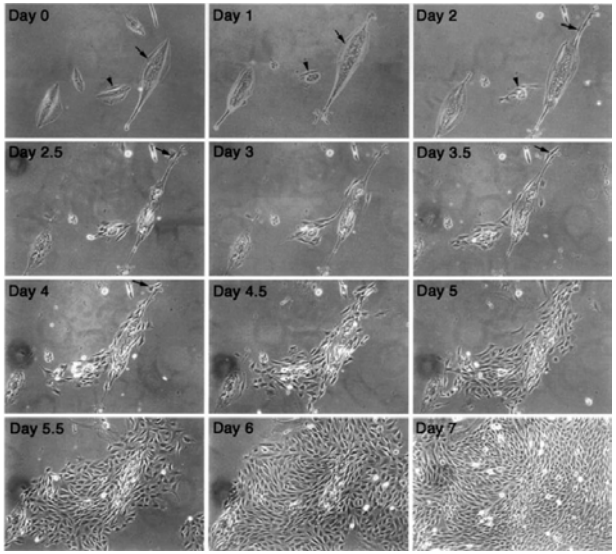

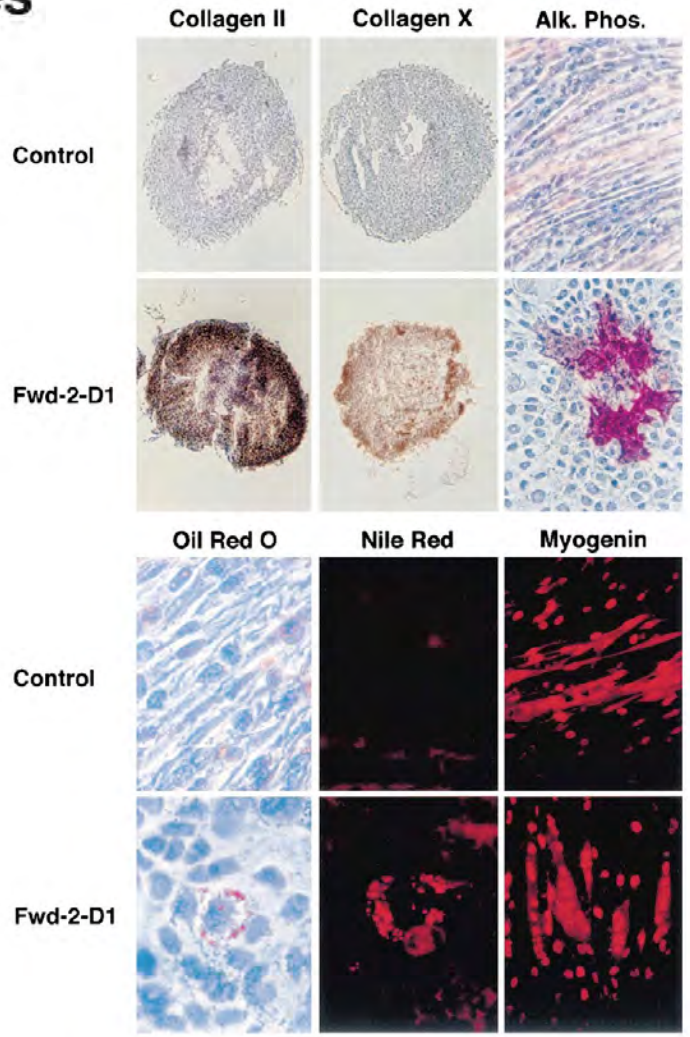

Mononucleated cells from dedifferentiated myotubes exhibit signs of pluripotency (subjected to chondrogenic, osteogenic, adipogenic, and myogenic inducing signals)

Mammalian cells might maintain the pathways required to respond to the proper “pro-regeneration” signals

Several factors could explain the absence of cellular dedifferentiation in mammals:

1. The extracellular factors that initiate dedifferentiation are not adequately expressed following amputation
2. The intrinsic cellular signaling pathways for dedifferentiation are absent
3. Differentiation factors are irreversibly expressed in mammalian cells
4. Structural characteristics of mammalian cells make dedifferentiation impossible

Mammalian myotube dedifferentiation induced by newt regeneration extract

Christopher J. McGann*†, Shannon J. Odelberg*†‡, and Mark T. Keating‡§¶||

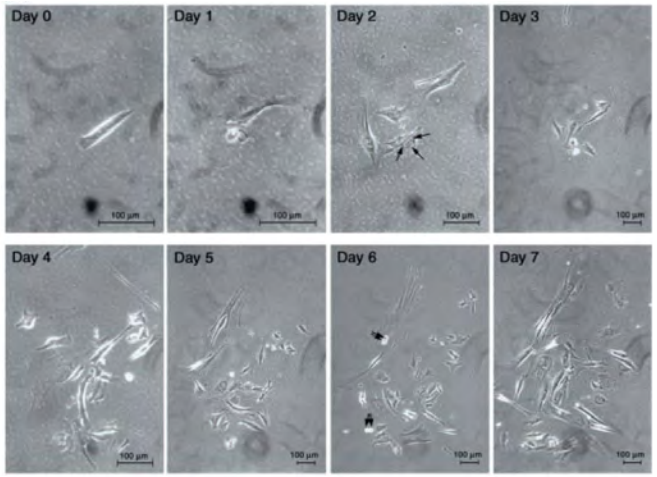

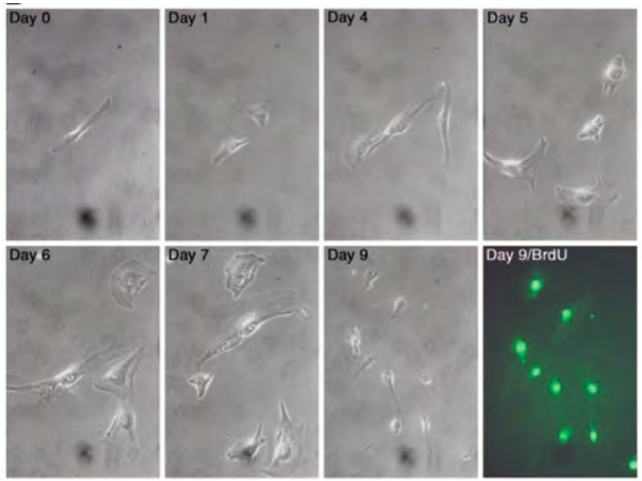

Mammalian cells retain the intracellular signaling pathways required for dedifferentiation, suggesting that mammals fail to exhibit *in vivo* cellular dedifferentiation because they lack the signals (proteins!) that initiate the process

PNAS | November 20, 2001 | vol. 98 | no. 24 | 13699–13704

Regeneration genetics in Zebrafish

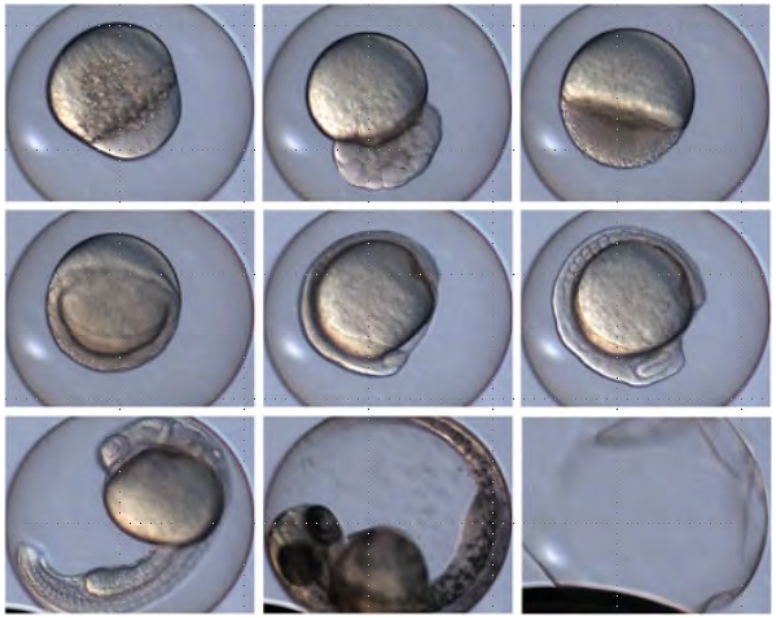

- Its fecundity makes it an optimal candidate for genetic and genomic analysis
- Eggs are fertilized outside the mother body - easy harvest and manipulation
- The embryo is transparent
- Thousands of mutations generated and characterized
- It regenerates fins, spinal cord, and optic nerve

Tales of Regeneration in Zebrafish

Kenneth D. Poss, Mark T. Keating, and Alex Nechiporuk*

DEVELOPMENTAL DYNAMICS 226:202–210, 2003

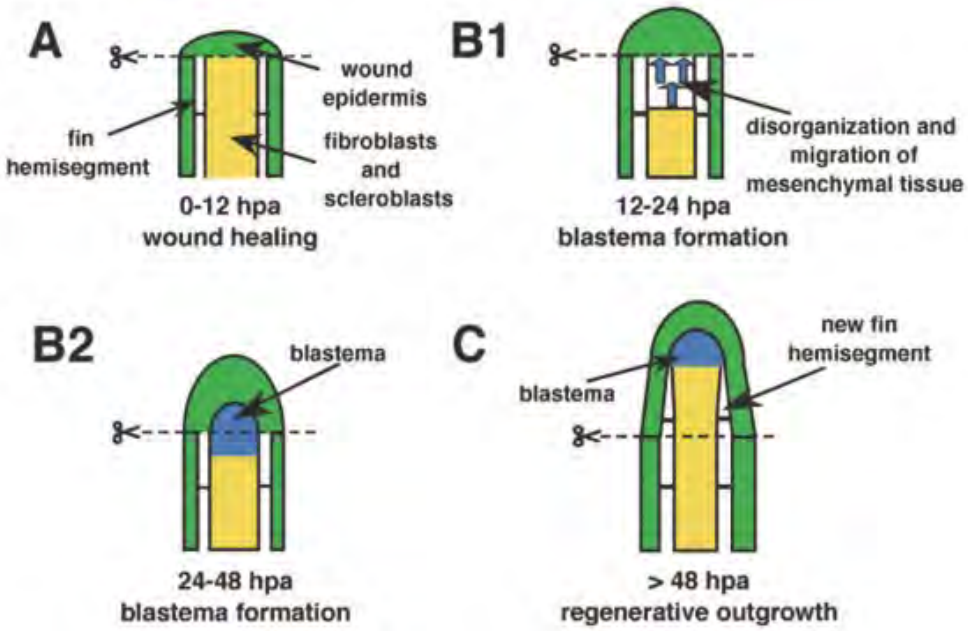

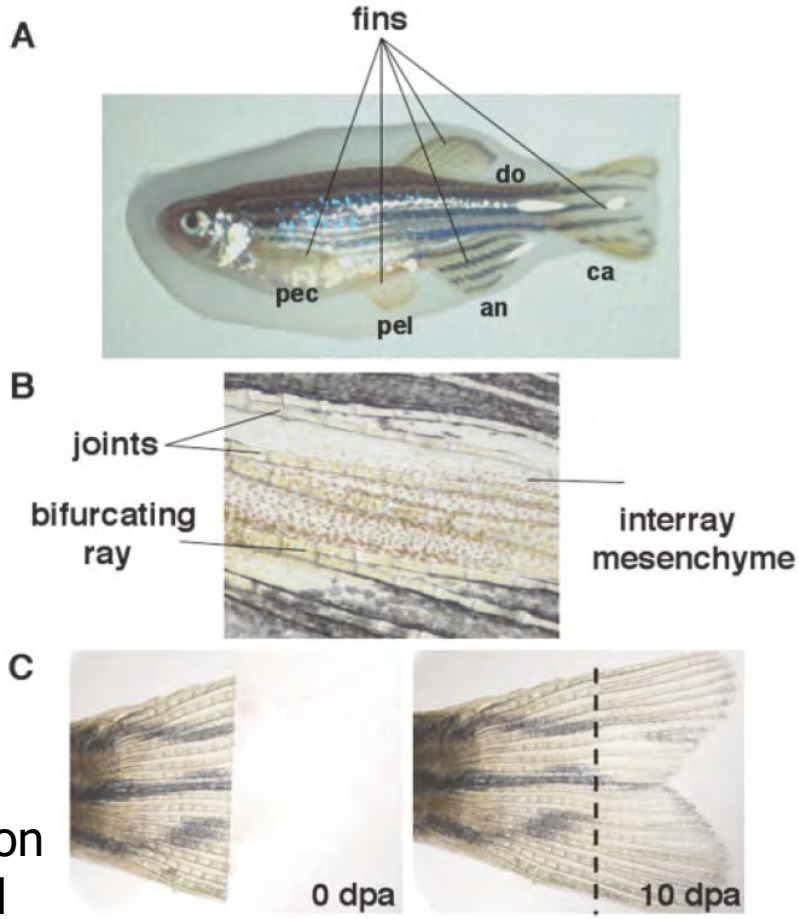

A hallmark of epimorphic limb or fin regeneration is formation of the **blastema**, a developmental event that distinguishes regeneration from embryogenesis.

Heart Regeneration in Zebrafish

Kenneth D. Poss,* Lindsay G. Wilson, Mark T. Keating*

Cardiac injury in mammals and amphibians typically leads to scarring, with minimal regeneration of heart muscle. Here, we demonstrate histologically that zebrafish fully regenerate hearts within 2 months of 20% ventricular resection. Regeneration occurs through robust proliferation of cardiomyocytes localized at the leading epicardial edge of the new myocardium. The hearts of zebrafish with mutations in the Mps1 mitotic checkpoint kinase, a critical cell cycle regulator, failed to regenerate and formed scars. Thus, injury-induced cardiomyocyte proliferation in zebrafish can overcome scar formation, allowing cardiac muscle regeneration. These findings indicate that zebrafish will be useful for genetically dissecting the molecular mechanisms of cardiac regeneration.

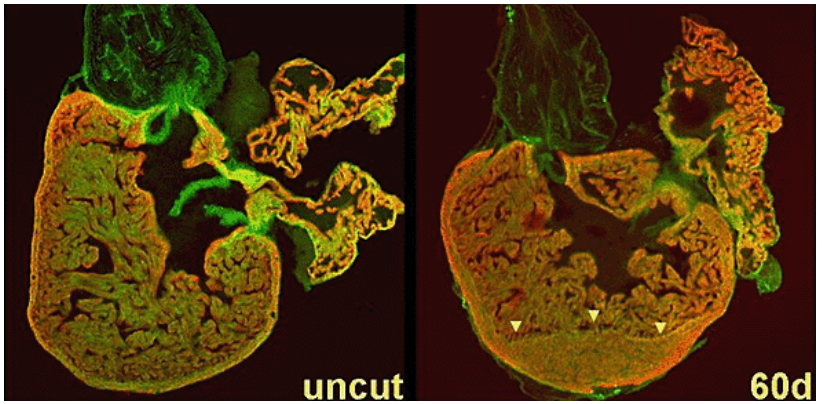

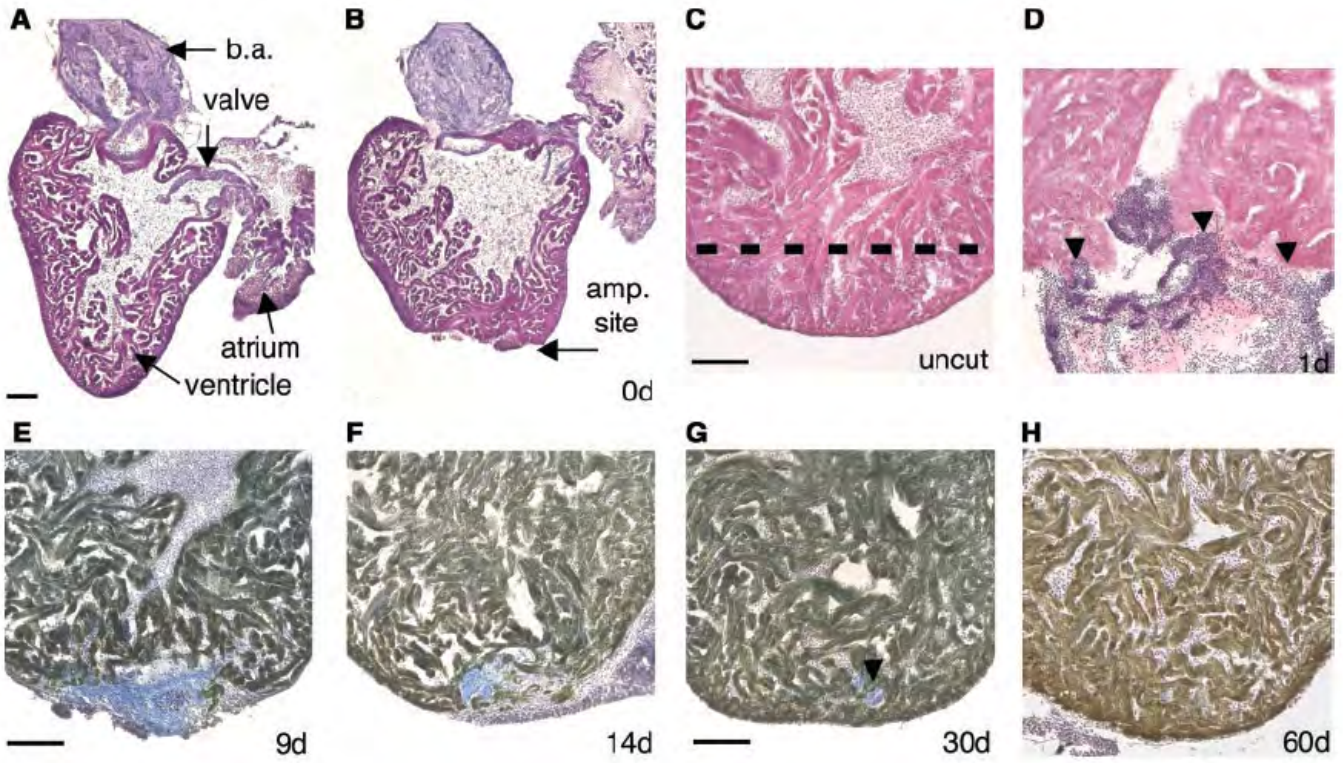

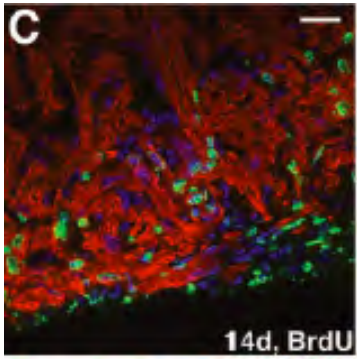

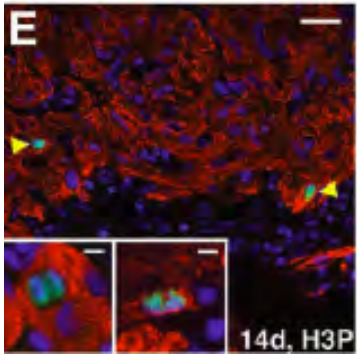

Heart Regeneration in Zebrafish

Kenneth D. Poss,* Lindsay G. Wilson, Mark T. Keating*

Cardiac injury in mammals and amphibians typically leads to scarring, with minimal regeneration of heart muscle. Here, we demonstrate histologically that zebrafish fully regenerate hearts within 2 months of 20% ventricular resection. Regeneration occurs through robust proliferation of cardiomyocytes localized at the leading epicardial edge of the new myocardium. The hearts of zebrafish with mutations in the Mps1 mitotic checkpoint kinase, a critical cell cycle regulator, failed to regenerate and formed scars. Thus, injury-induced cardiomyocyte proliferation in zebrafish can overcome scar formation, allowing cardiac muscle regeneration. These findings indicate that zebrafish will be useful for genetically dissecting the molecular mechanisms of cardiac regeneration.

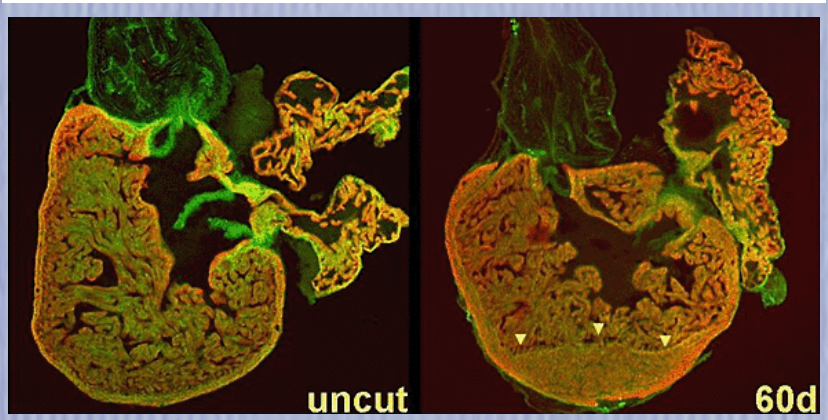

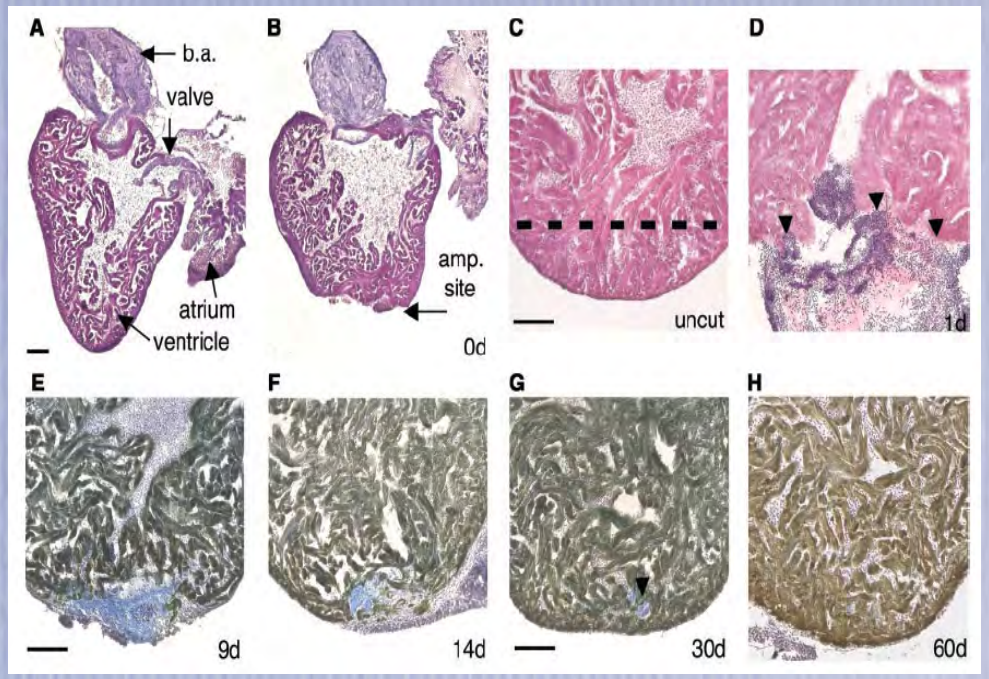

SCIENCE VOL 298 13 DECEMBER 2002

Primary contribution to zebrafish heart regeneration by *gata4*$^{+}$ cardiomyocytes

Kazu Kikuchi[1,2], Jennifer E. Holdway[1,2], Andreas A. Werdich[4], Ryan M. Anderson[5], Yi Fang[1,2], Gregory F. Egnaczyk[1,2,3], Todd Evans[6], Calum A. MacRae[4], Didier Y. R. Stainier[5] & Kenneth D. Poss[1,2]

Cardiomyocytes are the source of the regenerating tissues and expressed a marker of regeneration called *gata4*—a transcription fac involved in normal development of the heart

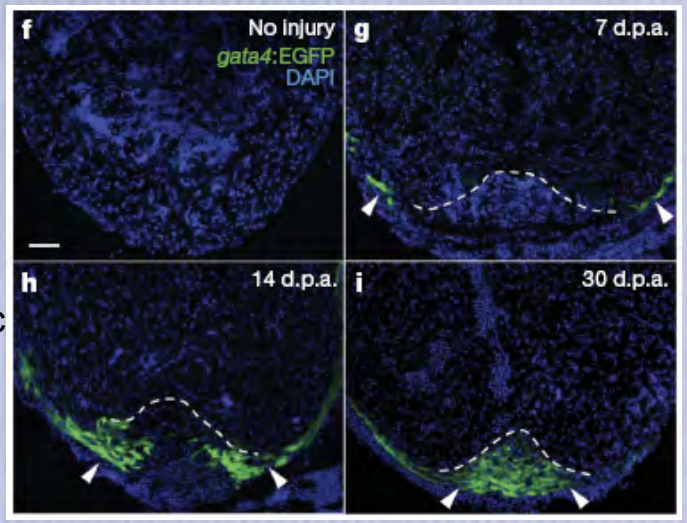

NATURE | Vol 464 | 25 March 2010

Why do zebrafish respond to cardiac injury with regeneration, whereas fibrosis predominates in other vertebrates?

mps1 mutant zebrafish form normal fibrin clots by day 8, but cardiac myofibers do not penetrate the clot

In these mutants, the ventricular wall cannot be restored; instead, the injured hearts retained fibrin deposits and developed large connective-tissue scars

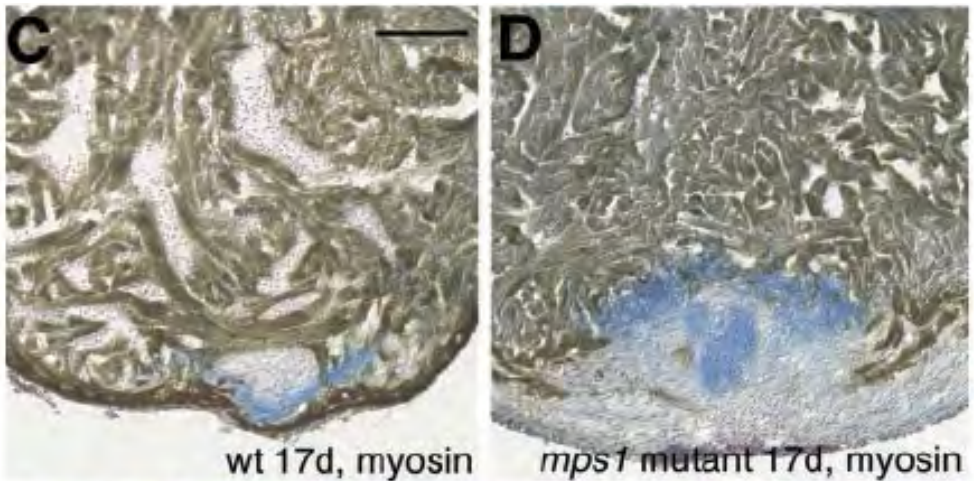

Mps1 *is a mitotic checkpoint kinase that is up-regulated in many proliferative cell types*

Scarring might complement regeneration, so that the vigor of myocyte proliferation within a given species would determine the predominant response. According to this model, the inhibition of regeneration would lead to scarring

Activation of Notch signaling pathway precedes heart regeneration in zebrafish

Ángel Raya*†, Christopher M. Koth*†, Dirk Büscher*†, Yasuhiko Kawakami*†, Tohru Itoh*†, R. Marina Raya*, Gabriel Sternik*, Huai-Jen Tsai‡, Concepción Rodríguez-Esteban*, and Juan Carlos Izpisúa-Belmonte*§

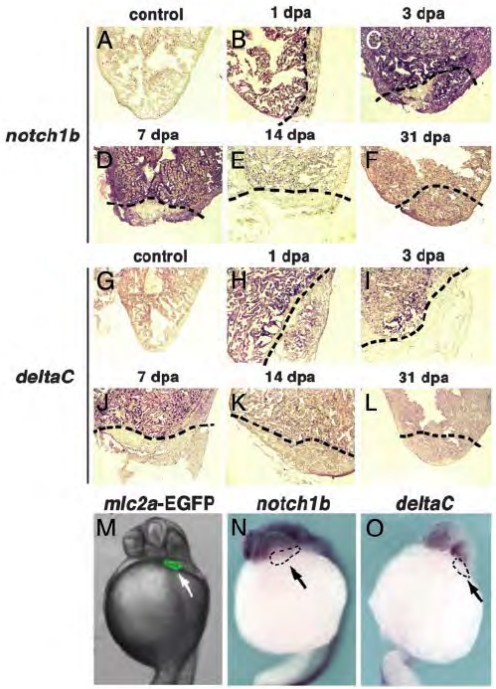

notch1b and ***deltaC*** are up-regulated during heart regeneration but not in the developing heart

Heart regeneration in zebrafish is accompanied by up-regulation of components of the Notch pathway, followed by members of the Msx family. These genes are not expressed during zebrafish heart development, indicating that **regeneration** involves the execution of a specific genetic program, rather than redeployment of a developmental program.

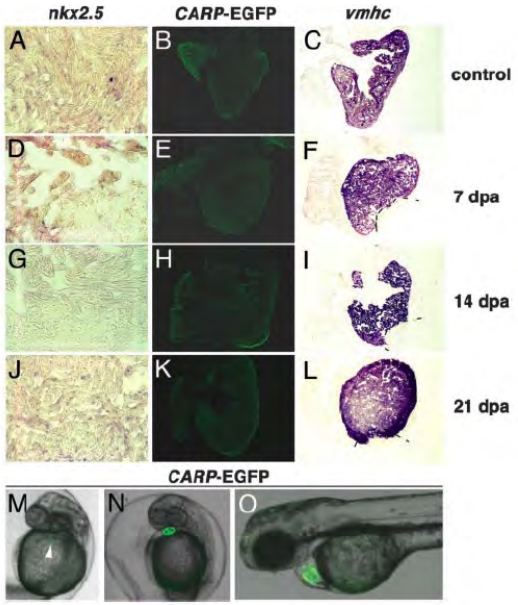

Markers of early cardiac development are not up-regulated during heart regeneration

msxC and msxB are expressed in the regenerating heart but not in 24- to 48-hpf embryos. However, both genes are expressed after removal of 50% of the developing heart

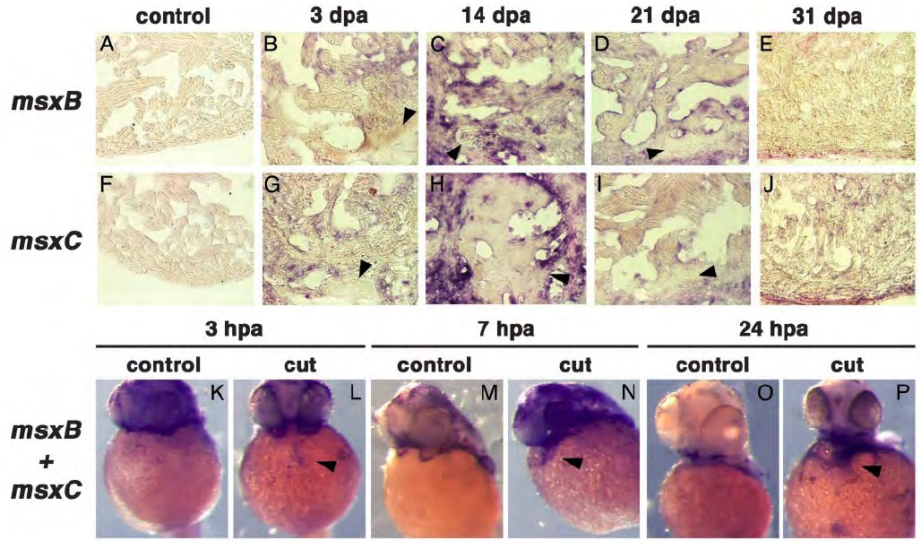

Many different hypothesis for the BrdU labeling results:

- First, differentiated, contracting CMs in existing myofibers could be stimulated to enter the cell cycle, divide, and reform the apex.
- Second, regeneration could proceed through the recruitment of undifferentiated progenitor cells that form new, proliferative CMs.
- A third conceivable mechanism for the origin of regenerative muscle is a chimera of these two mechanisms called "dedifferentiation", in which existing muscle would downregulate contractile genes toward creation of undifferentiated or poorly differentiated cells.

nature Vol 464|25 March 2010|doi:10.1038/nature08899

LETTERS

Zebrafish heart regeneration occurs by cardiomyocyte dedifferentiation and proliferation

Chris Jopling[1], Eduard Sleep[1,2]†, Marina Raya[1]†, Mercè Martí[1], Angel Raya[1,2,3]† & Juan Carlos Izpisúa Belmonte[1,2,4]

Although mammalian hearts show almost no ability to regenerate, there is a growing initiative to determine whether existing cardiomyocytes or progenitor cells can be coaxed into eliciting a regenerative response. In contrast to mammals, several non-mammalian vertebrate species are able to regenerate their hearts[1–3], including the zebrafish[4,5], which can fully regenerate its heart after amputation of up to 20% of the ventricle. To address directly the source of newly formed cardiomyocytes during zebrafish heart regeneration, we first established a genetic strategy to trace the lineage of cardiomyocytes in the adult fish, on the basis of the Cre/*lox* system widely used in the mouse[6]. Here we use this system to show that regenerated heart muscle cells are derived from the proliferation of differentiated cardiomyocytes. Furthermore, we show that proliferating cardiomyocytes undergo limited dedifferentiation characterized by the disassembly of their sarcomeric structure, detachment from one another and the expression of regulators of cell-cycle progression. Specifically, we show that the gene product of *polo-like kinase 1* (*plk1*) is an essential component of cardiomyocyte proliferation during heart regeneration. Our data provide the first direct evidence for the source of proliferating cardiomyocytes during zebrafish heart regeneration and indicate that stem or progenitor cells are not significantly involved in this process.

Regenerated cardiomyocytes are derived from differentiated, pre-existing cardiomyocytes

has been regenerated by cardiomyocytes. The exact source of these new cardiomyocytes is not yet known definitively. To address this question we developed and successfully implemented the 4-hydroxy-tamoxifen (4-OHT)-inducible Cre/*lox* approach in zebrafish to label regenerating cardiomyocytes genetically (for a detailed description of the lines generated and/or methodologies, see Methods and Supplementary Figs 1–9).

genetically labelled 48 h after fertilization. About 20% of the ventricle was removed, and cardiac regeneration was subsequently assessed at 7, 14 and 30 days after amputation. At 7 days after amputation, the remaining cardiac tissue was uniformly positive for green fluorescent protein (GFP) (Fig. 1a, b), with much of the missing tissue now replaced by a fibrin/collagen clot ($n = 5$ hearts) (Fig. 1c). At 14 days

($n = 7$ hearts; Fig. 1f). These results suggest that the regenerated cardiomyocytes arise from differentiated GFP-positive cardiomyocytes. These findings were substantiated at 30 days after amputation, when regeneration is nearly complete; all of the cardiomyocytes within the

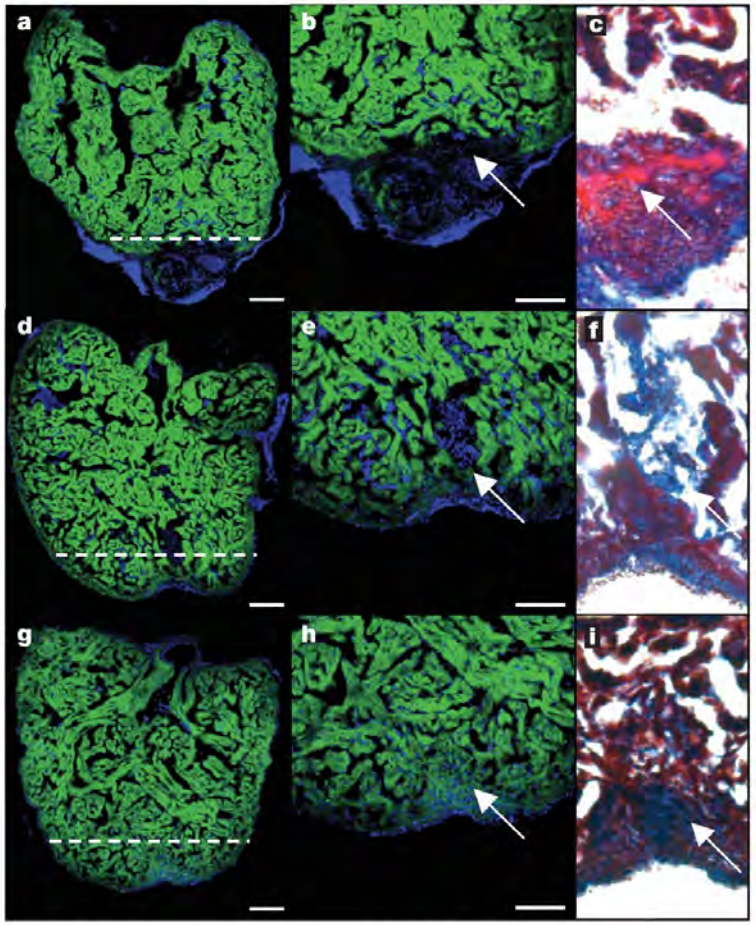

Figure 1 | Regenerated cardiomyocytes are derived from differentiated cardiomyocytes. Cardiomyocytes in transgenic zebrafish (tg-cmlc2a-Cre-Ert2: tg-cmlc2a-LnL–GFP) were genetically labelled at 48 h after fertilization by inducing Cre activity with tamoxifen. These embryos were then grown to adulthood (3 months or sexually mature), at which point the heart was amputated and allowed to regenerate for 7 (**a**–**c**), 14 (**d**–**f**) or 30 (**g**–**i**) days. The dashed white line represents the plane of amputation. At 7 days after amputation (**a**; enlargement in **b**) relatively little regeneration has occurred. Trichromic staining indicates that a fibrin clot has formed adjacent to the wound (**c**). By 14 days after amputation, GFP-positive cardiomyocytes have regenerated a substantial amount of new cardiac tissue (**d**; enlargement in **e**) and the fibrin clot was decreased in size (**f**). At 30 days after amputation, heart regeneration is virtually complete (**g**; enlargement in **h**) and all of the regenerated tissue is composed of GFP-positive cardiomyocytes. The clot has been replaced by a small scar (**h**). Scale bars, 100 μm (**a**, **d**, **g**) and 75 μm (**b**, **e**, **h**). Panels **c**, **f** and **i** are ×2 magnifications of the areas indicated with a white arrow in **b**, **e** and **h**.

Differentiating cardiomyocytes re-enter the cell cycle

We next sought to determine whether GFP-positive cardiomyocytes had re-entered the cell cycle. Adult GFP-positive transgenic zebrafish were treated with bromodeoxyuridine (BrdU) for 7 days after amputation (Fig. 2a–f). Subsequently, at 14 days after amputation, we found a significant increase in the number of BrdU-positive/GFP-positive cardiomyocytes in regenerating hearts compared with non-amputated controls (Fig. 2g). From this we conclude that differentiated GFP-positive cardiomyocytes had re-entered the cell cycle and engaged in DNA replication. We also analysed the position of BrdU-labelled GFP-positive cardiomyocytes within the regenerating heart (Fig. 2h and inset). Whereas most BrdU-positive/GFP-positive labelled cardiomyocytes were concentrated around the wound, a proportion could also be found in regions far from the site of amputation. This suggests that the response to the injury affects the heart in a global manner.

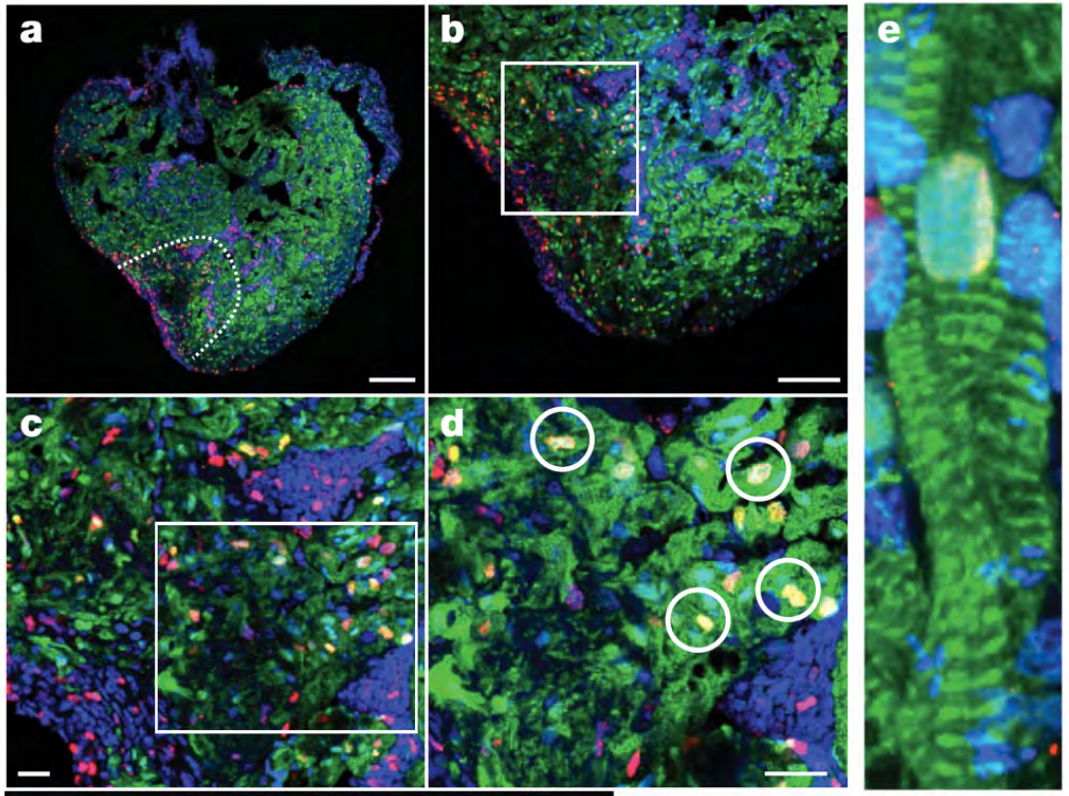

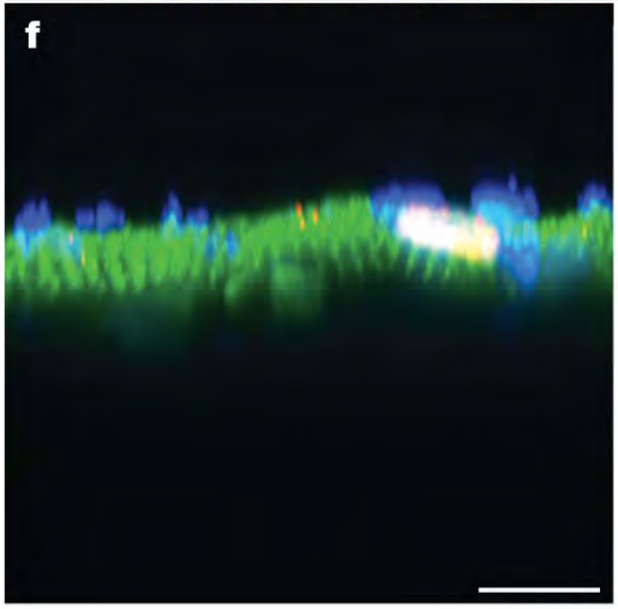

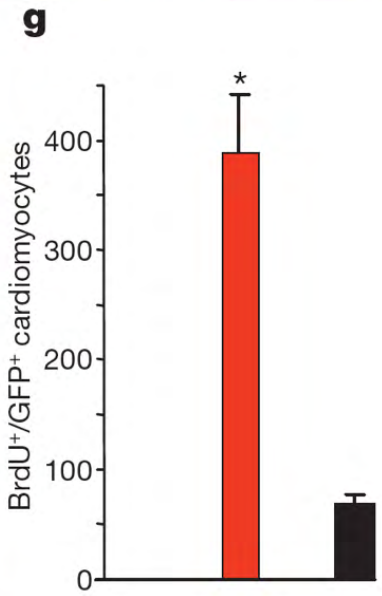

Figure 2 | Differentiated cardiomyocytes re-enter the cell cycle. (**a**–**f**) Transgenic zebrafish (tg-cmlc2a-Cre-Ert2: tg-cmlc2a-LnL–GFP) genetically labelled at 48 h after fertilization and grown to adulthood underwent cardiac amputation and were then treated with BrdU for 7 days after amputation. Hearts were isolated and processed at 14 days after amputation. Green, GFP-positive cardiomyocytes; red, BrdU-positive cells; blue, 4,6-diamidino-2-phenylindole stain for DNA; yellow, BrdU-positive/GFP-positive cardiomyocytes (white rings in **d**). **a**, Section of the entire heart, with a dashed white line representing the regenerating area. **b**, Enlargement of the regenerating area. **c**, **d**, Enlargements of the boxed areas in **b** and **c**, respectively. **e**, An *XY* reconstruction of an individual BrdU-positive/GFP-positive cardiomyocyte within a regenerating heart 14 days after amputation. **f**, An *XZ* reconstruction of the BrdU-positive/GFP-positive cardiomyocyte shown in **e**. **g**, The average number of BrdU-positive/GFP-positive cardiomyocytes per section (means and s.e.m.). Asterisk, $P < 0.01$ (*t*-test). Amputated (red bar), $n = 17$ sections from seven different animals; control (black bar), $n = 9$ sections from three different animals.

Regenerating cardiomyocyte partially disassemble the contractile apparatus but not revert to an embryonic stage

lineage they regress[7,8]. An increase in the expression of the cardiac-progenitor-associated genes *nkx2.5* and *hand2* during zebrafish heart regeneration has been reported[9]. However, our own *in situ* hybridization analyses failed to detect any significant upregulation of either transcript (data not shown), confirming previous results from our laboratory[5]. Furthermore, genome-wide transcriptome data[10,11] also failed to detect significant changes in the expression of either transcript during zebrafish heart regeneration. These results argue against an extensive dedifferentiation of cardiomyocytes as a prerequisite for their proliferation in the context of heart regeneration.

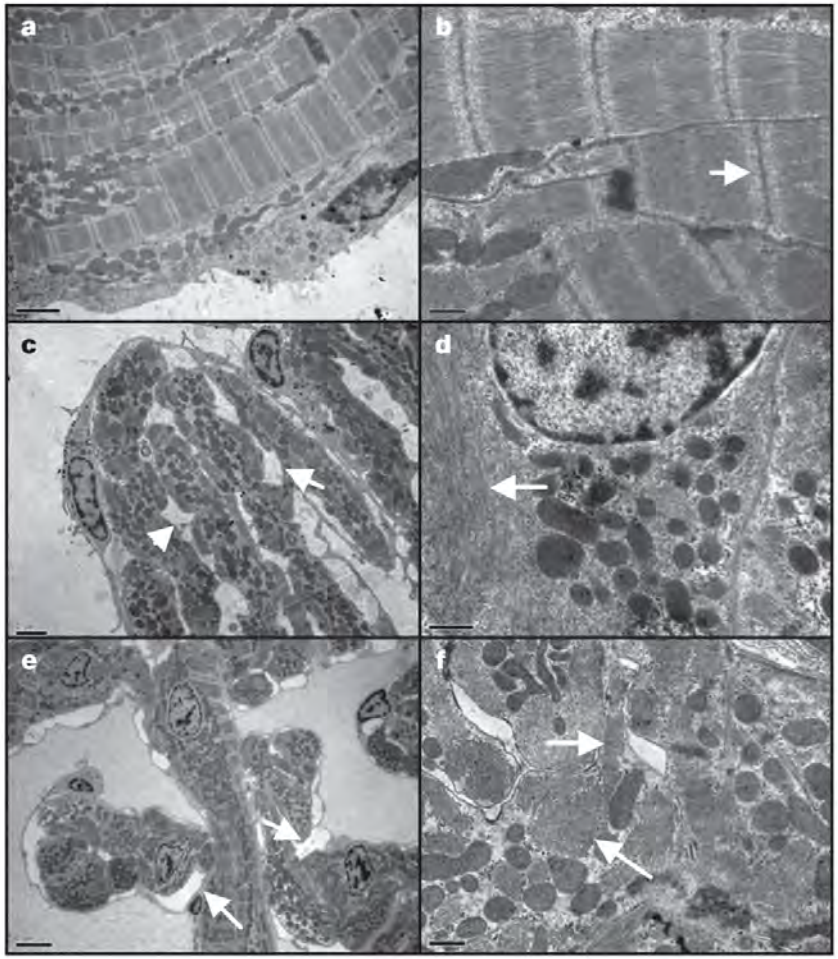

Figure 3 | Cardiomyocytes dedifferentiate, resulting in the disassembly of sarcomeric structure and detachment. Electron microscopy of sections of a control heart (**a**, **b**) and a regenerating heart at 5 days (**c**, **d**) and 7 days (**e**, **f**) after amputation. Cardiomyocytes in unamputated control samples show a tightly organized sarcomeric structure (**a**); at higher magnification (**b**) the Z-lines are clearly visible (arrow). At 5 days after amputation many of the cardiomyocytes have a disorganized sarcomeric structure (**c**) along with the appearance of intercellular spaces (arrows). Closer examination reveals a loss of Z-lines (**d**, arrow). At 7 days after amputation there is a similar loss of structure and appearance of intercellular spaces (**e**, arrows). At higher magnification (**f**) myosin fibres are visible (arrows); however, both longitudinal (upper arrow) and transverse (lower arrow) fibres are present within the same cardiomyocyte, indicating disorganized sarcomeric structure. Scale bars, 0.5 μm (**a**, **b**, **d**) and 2 μm (**c**, **e**, **f**).

What about mammals?

LETTER

doi:10.1038/nature11682

Mammalian heart renewal by pre-existing cardiomyocytes

Samuel E. Senyo[1], Matthew L. Steinhauser[1], Christie L. Pizzimenti[1], Vicky K. Yang[1], Lei Cai[1], Mei Wang[4,5], Ting-Di Wu[2,3], Jean-Luc Guerquin-Kern[2,3], Claude P. Lechene[4,5] & Richard T. Lee[1,6]

Although recent studies have revealed that heart cells are generated in adult mammals, the frequency of generation and the source of new heart cells are not yet known. Some studies suggest a high rate of stem cell activity with differentiation of progenitors to cardiomyocytes[1]. Other studies suggest that new cardiomyocytes are born at a very low rate[2–4], and that they may be derived from the division of pre-existing cardiomyocytes. Here we show, by combining two different pulse–chase approaches—genetic fate-mapping with stable isotope labelling, and multi-isotope imaging mass spectrometry—that the genesis of cardiomyocytes occurs at a low rate by the division of pre-existing cardiomyocytes during normal ageing, a process that increases adjacent to areas of myocardial injury. We found that cell cycle activity during normal ageing and after injury led to polyploidy and multinucleation, but also to new diploid, mononucleate cardiomyocytes. These data reveal pre-existing cardiomyocytes as the dominant source of cardiomyocyte replacement in normal mammalian myocardial homeostasis as well as after myocardial injury.

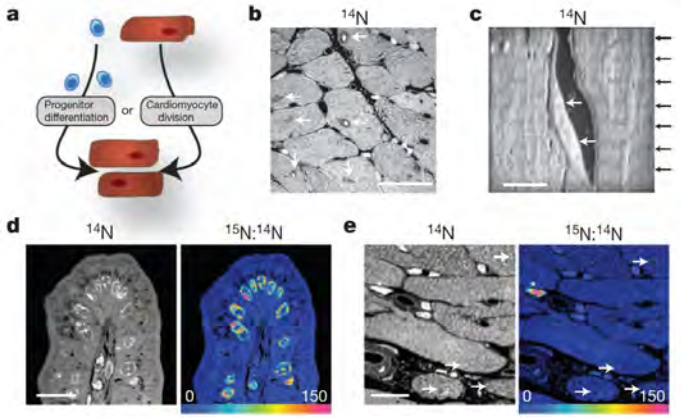

Figure 1 | Use of MIMS to study cardiomyocyte turnover. **a**, Primary question: are new cardiomyocytes derived from progenitors or from pre-existing cardiomyocytes? **b**, ^{14}N mass image. Subcellular details are evident, including cardiomyocyte nuclei (white arrows). Scale bar, 20 μm. **c**, MIMS resolves periodic sarcomeres (black arrows) in cardiomyocytes. Non-cardiomyocytes (white arrows) are seen outside cardiomyocyte borders. Scale bar, 5 μm. **d**, Right, ^{15}N:^{14}N hue–saturation–intensity image of small-intestinal epithelium after labelling with [^{15}N]thymidine. The scale ranges from blue, where the ratio is equivalent to natural ratio (0.37%, expressed as 0% above natural ratio (enrichment over natural ratio)), to red, where the ratio is 150% above natural ratio. ^{15}N labelling is concentrated in nuclei in a pattern resembling chromatin. Scale bar, 15 μm. **e**, Right, ^{15}N:^{14}N hue–saturation–intensity image of heart section (left ventricle). [^{15}N]Thymidine was administered for 1 week. Asterisk, rare $^{15}N^{+}$ interstitial cells. Cardiomyocyte nuclei (white arrows) are unlabelled. Scale bar, 15 μm.

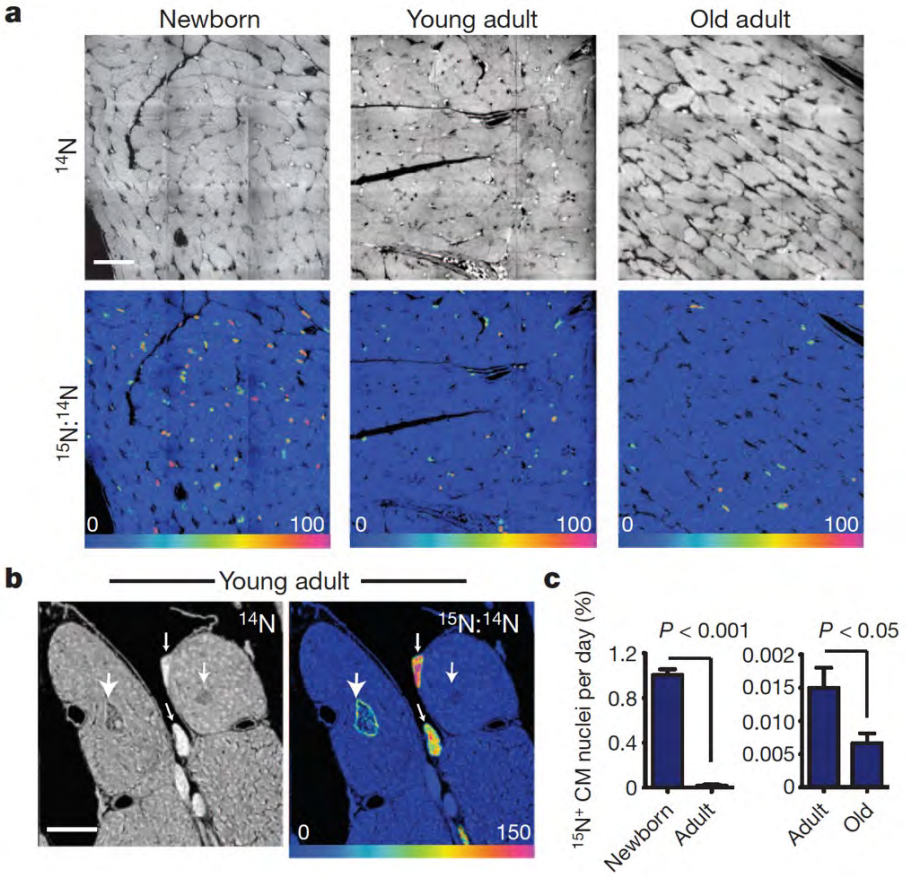

Figure 2 | Cardiomyocyte DNA synthesis decreases with age. **a**, [^{15}N]Thymidine was administered for 8 weeks to mice of different ages: newborn, starting at postnatal day 4; young adult, starting at 2 months; old adult, starting at 22 months. Top, ^{14}N mass images show histological details. Bottom, ^{15}N:^{14}N hue–saturation–intensity images show ^{15}N^{+} nuclei. Mosaics are constructed from nine tiles, 60 μm each. Scale bar, 30 μm. **b**, High-magnification analysis shows a cardiomyocyte from the young adult with nuclear ^{15}N labelling (large arrow), two labelled non-cardiomyocytes (small arrows) and an adjacent unlabelled cardiomyocyte nucleus (medium arrow). Scale bar, 10 μm. **c**, Age-related decline in cardiomyocyte DNA synthesis. Left, comparison of newborn with young adult. Right, scale reduced to compare young adult with old adult ($n = 3$ mice per group). Error bars indicate s.e.m.

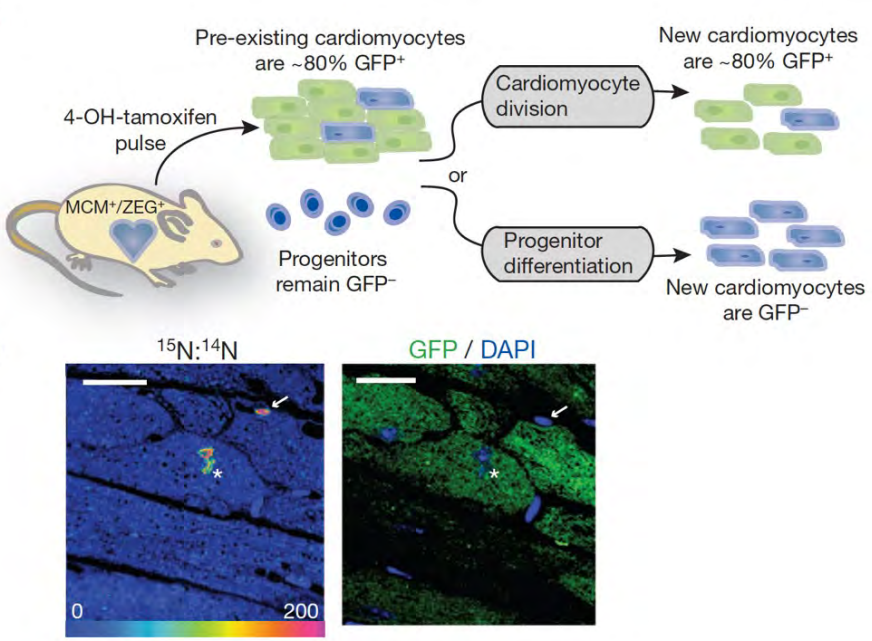

Figure 3 | New cardiomyocytes are derived from pre-existing cardiomyocytes during ageing. **a**, Experimental strategy. MerCreMer^{+}/ZEG^{+} (MCM^{+}ZEG^{+}) mice ($n = 4$) were treated for 2 weeks with 4-OH-tamoxifen to induce cardiomyocyte-specific GFP expression. [^{15}N]Thymidine was administered continuously during a 10-week chase, then cycling cells were identified by ^{15}N labelling. New cardiomyocytes (^{15}N^{+}) derived from pre-existing cardiomyocytes should express GFP at a rate similar to that of the surrounding quiescent (^{15}N^{-}) cardiomyocytes. New cardiomyocytes (^{15}N^{+}) derived from progenitors should be GFP^{-}. **b**, Left, ^{15}N:^{14}N hue–saturation–intensity image showing a [^{15}N]thymidine-labelled cardiomyocyte nucleus (white asterisk) and a ^{15}N^{+} non-cardiomyocyte (white arrow). Right, immunofluorescent image showing that the ^{15}N^{+} cardiomyocyte is GFP^{+}. Scale bars, 15 μm.

25 FEBRUARY 2011 VOL 331

Transient Regenerative Potential of the Neonatal Mouse Heart

Enzo R. Porrello,[1] Ahmed I. Mahmoud,[2] Emma Simpson,[3] Joseph A. Hill,[1,2] James A. Richardson,[1,3] Eric N. Olson,[1]* Hesham A. Sadek[2]*

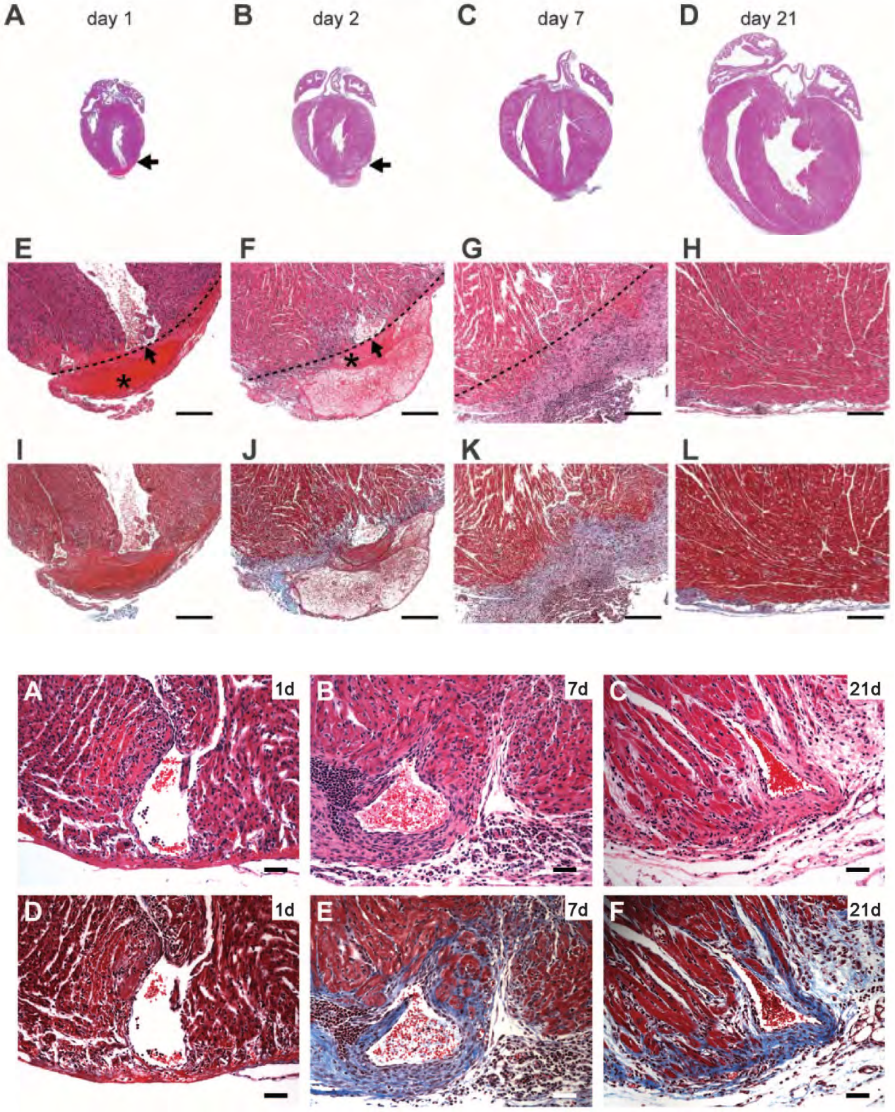

- Hearts of 1-day-old neonatal mice can regenerate after partial surgical resection, but this capacity is lost by 7 days of age.
- The regenerative response was characterized by cardiomyocyte proliferation with minimal hypertrophy or fibrosis.
- The majority of cardiomyocytes within the regenerated tissue originated from preexisting cardiomyocytes.

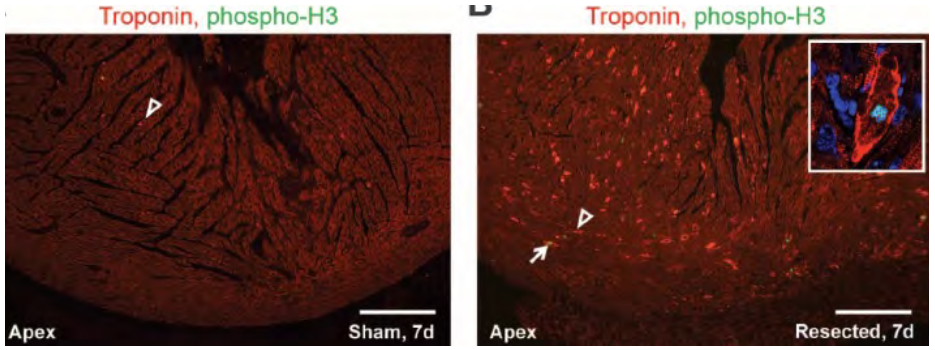

NATURE PROTOCOLS | VOL.9 NO.2 | 2014 | PROTOCOL

Surgical models for cardiac regeneration in neonatal mice

Ahmed I Mahmoud[1], Enzo R Porrello[2], Wataru Kimura[3], Eric N Olson[4] & Hesham A Sadek[3]

[1]Department of Medicine, Cardiovascular Division, Brigham and Women's Hospital and Harvard Medical School, Cambridge, Massachusetts, USA. [2]School of Biomedical Sciences, The University of Queensland, St. Lucia, Queensland, Australia. [3]Department of Internal Medicine, The University of Texas Southwestern Medical Center, Dallas, Texas, USA. [4]Department of Molecular Biology, The University of Texas Southwestern Medical Center, Dallas, Texas, USA. Correspondence should be addressed to H.A.S. (hesham.sadek@utsouthwestern.edu).

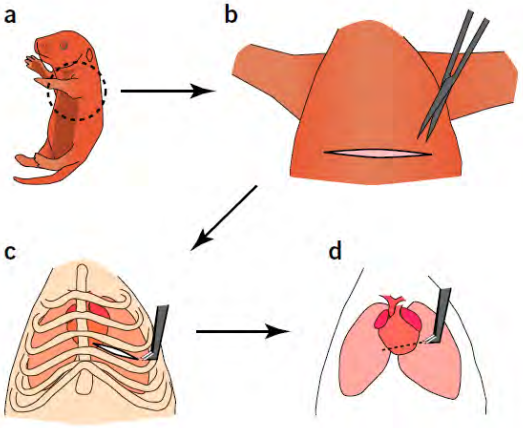

(Mahmoud et al., 2014)

Apical resection surgical model

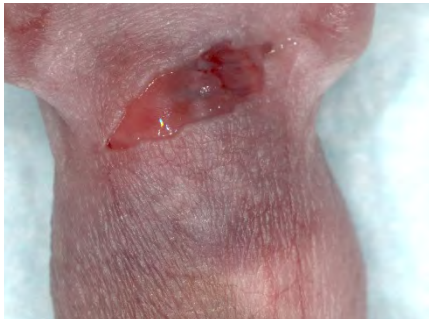

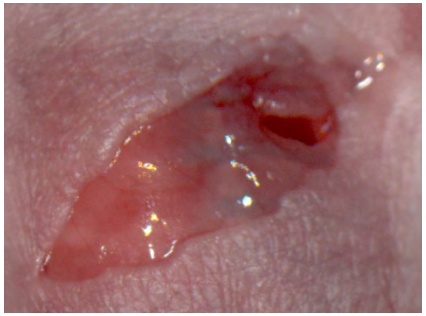

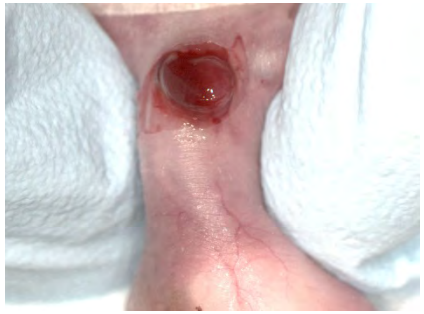

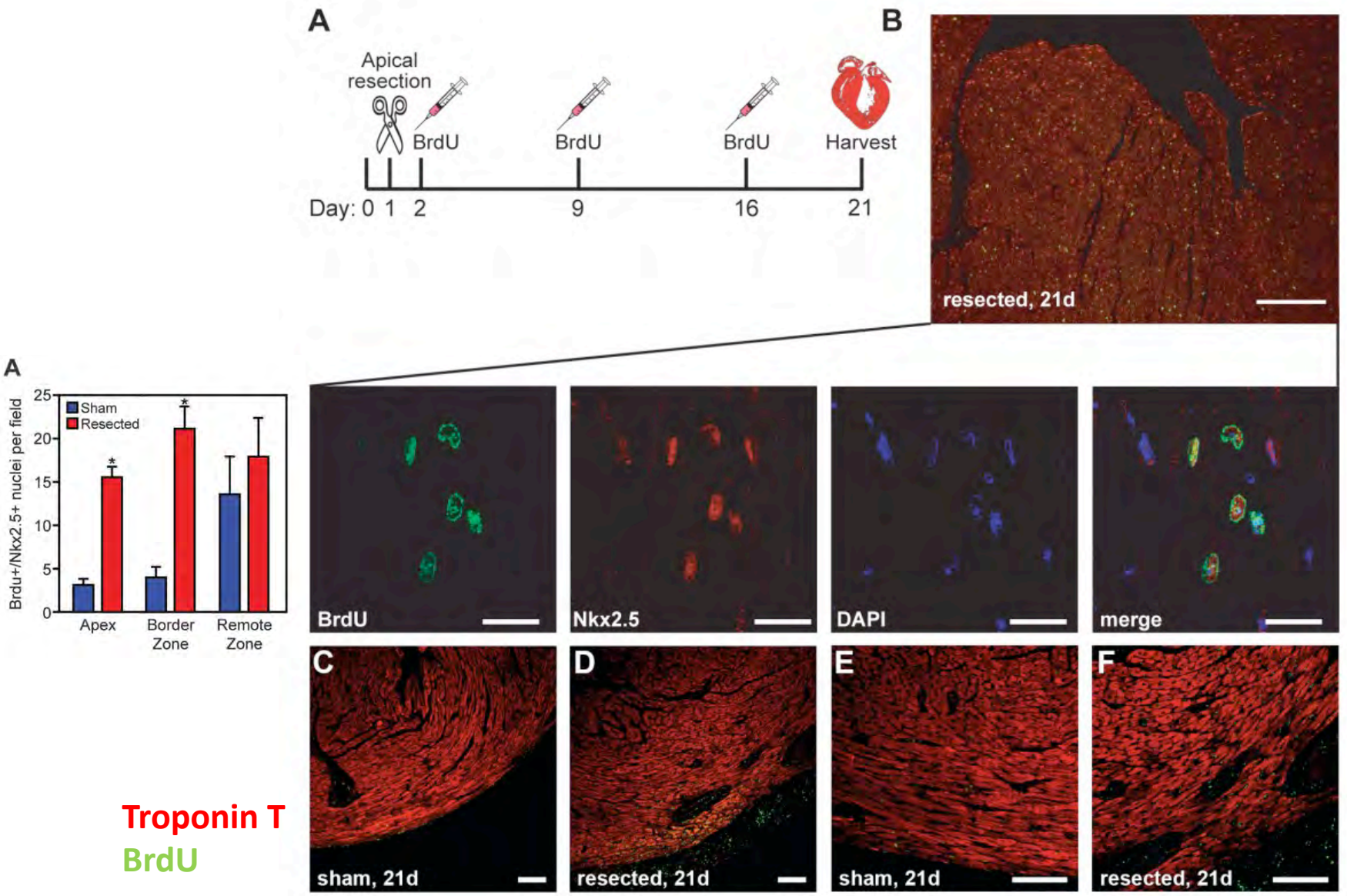

Newly formed cardiomyocytes

(Porrello et al., 2011)

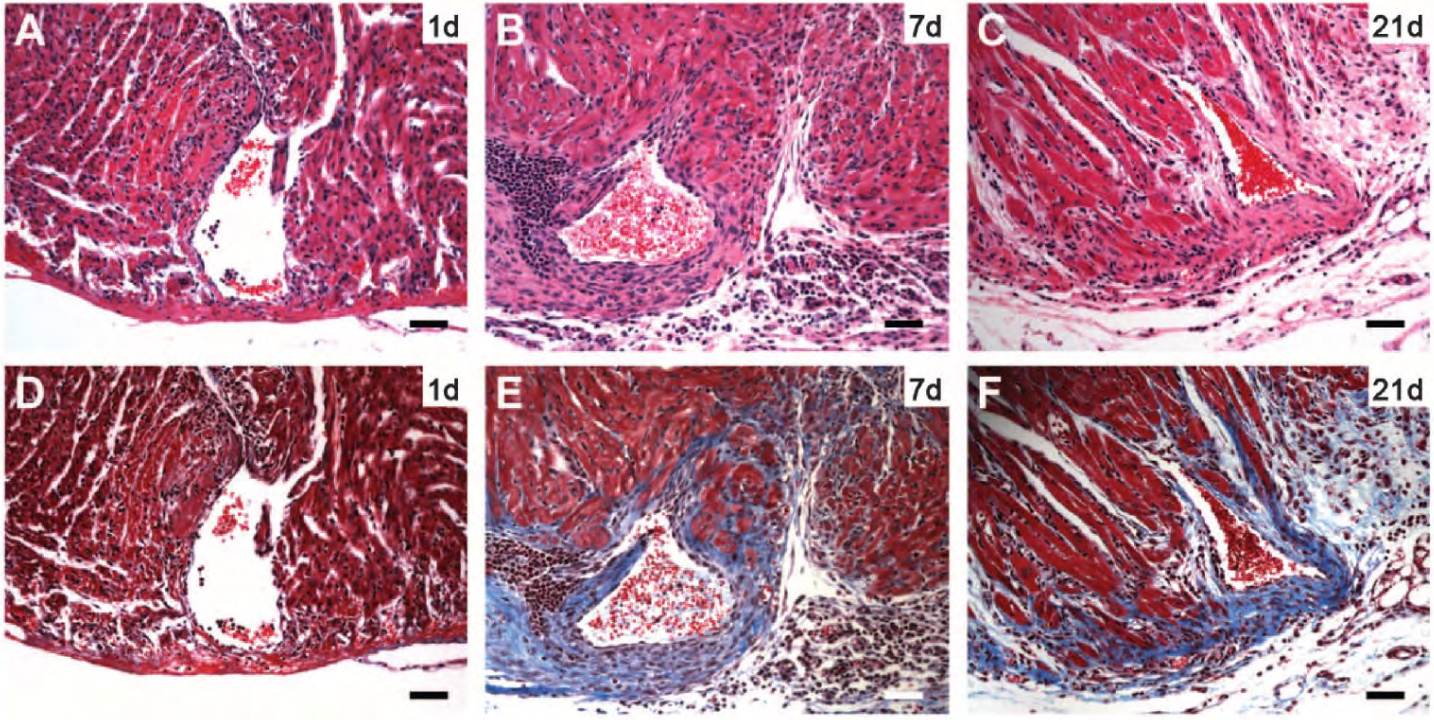

Fig. 4. Lack of regeneration after apical resection of 7-day-old mice. (**A** to **C**) H&E staining at 1, 7, and 21 dpr, respectively. (**D** to **F**) Trichrome staining at 1, 7, and 21 dpr. Note fibrotic scar (blue staining) surrounding resected ventricular chamber at 7 and 21 dpr [(E) and (F)]. Scale bars, 200 μm.

Which cells do they derive from ?

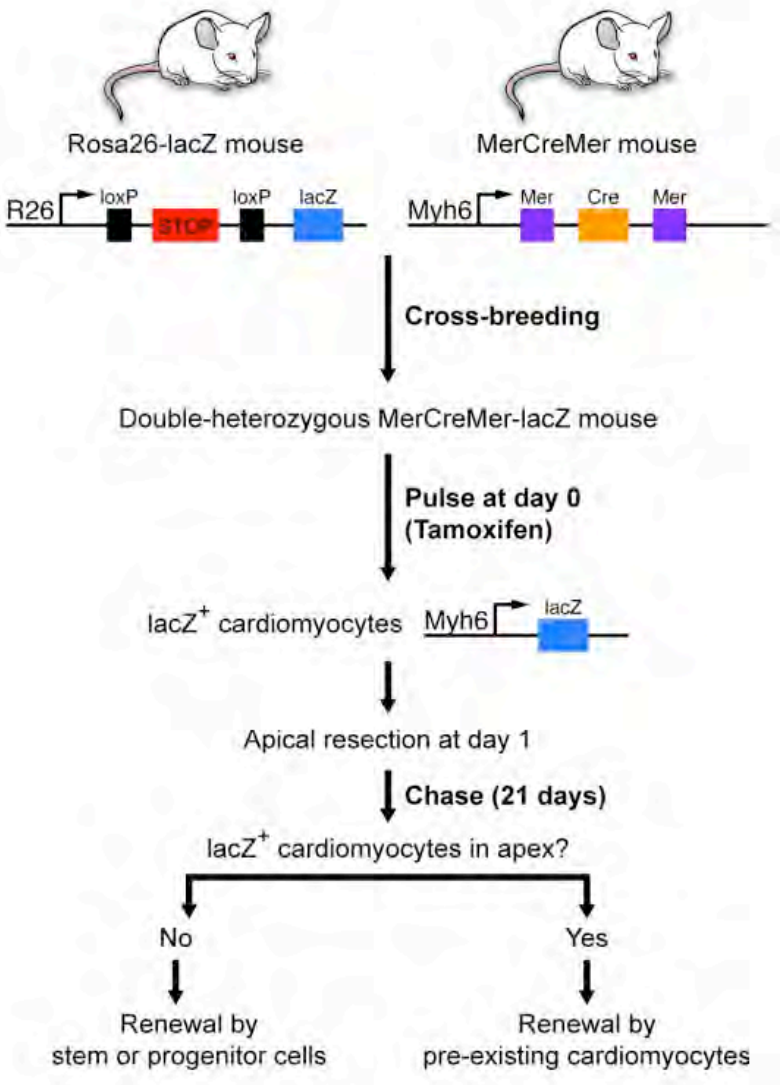

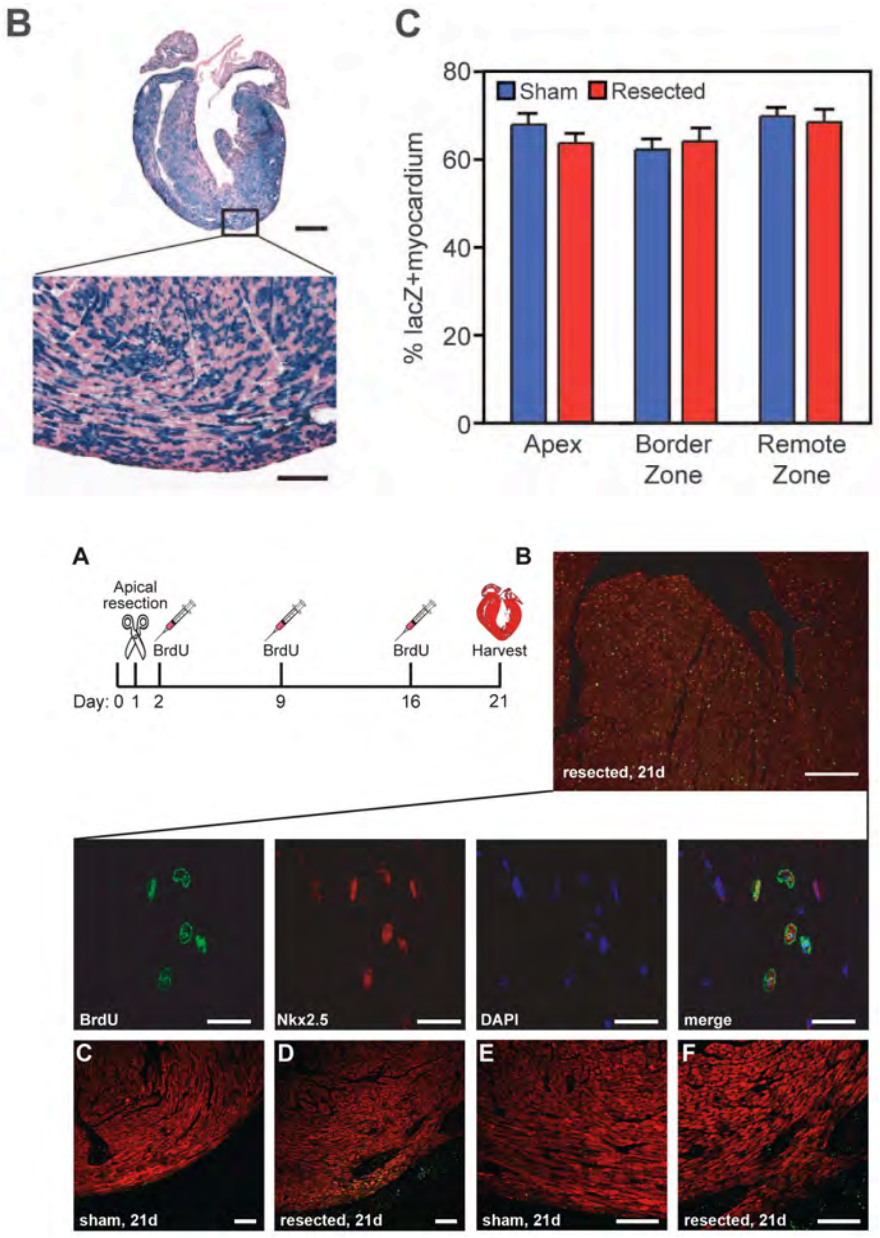

(Porrello et al., 2011)

Stem Cell Reports | Vol. 10 | 860–874 | March 13, 2018 | © 2018 The Author(s).

Stem Cell Reports

Article

ISSCR

OPEN ACCESS

Neonatal Apex Resection Triggers Cardiomyocyte Proliferation, Neovascularization and Functional Recovery Despite Local Fibrosis

Vasco Sampaio-Pinto,[1,2,3] Sílvia C. Rodrigues,[1,2] Tiago L. Laundos,[1,2,3] Elsa D. Silva,[1,2] Francisco Vasques-Nóvoa,[1,2,4] Ana C. Silva,[1,2,3,5] Rui J. Cerqueira,[4] Tatiana P. Resende,[1,2] Nicola Pianca,[6] Adelino Leite-Moreira,[4] Gabriele D'Uva,[6] Sólveig Thorsteinsdóttir,[7] Perpétua Pinto-do-Ó,[1,2,3,8] and Diana S. Nascimento[1,2,8,*]

SUMMARY

So far, opposing outcomes have been reported following neonatal apex resection in mice, questioning the validity of this injury model to investigate regenerative mechanisms. We performed a systematic evaluation, up to 180 days after surgery, of the pathophysiological events activated upon apex resection. In response to cardiac injury, we observed increased cardiomyocyte proliferation in remote and apex regions, neovascularization, and local fibrosis. In adulthood, resected hearts remain consistently shorter and display permanent fibrotic tissue deposition in the center of the resection plane, indicating limited apex regrowth. However, thickening of the left ventricle wall, explained by an upsurge in cardiomyocyte proliferation during the initial response to injury, compensated cardiomyocyte loss and supported normal systolic function. Thus, apex resection triggers both regenerative and reparative mechanisms, endorsing this injury model for studies aimed at promoting cardiomyocyte proliferation and/or downplaying fibrosis.

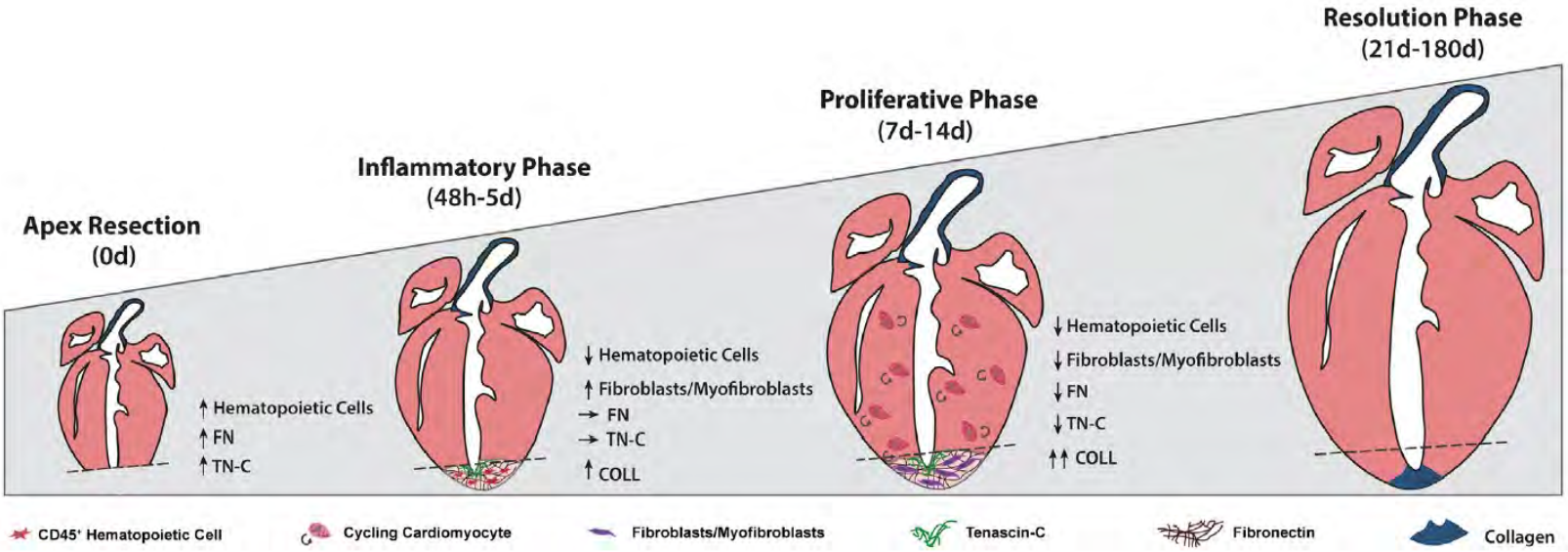

Apex resection promotes local infiltration of inflammatory cells in the first 48 hr, which leads to the deposition of a transient FN and TN-Crich ECM.

At 7 days post-injury, rates of CM proliferation are increased throughout the left ventricular myocardium and cardiac fibroblasts are activated at the injury site. These cellular dynamics result in a thickening of left ventricle walls, de novo vessel formation and deposition of a permanent fibrotic scar at the midpoint of the injured area.

Long-term evaluation showed preserved systolic function, shortened long-axis and thicker left ventricle, without hypertrophy and edema.

Is the heart really a post-mitotic organ?

Carbon dating of human tissues

After the Second World War, tests of nuclear bombs spewed carbon-14 pollution into the atmosphere. This isotope was incorporated into plants and the people who consumed them. After above-ground tests were stopped in 1963, levels of the isotope started to fall. The ^{14}C in a cell's DNA corresponds to the amount of the isotope in the atmosphere at the time it was dividing, providing a way to date a cell's birth.

People born before 1955 had levels of ^{14}C in their cardiomyocytes that were higher than was present in the atmosphere at the time of their birth, so some of these cells must have arisen later on in their lives. Further work and mathematical modelling allowed to calculate that a 50-year-old heart still contains more than half the cells it had at birth and that the turnover slows down with time. A 25-year-old heart replaces about 1% of all cardiomyocytes over a year; a 75-year-old about half that.

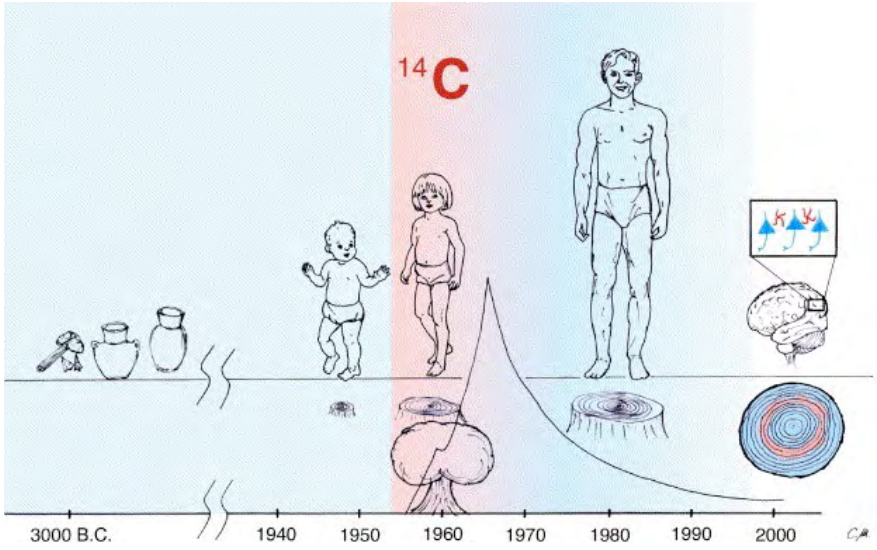

Although extensive regeneration is unlikely to occur in most of mammalian tissues, evidence has accumulated in recent years suggesting that mammalian cardiac myocytes do retain the capacity to divide. Carbon dating of cardiomyocytes in human hearts has been suggested to indicate a lifetime turnover rate of 50%.

Nevertheless, the ability of adult mammalian myocytes to regenerate injured tissue is limited. Perhaps during the course of evolution, mammalian hearts have simply lost the capacity for regeneration because it wasn't needed. After all, heart disease occurs later in life after we have reproduced. In addition, repair became more important. The mammalian heart works at high pressure, whereas the fish heart doesn't.

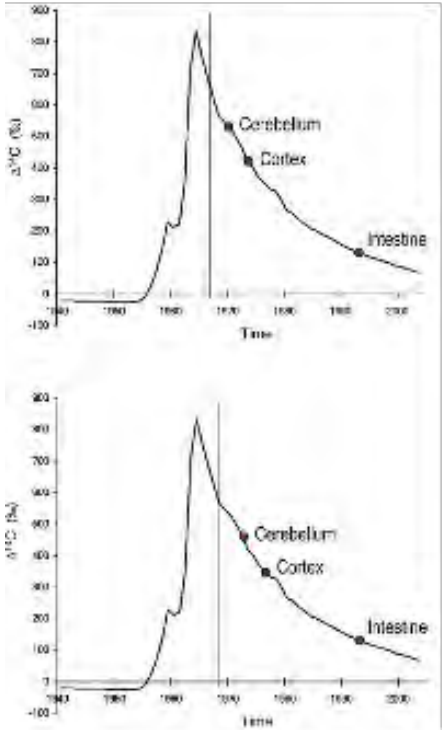

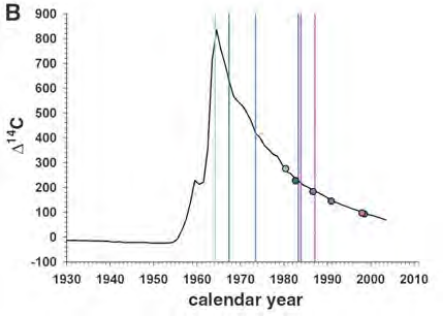

The vertical bar indicates the date of birth of each individual, and the similarly colored dots represent the ^{14}C data for the same individual.

3 APRIL 2009 VOL 324 SCIENCE

Evidence for Cardiomyocyte Renewal in Humans

Olaf Bergmann,[1]* Ratan D. Bhardwaj,[1]* Samuel Bernard,[2] Sofia Zdunek,[1] Fanie Barnabé-Heider,[1] Stuart Walsh,[3] Joel Zupicich,[1] Kanar Alkass,[4] Bruce A. Buchholz,[5] Henrik Druid,[4] Stefan Jovinge,[3,6] Jonas Frisén[1]†

It has been difficult to establish whether we are limited to the heart muscle cells we are born with or if cardiomyocytes are generated also later in life. We have taken advantage of the integration of carbon-14, generated by nuclear bomb tests during the Cold War, into DNA to establish the age of cardiomyocytes in humans. We report that cardiomyocytes renew, with a gradual decrease from 1% turning over annually at the age of 25 to 0.45% at the age of 75. Fewer than 50% of cardiomyocytes are exchanged during a normal life span. The capacity to generate cardiomyocytes in the adult human heart suggests that it may be rational to work toward the development of therapeutic strategies aimed at stimulating this process in cardiac pathologies.

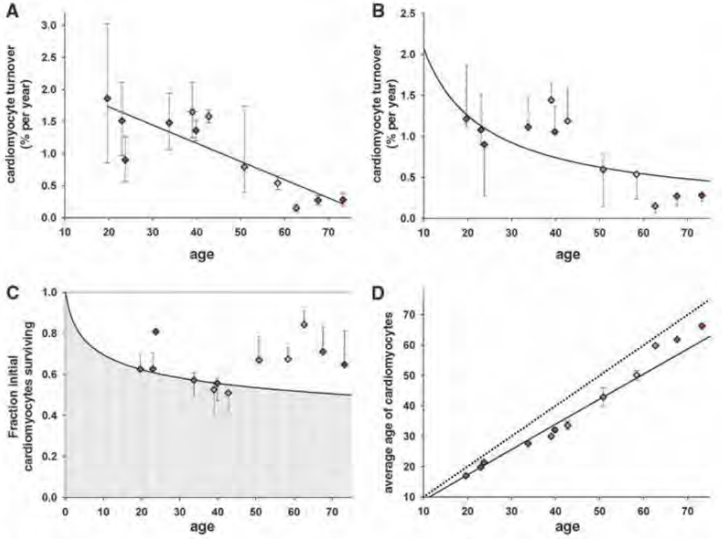

Fig. 4. Dynamics of cardiomyocyte turnover. (**A**) Individual data fitting assuming a constant turnover (see supporting online text) reveals an almost linear decline of cardiomyocyte turnover with age (R = −0.84; P = 0.001). A constant-turnover hypothesis might therefore not represent the turnover dynamics accurately. (**B**) Global fitting of all data points (see supporting online text, error sum of squares = 1.2×10^4) shows an age-dependent decline of cardiomyocyte turnover. (**C**) The gray area depicts the fraction of cardiomyocytes remaining from birth, and the white area is the contribution of new cells. Estimate is from the best global fitting. (**D**) Cardiomyocyte age estimates from the best global fitting. The dotted line represents the no-cell-turnover scenario, where the average age of cardiomyocytes equals the age of the individual. The black line shows the best global fitting. Colored diamonds indicate computed data points from ^{14}C-dated subjects. Error bars in (A) are calculated from the errors on ^{14}C measurements. Error bars in all other graphs are calculated for each subject individually and show the interval of possible values fitted with the respective mathematical scenario.

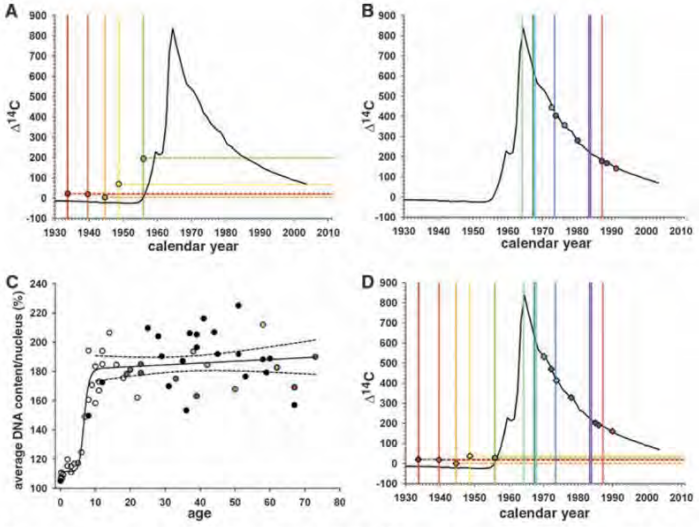

Fig. 3. Cardiomyocyte turnover in adulthood. (**A**) The ^{14}C concentrations in cardiomyocyte DNA from individuals born before the time of the atmospheric radiocarbon increase correspond to time points after the birth of all individuals. The vertical bar indicates year of birth, with the correspondingly colored data point indicating the Δ^{14}C value. (**B**) ^{14}C concentrations in cardiomyocyte DNA from individuals born after the time of the nuclear bomb test. (**C**) Average DNA content ($2n$ = 100%) per cardiomyocyte nucleus from individuals (without severe heart enlargement; see fig. S5) of different ages. Ploidy was measured by flow cytometry. Colored data points identify individuals analyzed for ^{14}C (n = 13). Black data points are from individuals analyzed only with regard to ploidy level (n = 23), and white data points are taken from Adler *et al.* (n = 26) (*24*, *26*). The dashed lines indicate the 95% confidence interval for the regression curve. (**D**) ^{14}C values corrected for the physiologically occurring polyploidization of cardiomyocytes during childhood for individuals born before and after the bomb-induced spike in ^{14}C concentrations, calculated on the basis of the individual average DNA content per cardiomyocyte nucleus. The ^{14}C content is not affected in individuals where the polyploidization occurred before the increase in atmospheric ^{14}C concentrations.

A considerable amount of cardiomyocyte division was shown in the failing and infarcted human myocardium (mitotic index of 0.015% and 0.08%, respectively)

The New England Journal of Medicine

EVIDENCE THAT HUMAN CARDIAC MYOCYTES DIVIDE AFTER MYOCARDIAL INFARCTION

ANTONIO P. BELTRAMI, M.D., KONRAD URBANEK, M.D., JAN KAJSTURA, PH.D., SHAO-MIN YAN, M.D., NICOLETTA FINATO, M.D., ROSSANA BUSSANI, M.D., BERNARDO NADAL-GINARD, M.D., PH.D., FURIO SILVESTRI, M.D., ANNAROSA LERI, M.D., C. ALBERTO BELTRAMI, M.D., AND PIERO ANVERSA, M.D.

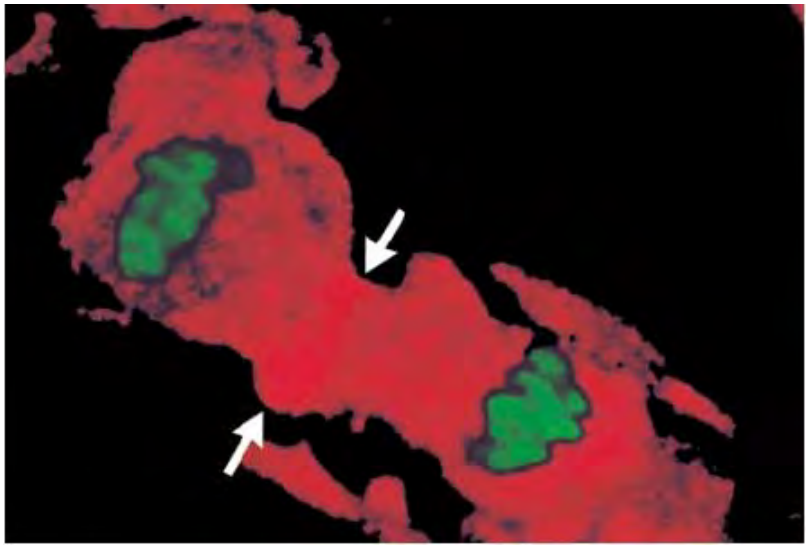

NEJM, 2001

When does cardiomyocyte proliferation stop?

Proliferating neonatal cardiomyocytes express Notch1

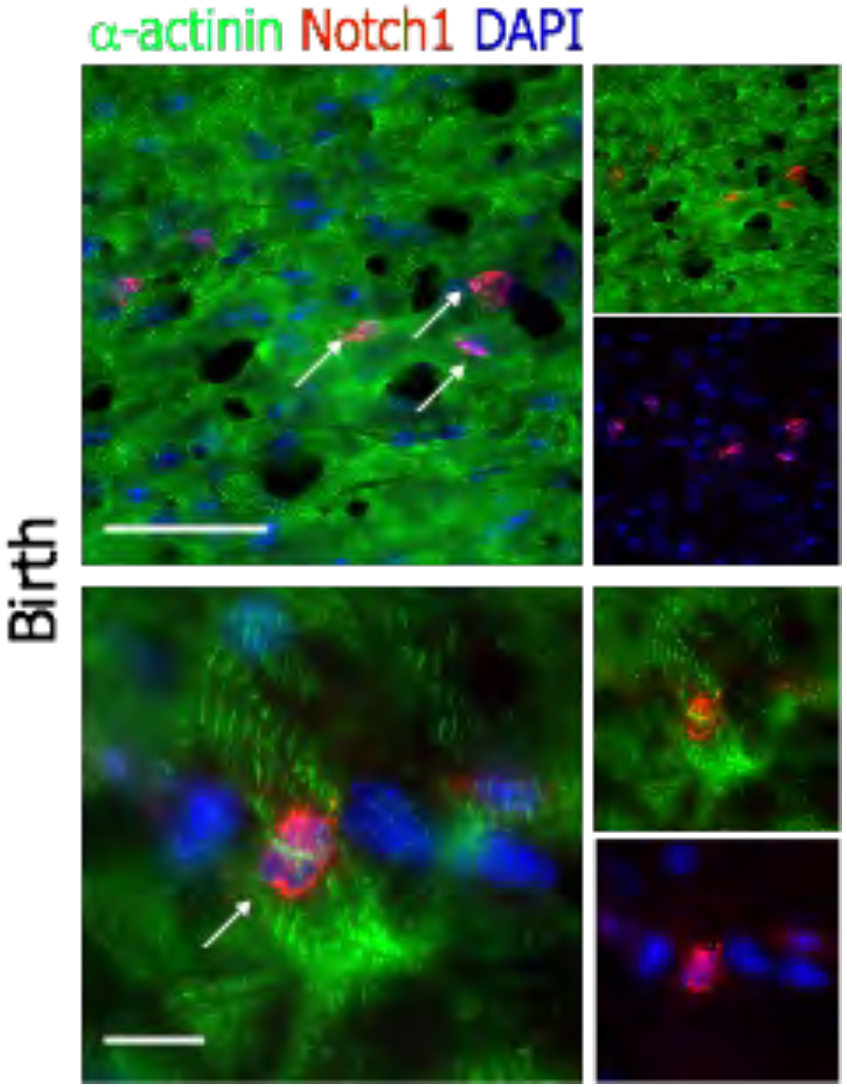

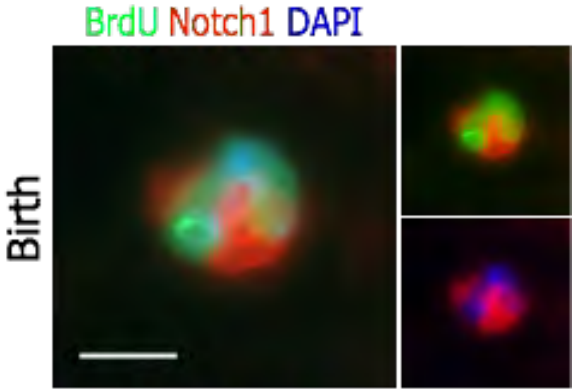

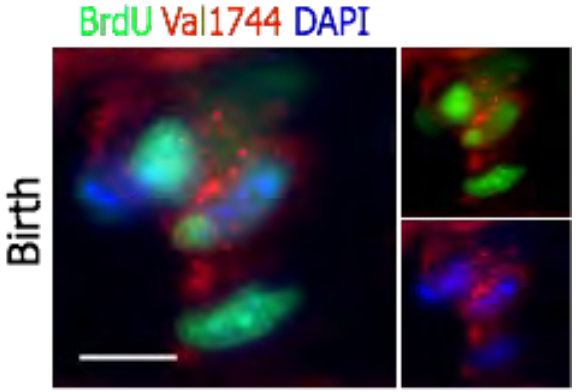

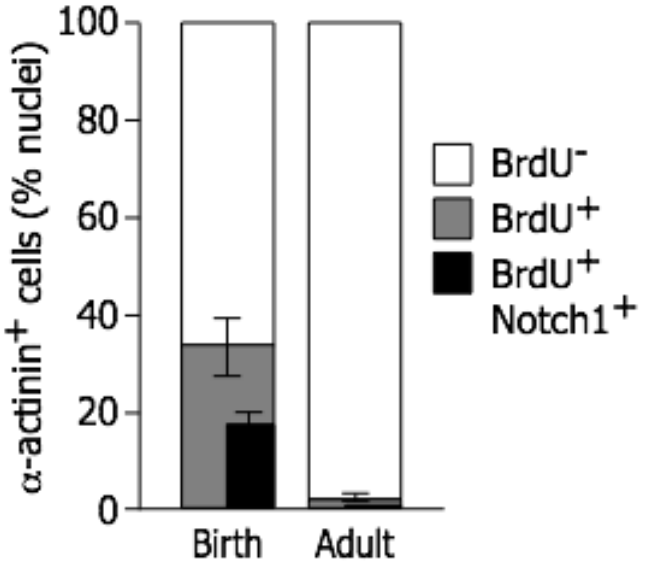

Proliferative potential of neonatal cardiomyocytes is rapidly lost in culture

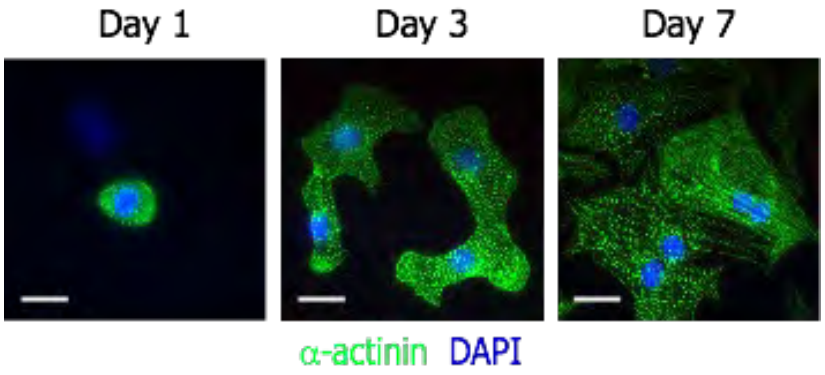

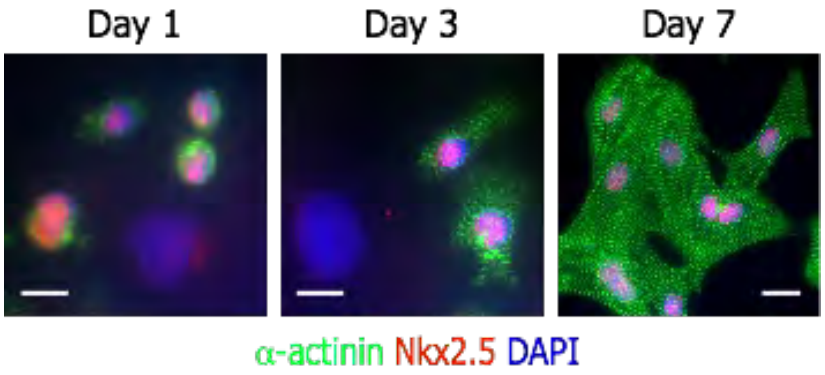

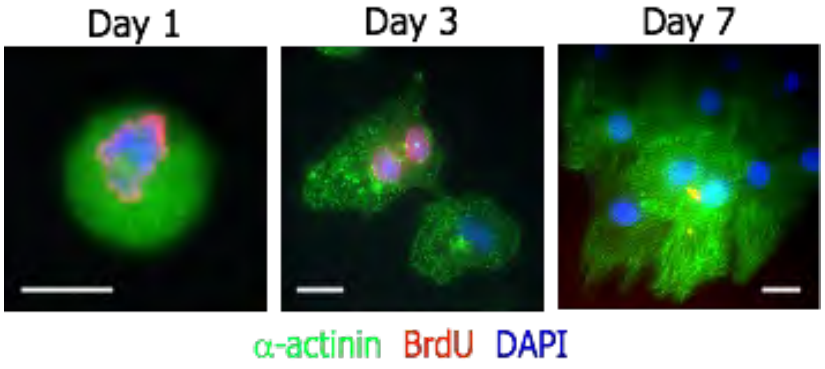

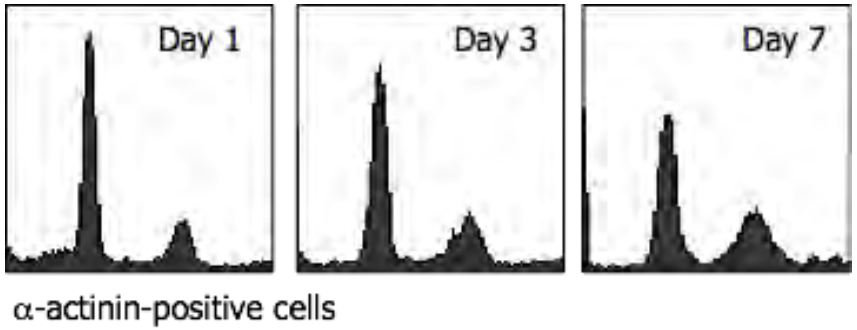

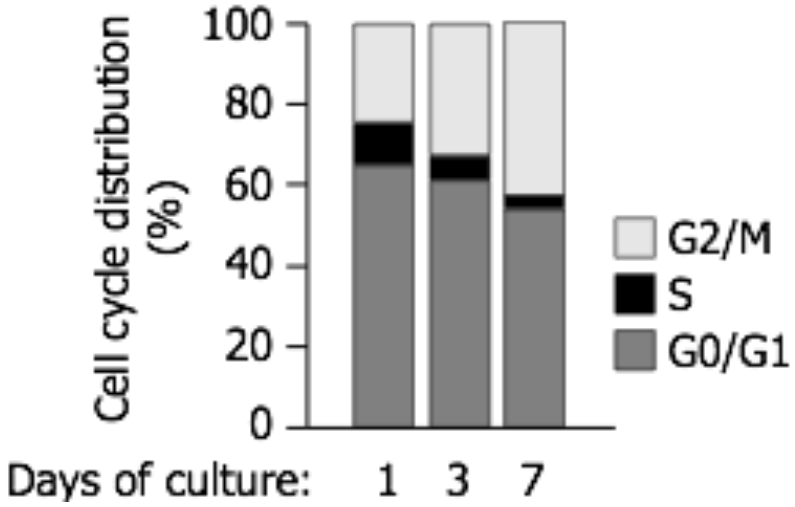

Loss of cardiomyocyte replicative potential correlates with loss of Notch1

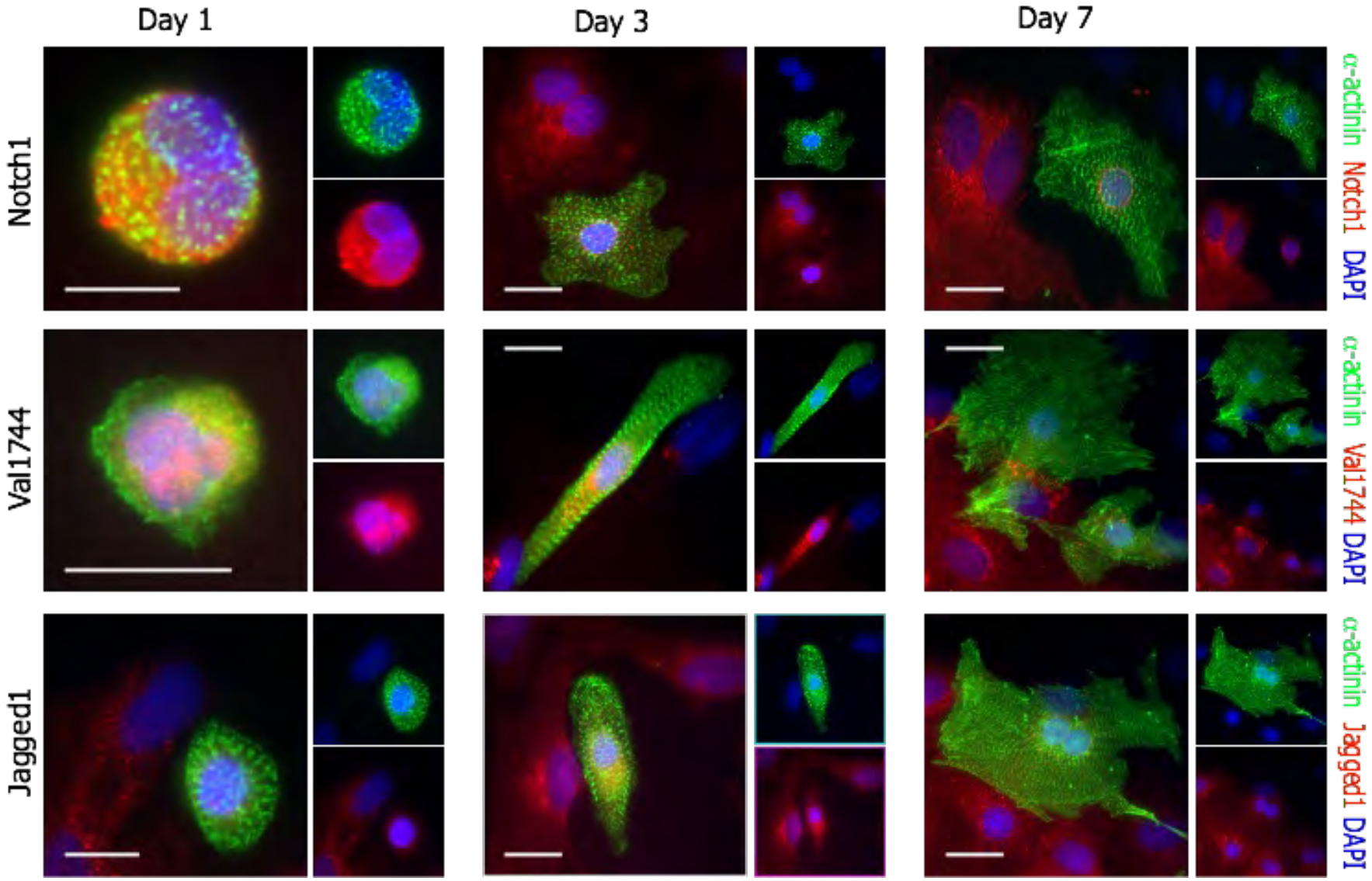

Published September 29, 2008

JCB: ARTICLE

Notch1 signaling stimulates proliferation of immature cardiomyocytes

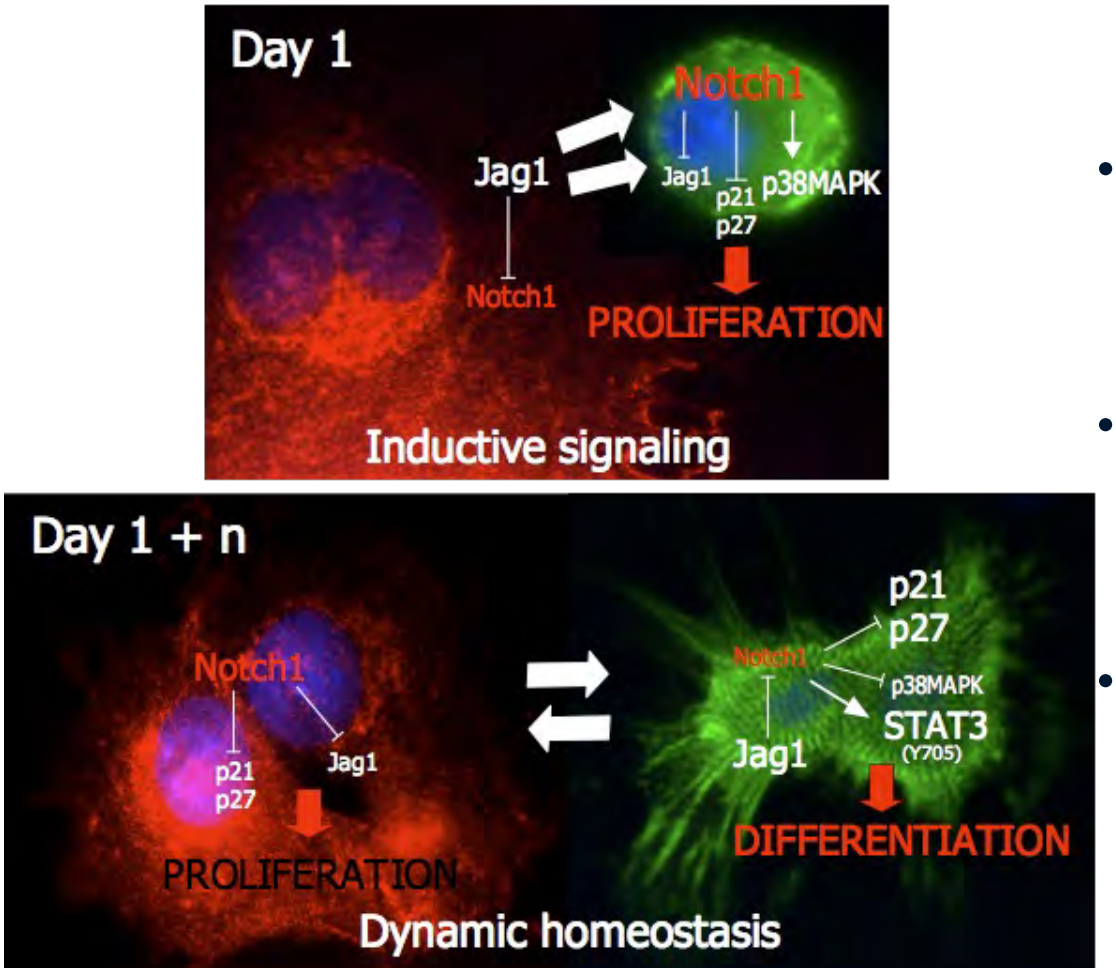

- Loss of cardiomyocyte proliferation after birth in vivo parallels loss of Notch signaling
- Neonatal cardiomyocyte proliferation in vitro requires activated Notch ICD
- Cardiomyocyte proliferation in vitro can be stimulated by Notch pathway stimulation
- In vivo, AAV9-N1ICD transduction induces the infiltration of the myocardium with BrdU+, proliferating cells.

Published October 6, 2008

Notch activates cell cycle reentry and progression in quiescent cardiomyocytes

Víctor M. Campa, Raquel Gutiérrez-Lanza, Fabio Cerignoli, Ramón Díaz-Trelles, Brandon Nelson, Toshiya Tsuji, Maria Barcova, Wei Jiang, and Mark Mercola

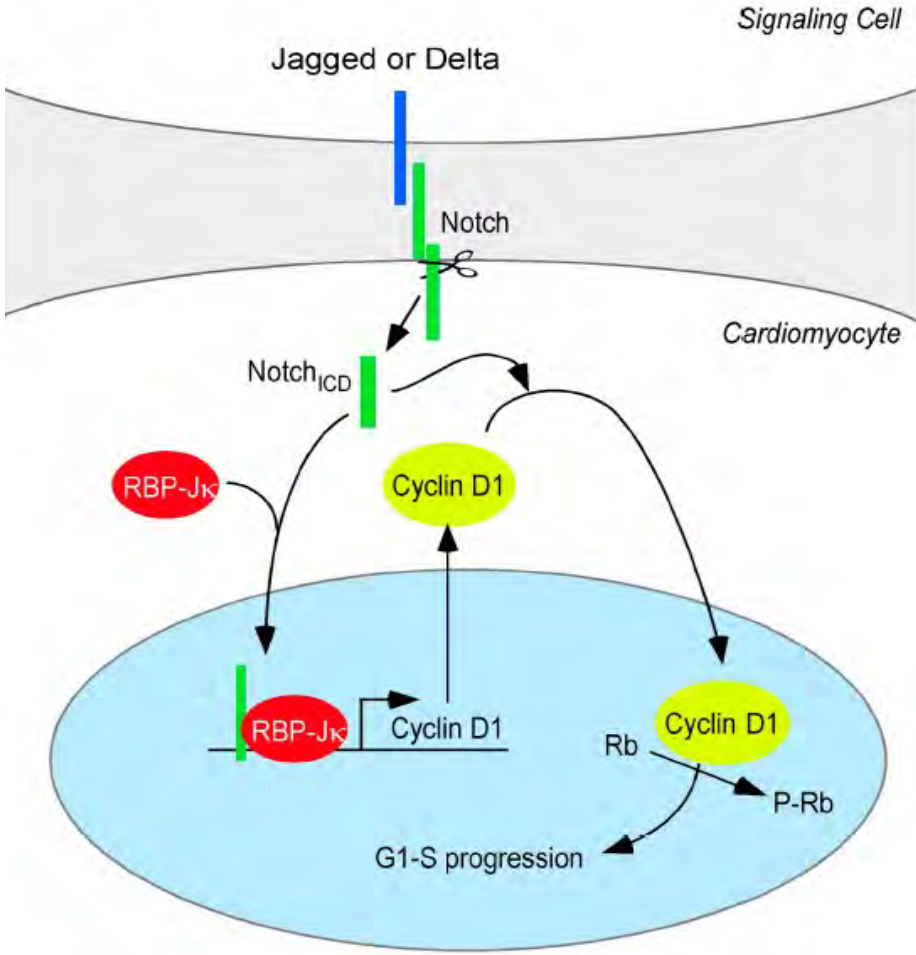

Figure 9. **Summary of Notch2-induced cell cycle entry.** RBP-Jκ–dependent transcription leads to accumulation of cyclin D1 in the cytosol. Notch ICD regulates entry into the cell cycle by controlling nuclear localization of cyclin D1 independently of RBP-Jκ.

What about adult cardiomyocytes?

Loss of cardiomyocyte proliferative potential correlates with downregulation of Notch1 and its target genes

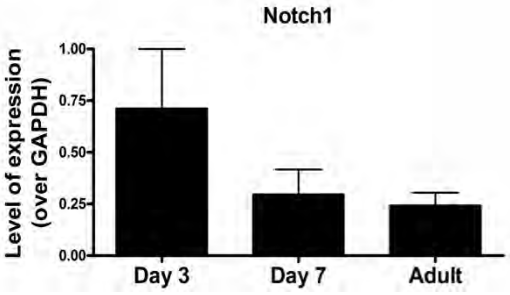

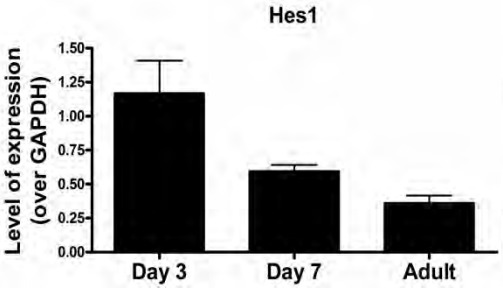

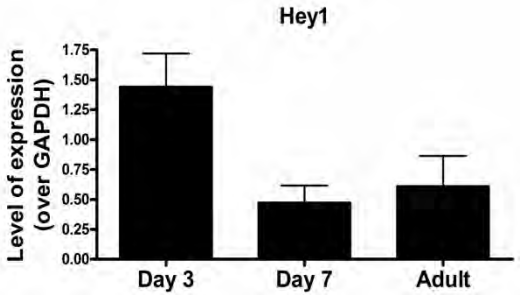

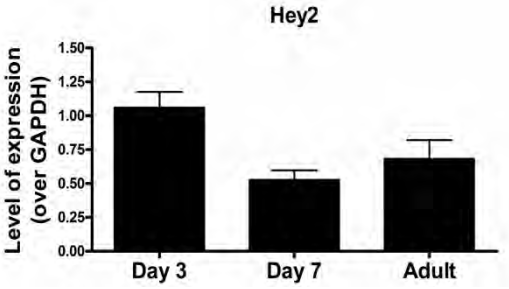

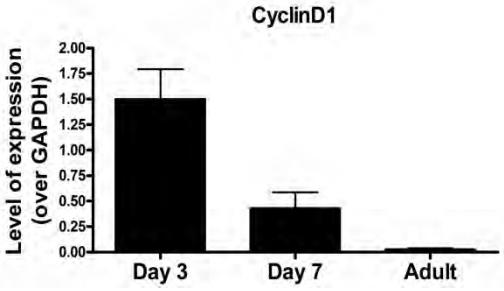

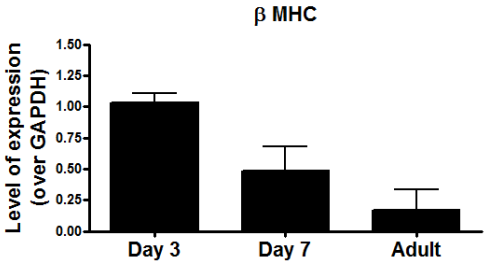

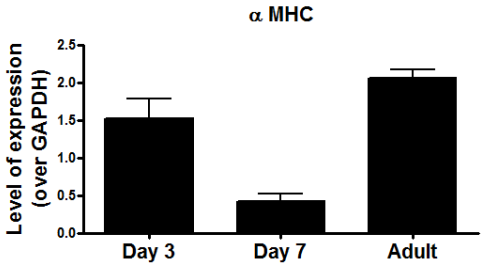

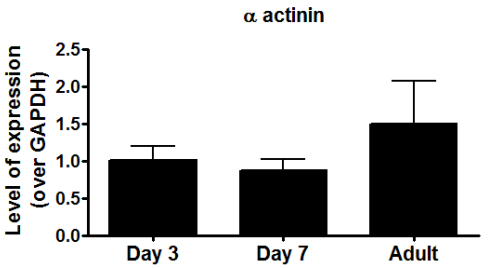

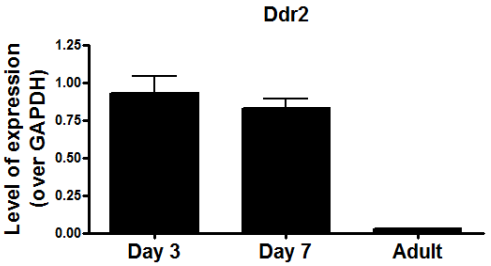

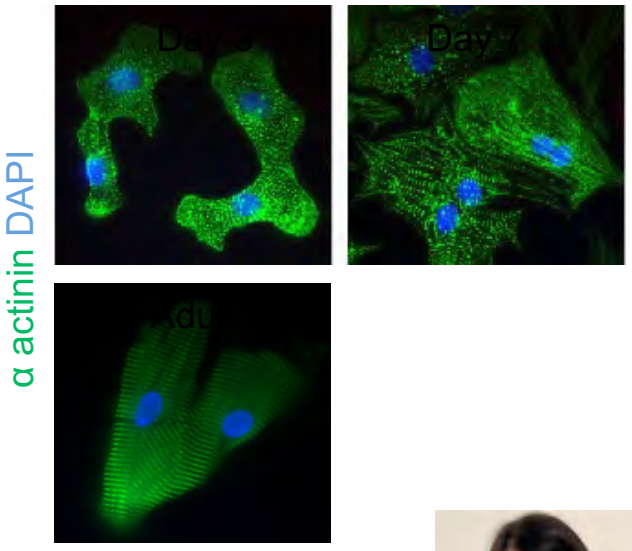

Giulia Felician

Methylation of promoters of Notch target genes impairs AAV9-sJagged1 and AAV9-N1ICD effect

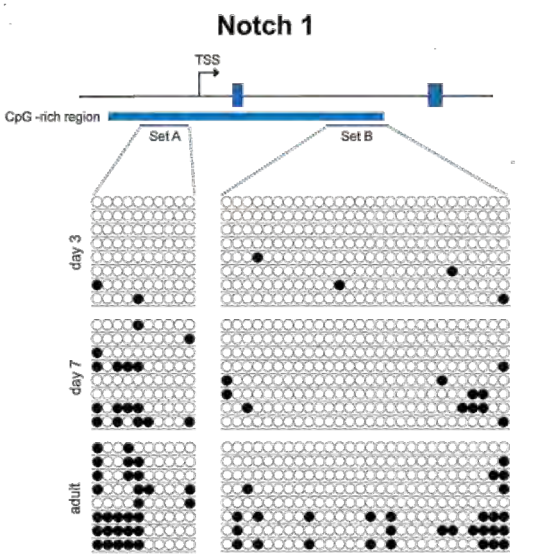

	day 3	day 7	adult
Set A	2/80 (2.5%)	16/80 (20.0%)	29/80 (36.2%)
Set B	4/224 (1.8%)	11/224 (4.9%)	29/224 (12.9%)

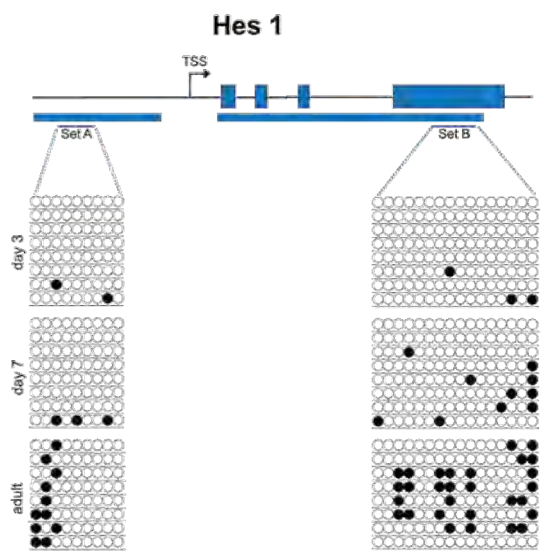

	day 3	day 7	adult
Set A	2/72 (2.7%)	3/72 (4.2%)	11/72 (15.3%)
Set B	3/128 (2.3%)	11/128 (8.6%)	29/128 (22.7%)

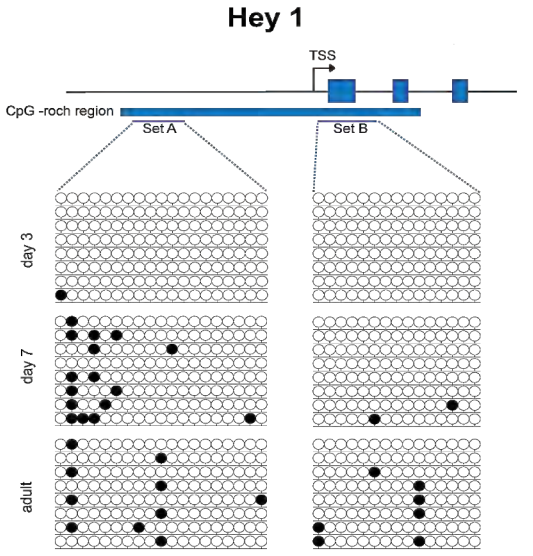

	day 3	day 7	adult
Set A	1/152 (0.6%)	16/152 (10.5%)	10/152 (6.6%)
Set B	0/120 (0%)	2/120 (1.7%)	7/120 (5.8%)

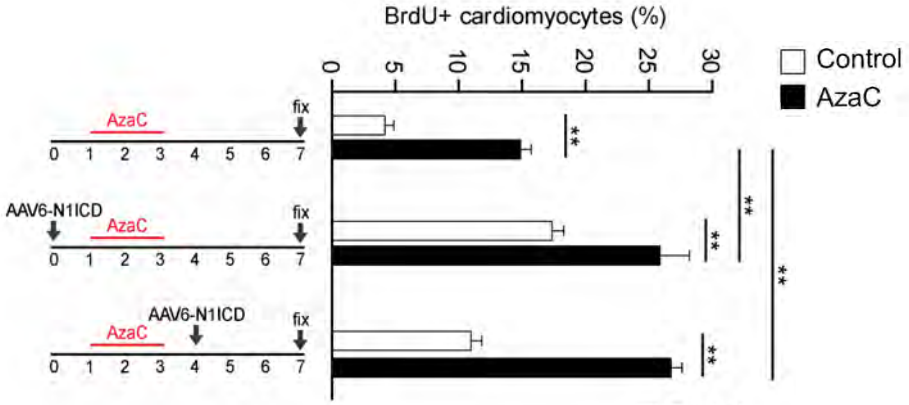

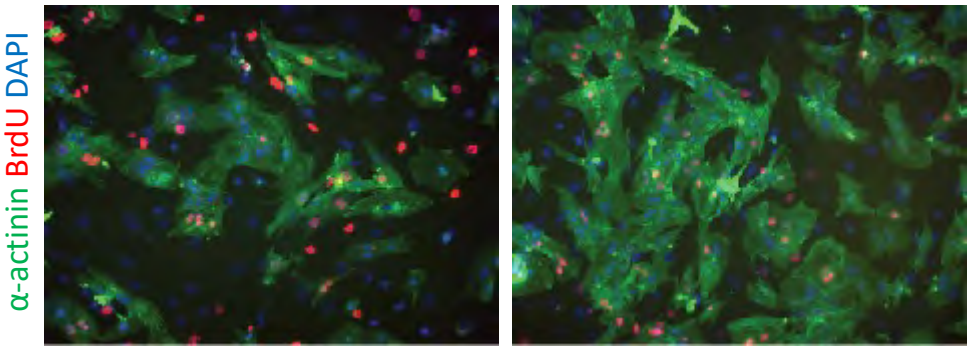

Felician G. et al., Circ. Res., 2014

Cardiac resident stem cells?

Cardiac stem cells (CSCs): do they exist?

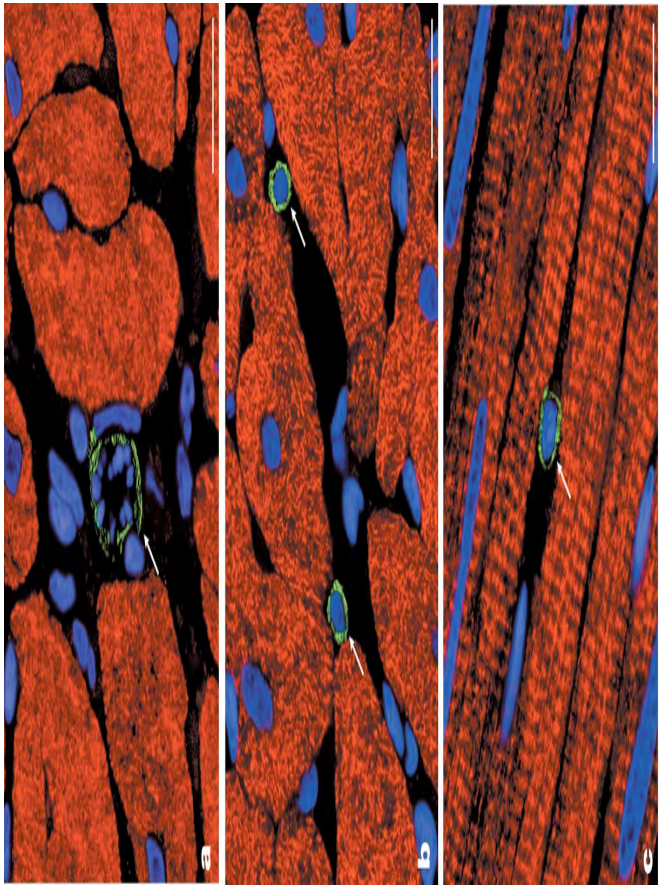

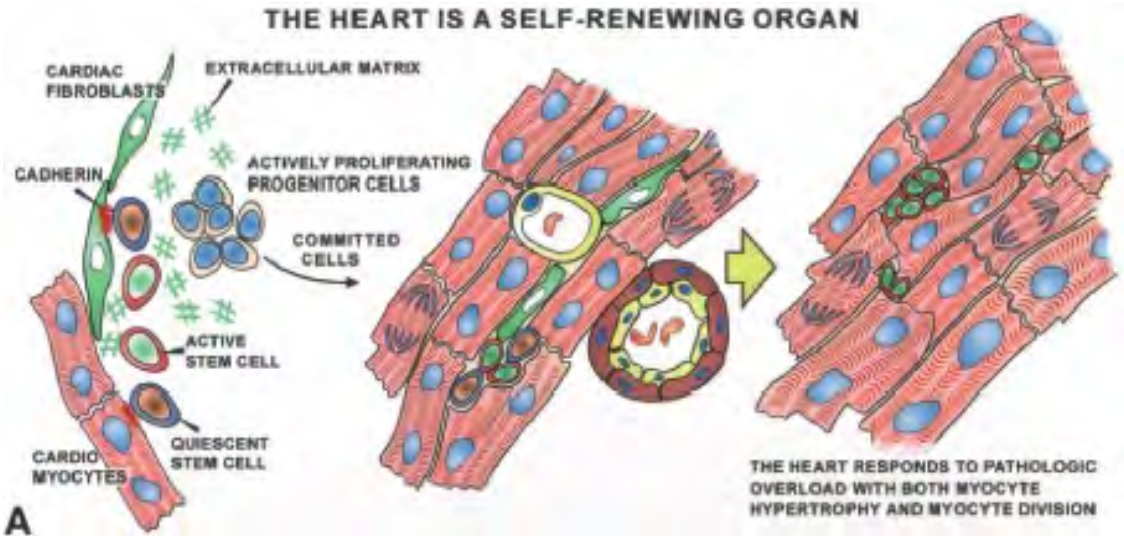

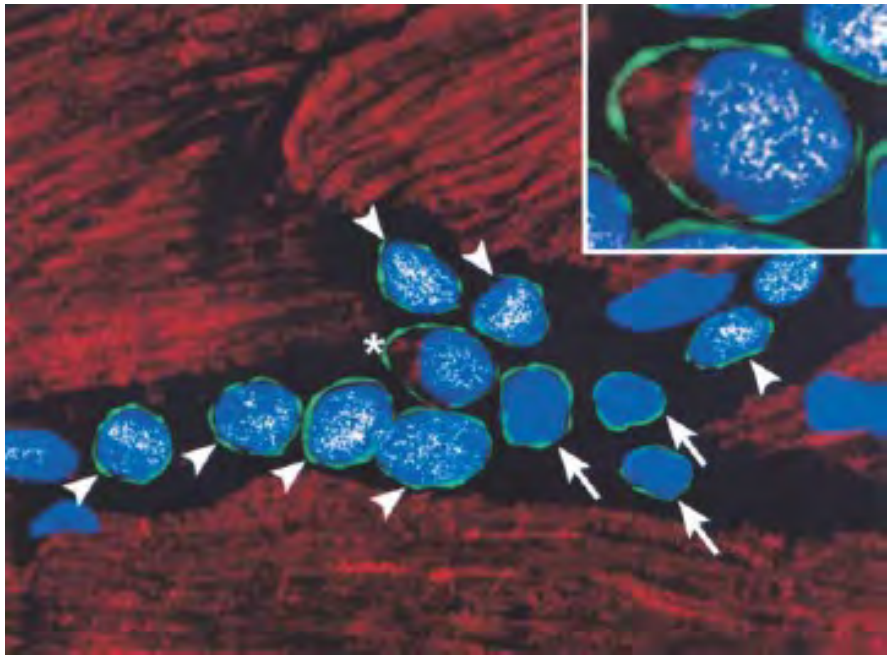

Adult cardiac stem cells are multipotent and support myocardial regeneration.
Beltrami AP, Barlucchi L, Torella D, Baker M, Limana F, Chimenti S, Kasahara H, Rota M, Musso E, Urbanek K, Leri A, Kajstura J, Nadal-Ginard B, Anversa P.

Life and Death of Cardiac Stem Cells

A Paradigm Shift in Cardiac Biology

Piero Anversa, MD; Jan Kajstura, PhD; Annarosa Leri, MD; Roberto Bolli, MD

Circulation March 21, 2006

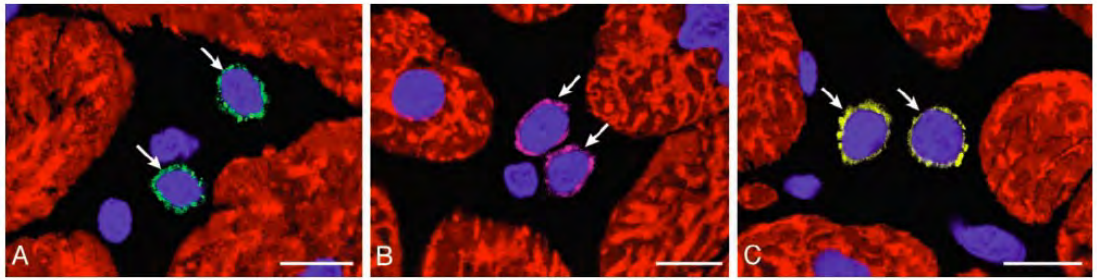

Fig. 1. Putative cardiac stem cells. Shown are detection of c-kit (*A*, green), MDR1 (*B*, purple), and Sca-1-reactive protein (*C*, yellow) in primitive cells (arrows) of hypertrophied hearts. Nuclei are stained by propidium iodide (PI; blue) and myocytes by cardiac myosin (red). (Bars = 10 μm.)

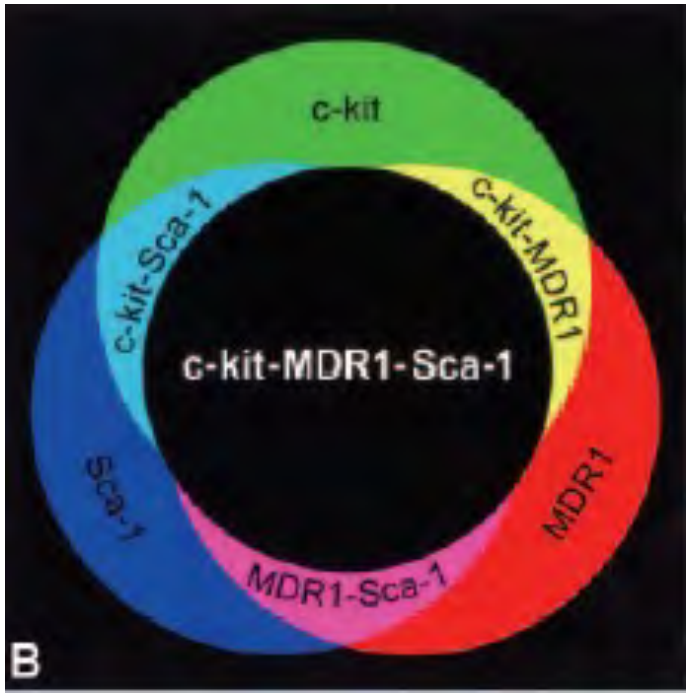

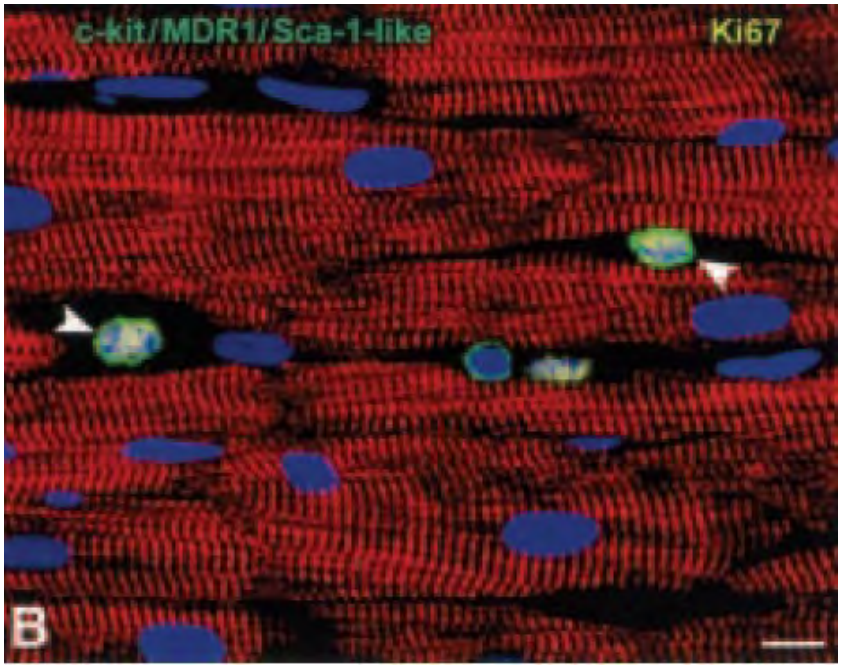

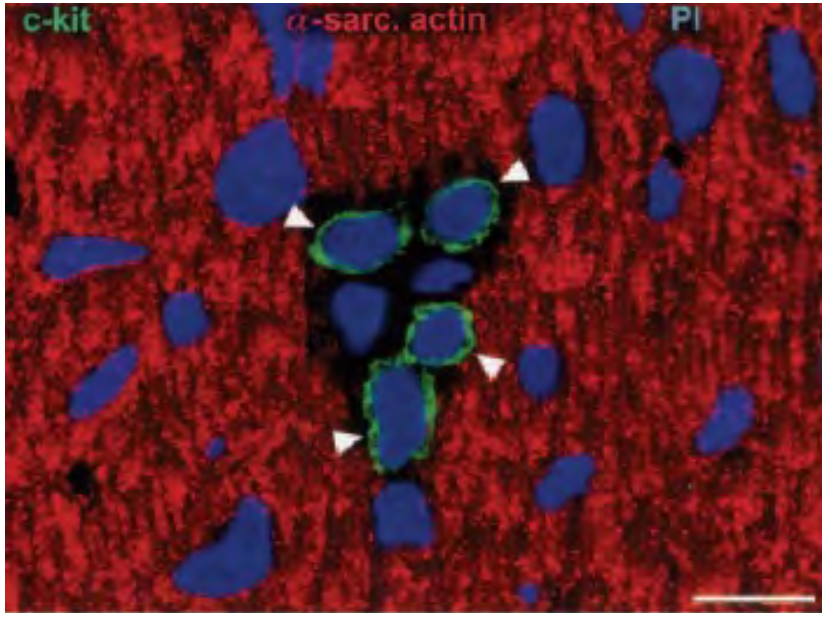

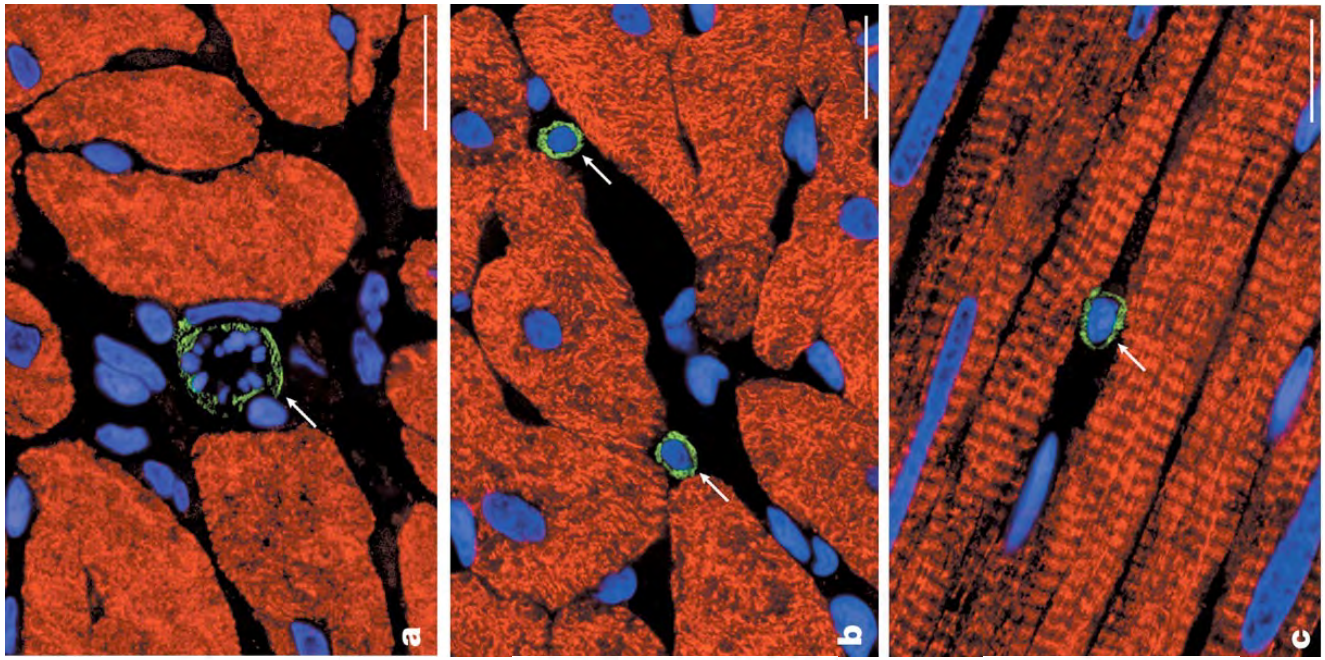

c-*kit*

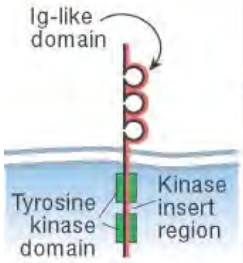

Distribution

- Melanocytes
- Mast cells
- Germ cells
- Stem cells

Functions

- Proliferation
- Migration
- Differentiation
- Secretion

P-glycoprotein or MRD1

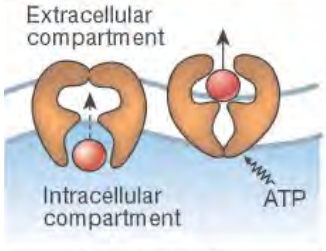

Distribution

- Hepatocytes–cholangiocytes
- Brush border cells
- Renal tubular cells
- Endothelial cells (brain)
- Cancer cells
- Stem cells

Functions

- Transmembrane efflux pump
- Inhibition of apoptosis

Sca-1

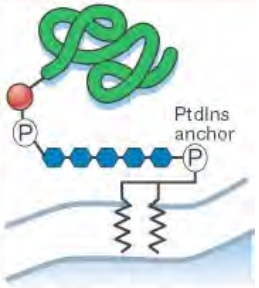

Distribution

- Vessel wall
- Kidney cortical tubules
- Thymus, spleen
- T lymphocytes
- Stem cells

Functions

- Cell adhesion
- Cell signalling
- T-cell activation

Cardiac stem cells delivered intravascularly traverse the vessel barrier, regenerate infarcted myocardium, and improve cardiac function

Buddhadeb Dawn*, Adam B. Stein*, Konrad Urbanek†, Marcello Rota†, Brian Whang†, Raffaella Rastaldo†, Daniele Torella†, Xian-Liang Tang*, Arash Rezazadeh*, Jan Kajstura†, Annarosa Leri†, Greg Hunt*, Jai Varma*, Sumanth D. Prabhu*, Piero Anversa†, and Roberto Bolli*‡

GFP-labeled CSCs delivered to the coronary arteries 4 hr after ischemia-reperfusion

Ventricular function monitored by echocardiography

Myocardial regeneration by histology

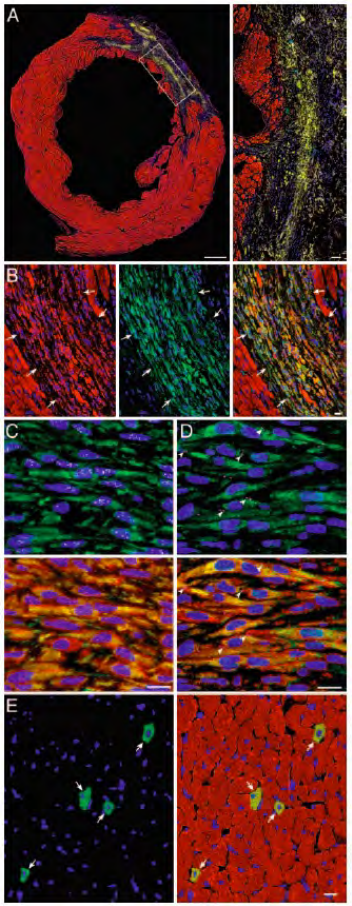

3766–3771 | PNAS | March 8, 2005 | vol. 102 | no. 10

Adult cardiac stem cells are multipotent and support myocardial regeneration.

Beltrami AP, Barlucchi L, Torella D, Baker M, Limana F, Chimenti S, Kasahara H, Rota M, Musso E, Urbanek K, Leri A, Kajstura J, Nadal-Ginard B, Anversa P.

Cardiovascular Research Institute, Department of Medicine, New York Medical College, Valhalla, NY 10595, USA

The notion of the adult heart as terminally differentiated organ without self-renewal potential has been undermined by the existence of a subpopulation of replicating myocytes in normal and pathological states. The origin and significance of these cells has remained obscure for lack of a proper biological context. We report the existence of Lin(-) c-kit(POS) cells with the properties of cardiac stem cells. They are self-renewing, clonogenic, and multipotent, giving rise to myocytes, smooth muscle, and endothelial cells. When injected into an ischemic heart, these cells or their clonal progeny reconstitute well-differentiated myocardium, formed by blood-carrying new vessels and myocytes with the characteristics of young cells, encompassing approximately 70% of the ventricle. Thus, the adult heart, like the brain, is mainly composed of terminally differentiated cells, but is not a terminally differentiated organ because it contains stem cells supporting its regeneration. The existence of these cells opens new opportunities for myocardial repair.

Cell, 2003 Sep 19

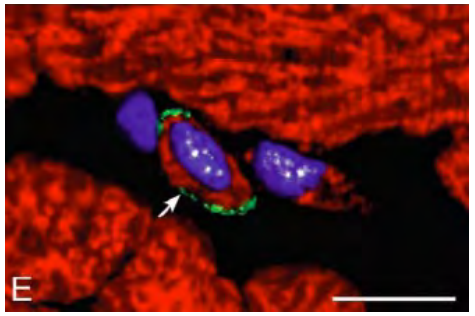

Red: MHC
Green: c-kit
White: MEF2
Blue: DAPI

Intense myocyte formation from cardiac stem cells in human cardiac hypertrophy

Konrad Urbanek*, Federico Quaini*, Giordano Tasca†, Daniele Torella*, Clotilde Castaldo*, Bernardo Nadal-Ginard*, Annarosa Leri*, Jan Kajstura*, Eugenio Quaini‡, and Piero Anversa*§

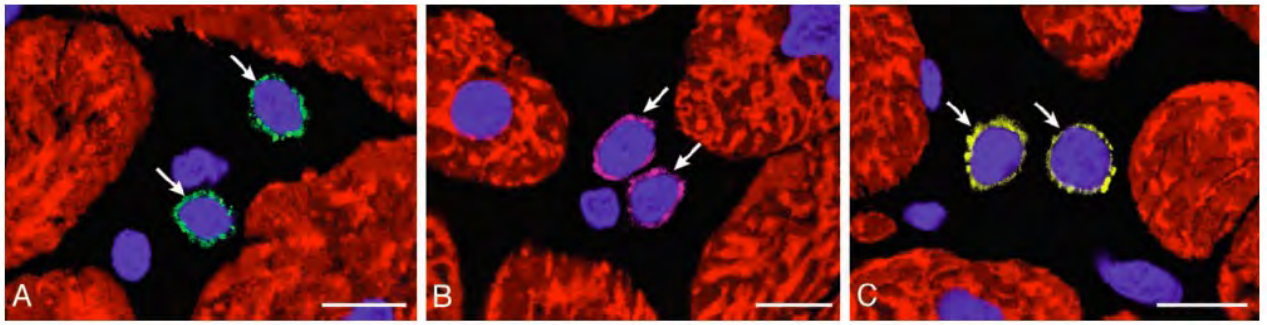

Fig. 1. Putative cardiac stem cells. Shown are detection of c-kit (*A*, green), MDR1 (*B*, purple), and Sca-1-reactive protein (*C*, yellow) in primitive cells (arrows) of hypertrophied hearts. Nuclei are stained by propidium iodide (PI; blue) and myocytes by cardiac myosin (red). (Bars = 10 μm.)

Resident cardiac stem cells

c-Kit+ cells (Anversa)
Sca-1 cells (Schneider)
Side population cells (Liao)
Islet-1 cells (Chien)
Cardiosphere-forming cells (Messina/Marban)
SSea-4+ cells (Taylor)

One of the least regenerative organ in the body has multiple non-overlapping populations of cardiomyocyte progenitors??

Cardiac stem cells in patients with ischaemic cardiomyopathy (SCIPIO): initial results of a randomised phase 1 trial

Roberto Bolli, Atul R Chugh, Domenico D'Amario, John H Loughran, Marcus F Stoddard, Sohail Ikram, Garth M Beache, Stephen G Wagner, Annarosa Leri, Toru Hosoda, Fumihiro Sanada, Julius B Elmore, Polina Goichberg, Donato Cappetta, Naresh K Solankhi, Ibrahim Fahsah, D Gregg Rokosh, Mark S Slaughter, Jan Kajstura, Piero Anversa

Summary

Background c-kit-positive, lineage-negative cardiac stem cells (CSCs) improve post-infarction left ventricular (LV) dysfunction when administered to animals. We undertook a phase 1 trial (Stem Cell Infusion in Patients with Ischemic cardiOmyopathy [SCIPIO]) of autologous CSCs for the treatment of heart failure resulting from ischaemic heart disease.

Methods In stage A of the SCIPIO trial, patients with post-infarction LV dysfunction (ejection fraction [EF] ≤40%) before coronary artery bypass grafting were consecutively enrolled in the treatment and control groups. In stage B, patients were randomly assigned to the treatment or control group in a 2:3 ratio by use of a computer-generated block randomisation scheme. 1 million autologous CSCs were administered by intracoronary infusion at a mean of 113 days (SE 4) after surgery; controls were not given any treatment. Although the study was open label, the echocardiographic analyses were masked to group assignment. The primary endpoint was short-term safety of CSCs and the secondary endpoint was efficacy. A per-protocol analysis was used. This study is registered with ClinicalTrials.gov, number NCT00474461.

Findings This study is still in progress. 16 patients were assigned to the treatment group and seven to the control group; no CSC-related adverse effects were reported. In 14 CSC-treated patients who were analysed, LVEF increased from 30·3% (SE 1·9) before CSC infusion to 38·5% (2·8) at 4 months after infusion (p=0·001). By contrast, in seven control patients, during the corresponding time interval, LVEF did not change (30·1% [2·4] at 4 months after CABG *vs* 30·2% [2·5] at 8 months after CABG). Importantly, the salubrious effects of CSCs were even more pronounced at 1 year in eight patients (eg, LVEF increased by 12·3 ejection fraction units [2·1] *vs* baseline, p=0·0007). In the seven treated patients in whom cardiac MRI could be done, infarct size decreased from 32·6 g (6·3) by 7·8 g (1·7; 24%) at 4 months (p=0·004) and 9·8 g (3·5; 30%) at 1 year (p=0·04).

Interpretation These initial results in patients are very encouraging. They suggest that intracoronary infusion of autologous CSCs is effective in improving LV systolic function and reducing infarct size in patients with heart failure after myocardial infarction, and warrant further, larger, phase 2 studies.

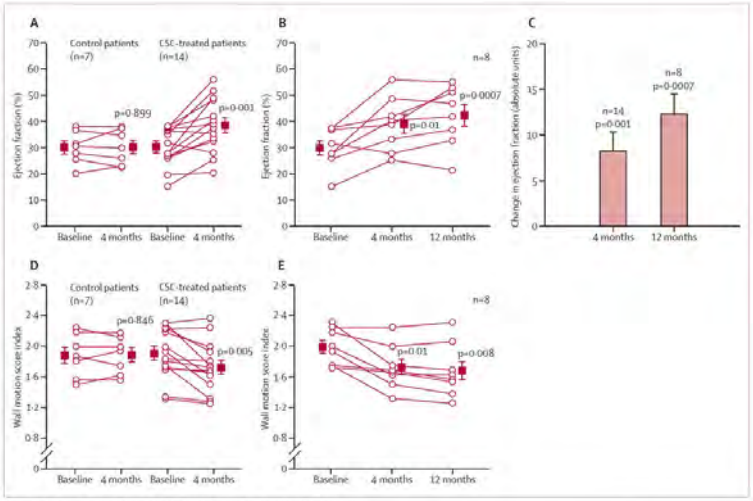

Figure 4: Echocardiographic analysis of CSC-treated patients and controls
(A) Left ventricular ejection fraction (measured by use of three-dimensional echocardiography) at 4 months after baseline in control and CSC-treated patients. (B) Ejection fraction at 4 months and 12 months after baseline in the CSC-treated patients who had 1 year of follow-up. (C) Change in ejection fraction from baseline at 4 months and 12 months in CSC-treated patients. (D) Wall motion score index at 4 months after baseline in control and CSC-treated patients. (E) Wall motion score index at 4 months and 12 months after baseline in the CSC-treated patients who had 1 year of follow-up. Boxes represent the mean values and error bars represent SE. p values are reported for difference between baseline and 4 months and between baseline and 12 months. CSC=cardiac stem cell.

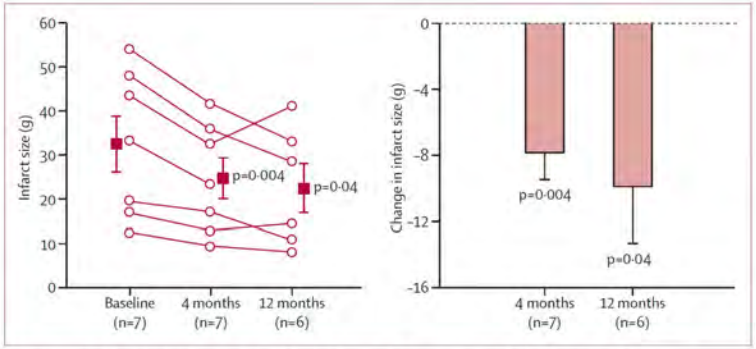

Figure 5: **Infarct size and change in infarct size at 4 months and 12 months after baseline in patients administered cardiac stem cells**
p values are reported for difference between baseline and 4 months and between baseline and 12 months. Boxes and bars represent the mean values and error bars represent the SE.

Cardiospheres

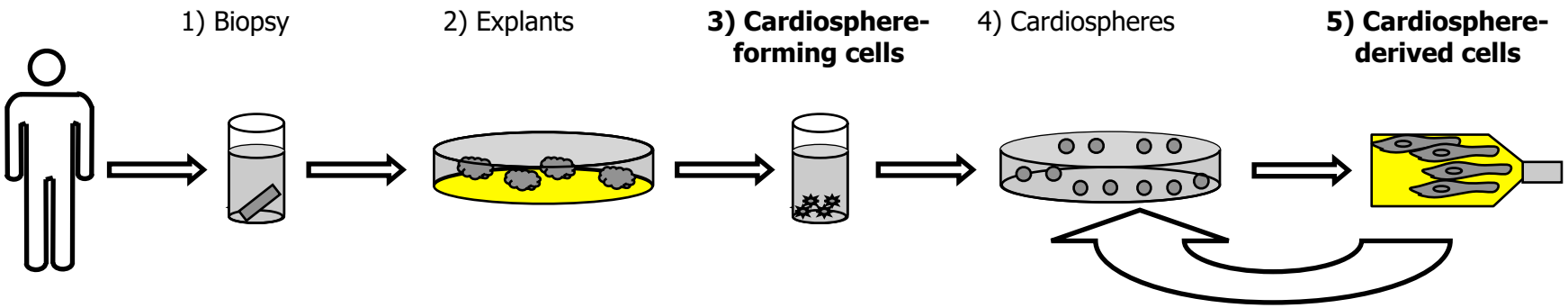

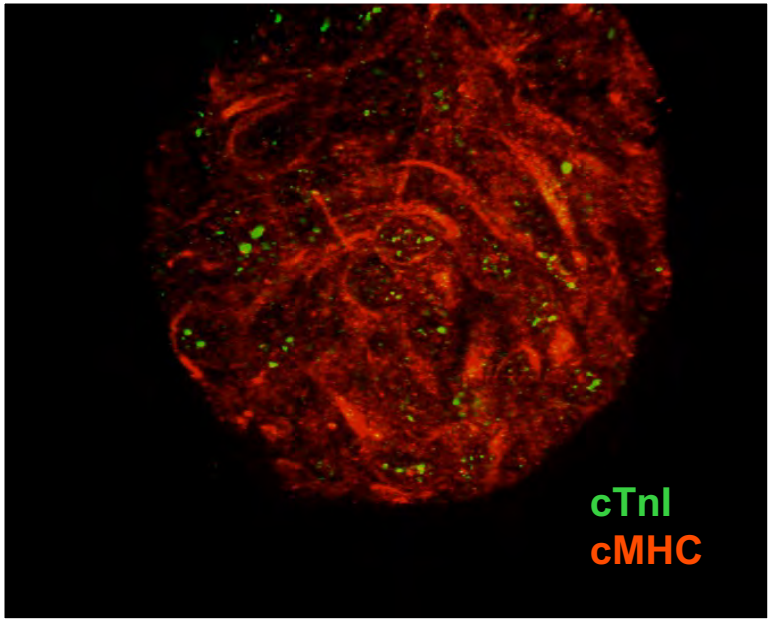

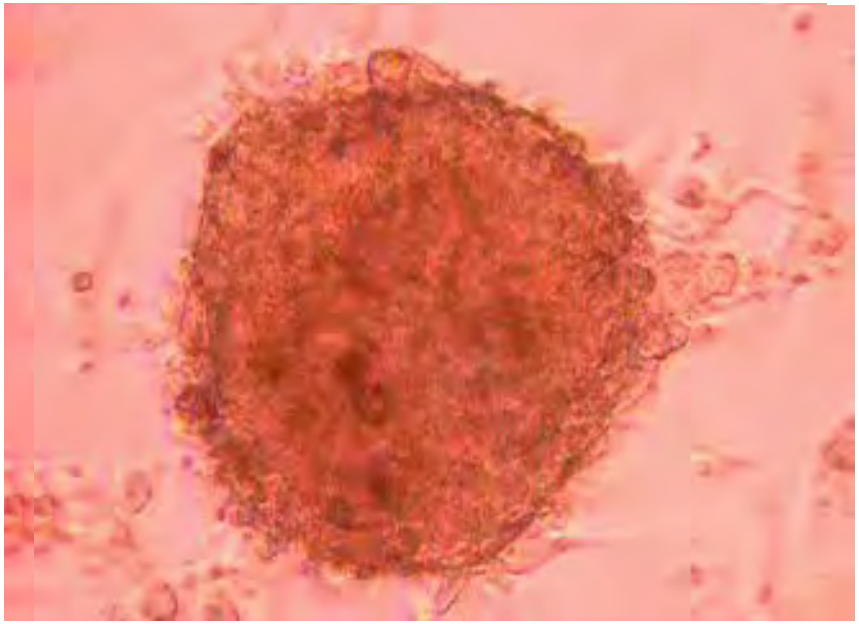

Isolation and Expansion of Adult Cardiac Stem Cells From Human and Murine Heart

Elisa Messina, Luciana De Angelis, Giacomo Frati, Stefania Morrone, Stefano Chimenti, Fabio Fiordaliso, Monica Salio, Massimo Battaglia, Michael V.G. Latronico, Marcello Coletta, Elisabetta Vivarelli, Luigi Frati, Giulio Cossu, Alessandro Giacomello

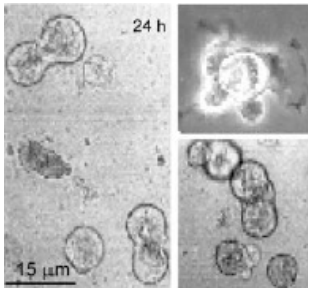

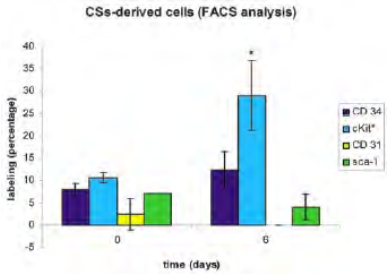

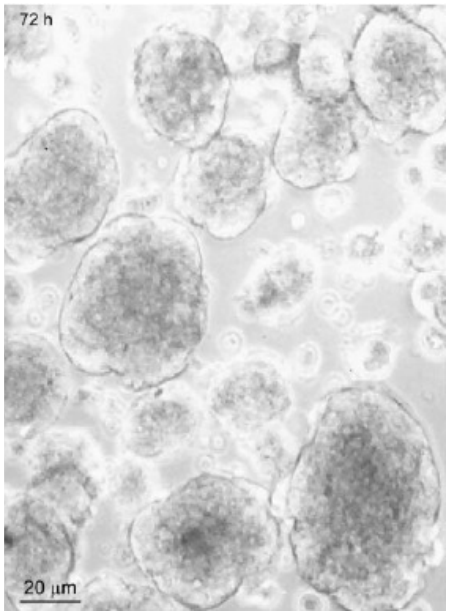

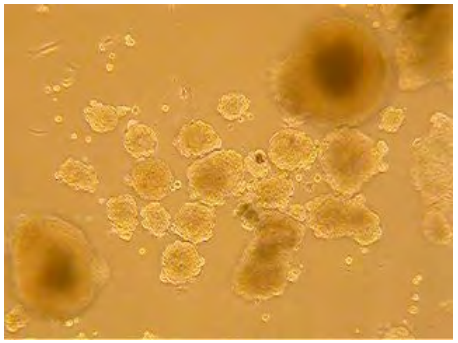

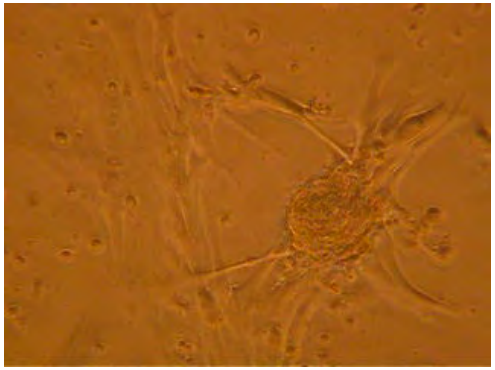

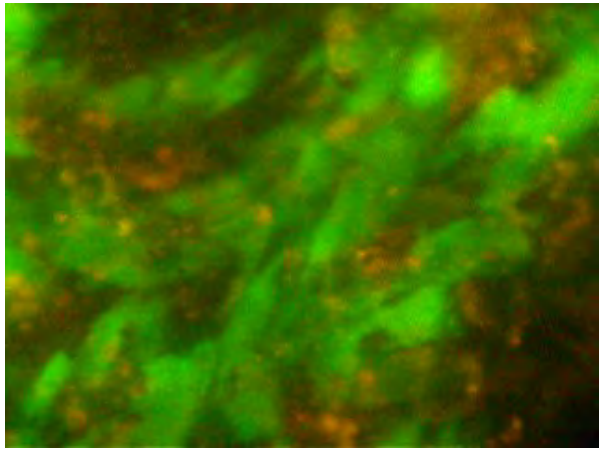

Mild enzymatic digestion
EDTA and mild trypsinization
Low serum, serum substitute B27, EGF, bFGF, cardiotrophin-1, **thrombin** (7-fold increase in the number of spheres)

PNAS | October 7, 2008 | vol. 105 | no. 40 | 15529–15534

Notch1 regulates the fate of cardiac progenitor cells

Alessandro Boni*†, Konrad Urbanek*†, Angelo Nascimbene*†, Toru Hosoda†, Hanqiao Zheng†, Francesca Delucchi†, Katsuya Amano†, Arantxa Gonzalez†, Serena Vitale†, Caroline Ojaimi‡, Roberto Rizzi†, Roberto Bolli§, Katherine E. Yutzey¶, Marcello Rota†, Jan Kajstura†, Piero Anversa†, and Annarosa Leri†‖

†Departments of Anesthesia and Medicine and Division of Cardiology, Brigham and Women's Hospital, Harvard Medical School, Boston, MA 02115; ‡Department of Physiology, New York Medical College, Valhalla, NY 10595; §Institute of Molecular Cardiology, University of Louisville, Louisville, KY 40292; and ¶Divison of Molecular Cardiovascular Biology, Children's Medical Center, Cincinnati, OH 45229

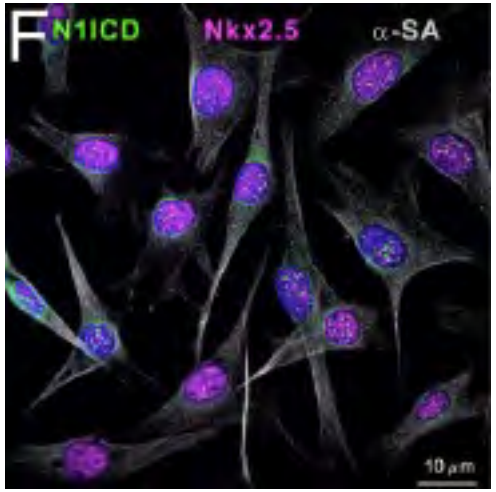

- Cardiac progenitor cells (CPCs) in the niches express Notch1 receptor, and the supporting cells exhibit the Notch ligand Jagged1.
- N1ICD and RBP-Jk form a protein complex, which in turn binds to the Nkx2.5 promoter initiating transcription and myocyte differentiation.

- Notch1 favors the early specification of CPCs to the myocyte phenotype but maintains the newly formed cells in a highly proliferative state.

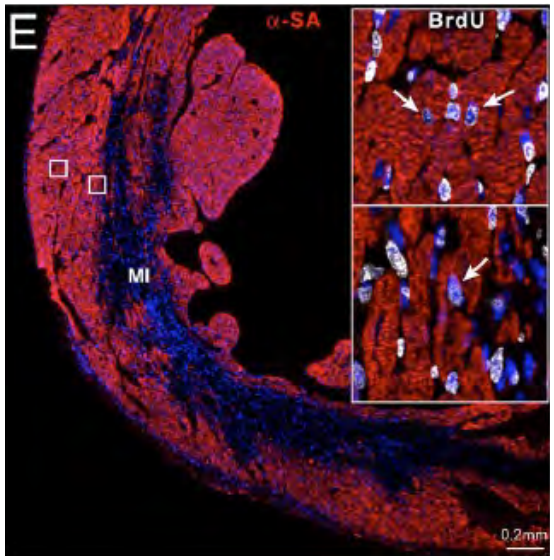

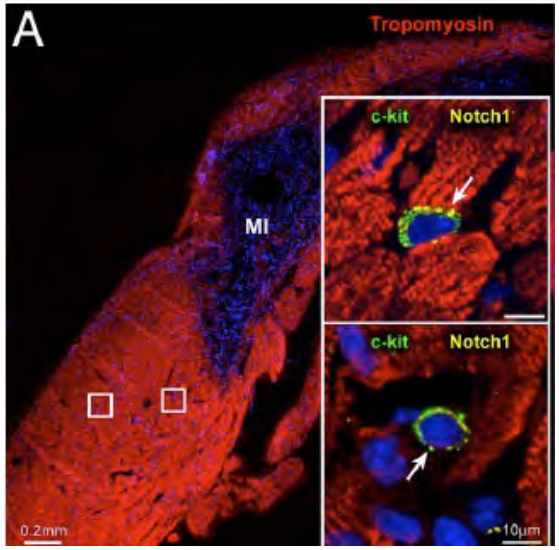

Screening for cardiomyocyte proliferation using a library of microRNA mimics

microRNA mimics
arrayed on 96-well plates
(988 mature sequences)

0h — add transfection reagent
add cardiomyocytes isolated from newborn rats

52h — add EdU

72h

cell fixation and fluorescence staining
(Hoechst, alpha-actinin, Ki-67 and EdU)

Ana Eulalio

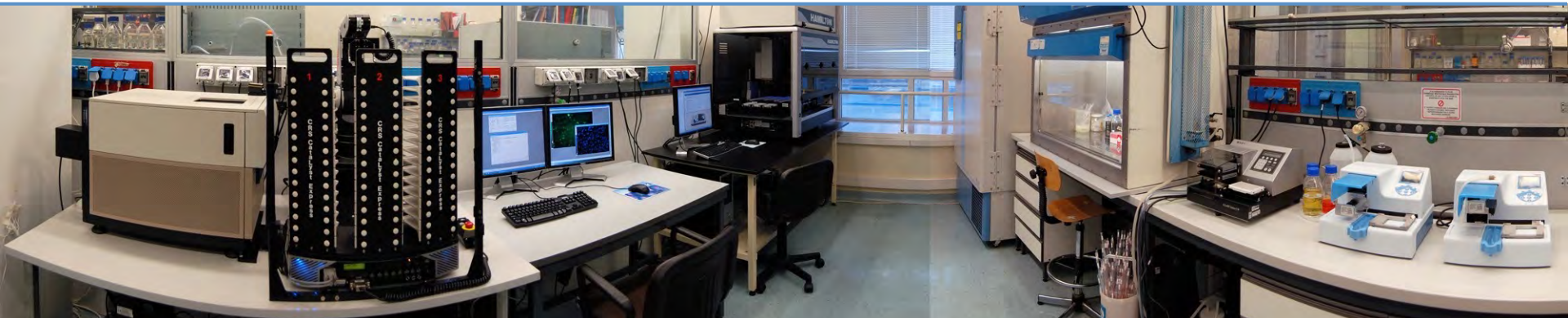

40 human miRNAs increase both rat and mouse cardiomyocyte proliferation

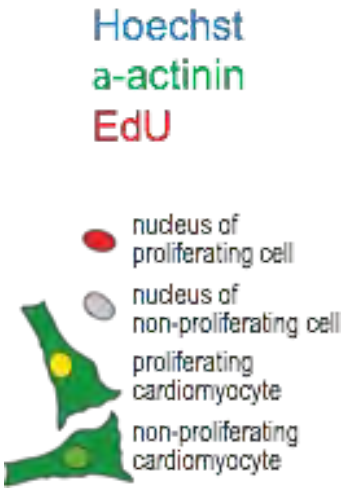

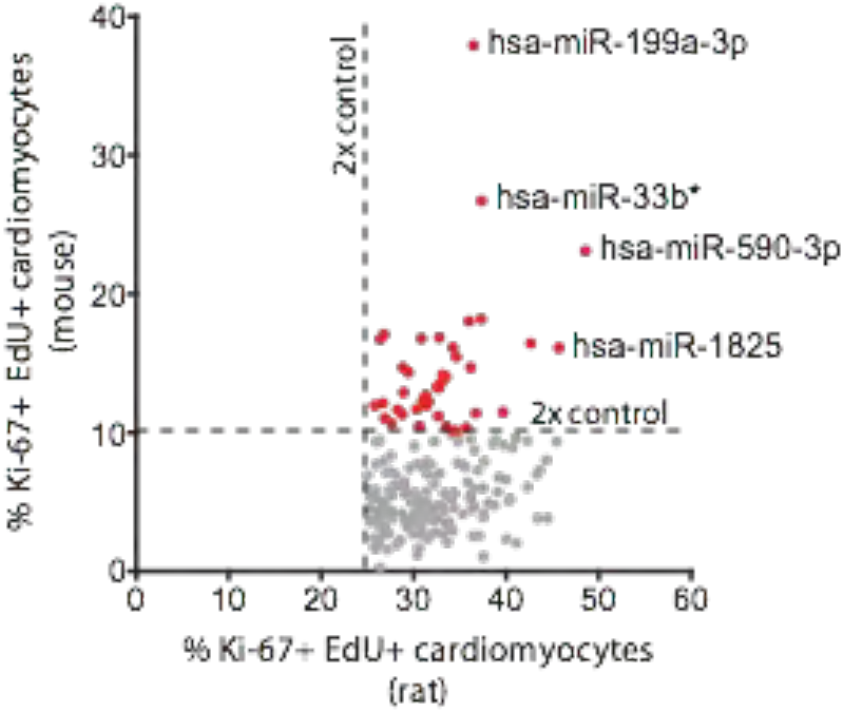

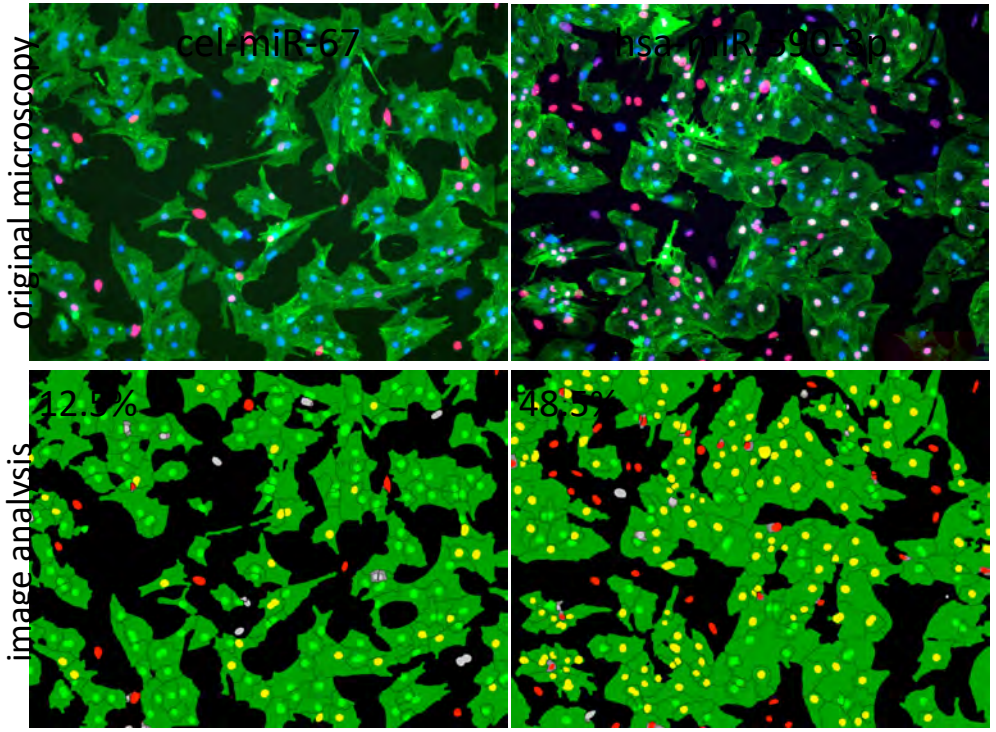

Intracardiac injection of the miRNAs increasing cardiomyocyte proliferation in the newborn rat heart

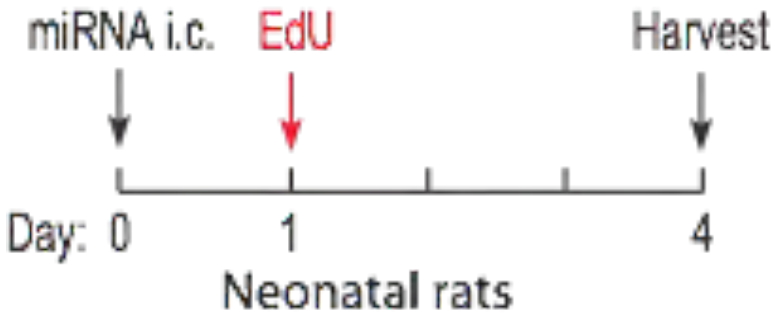

cel-miR-67 | hsa-miR-199a | hsa-miR-590

α-actinin / EdU

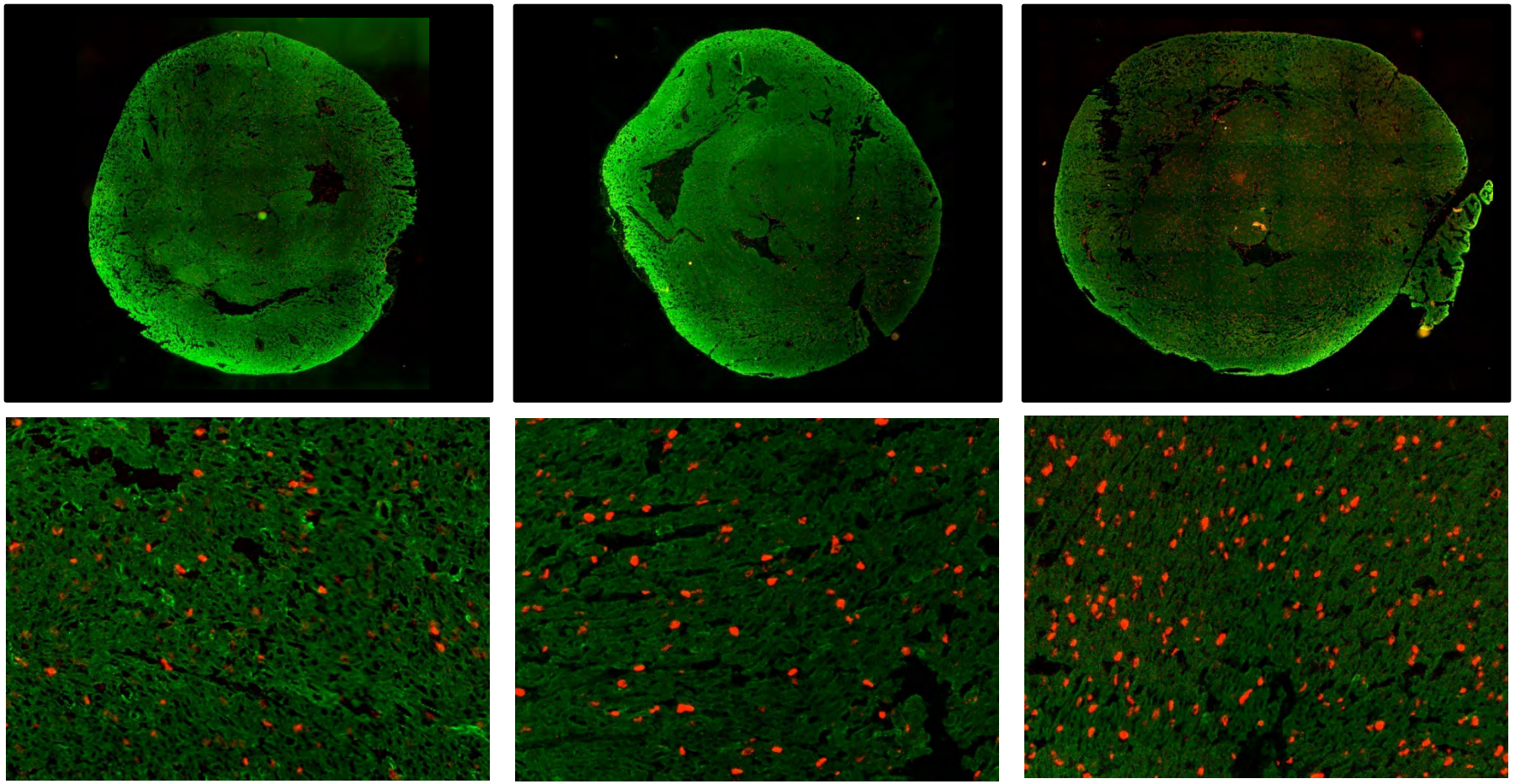

miRNAs increasing CM proliferation *in vivo*

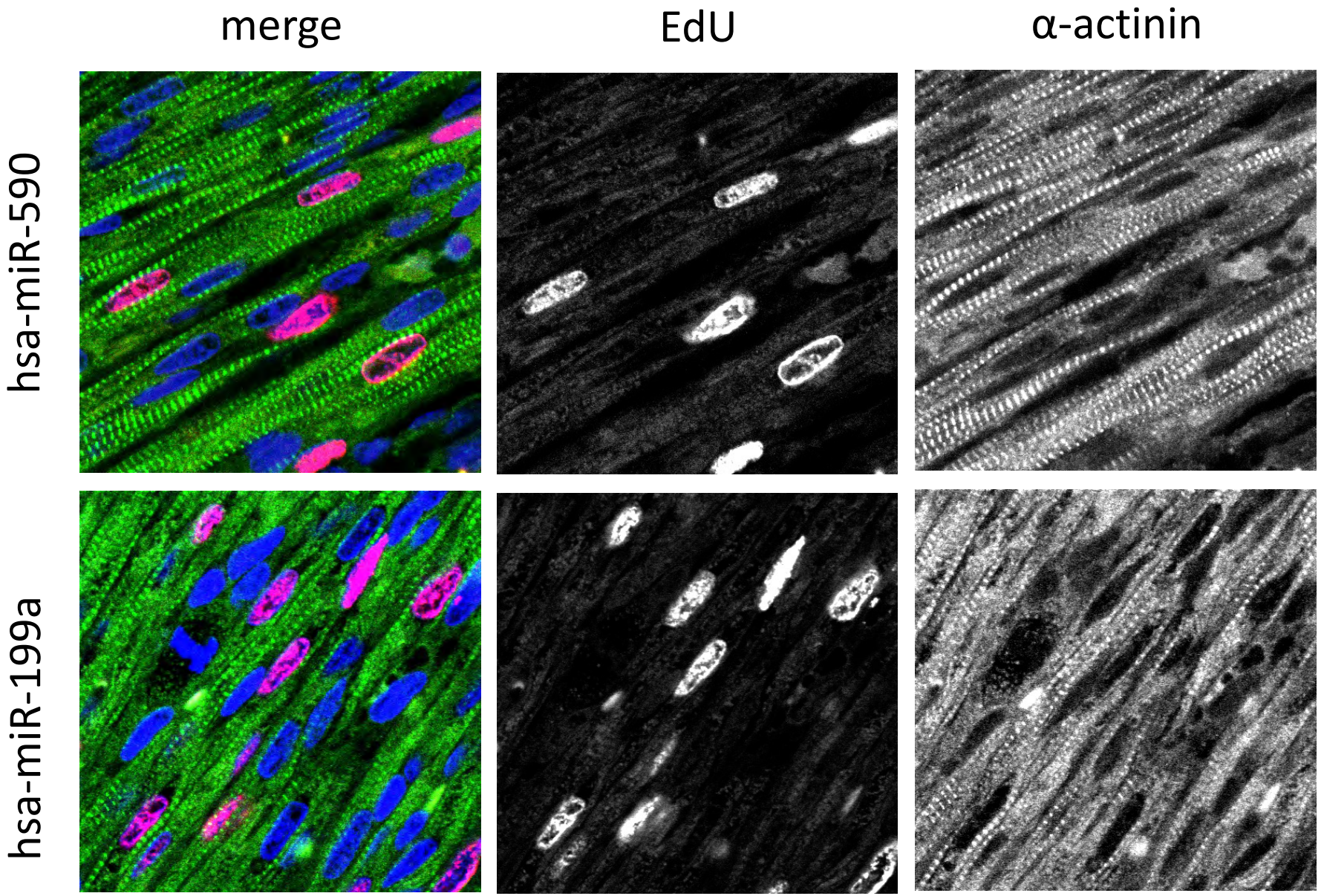

Effect of miRNA prolonged expression in vivo?

miR-590 and miR-199a markedly reduce infarct size

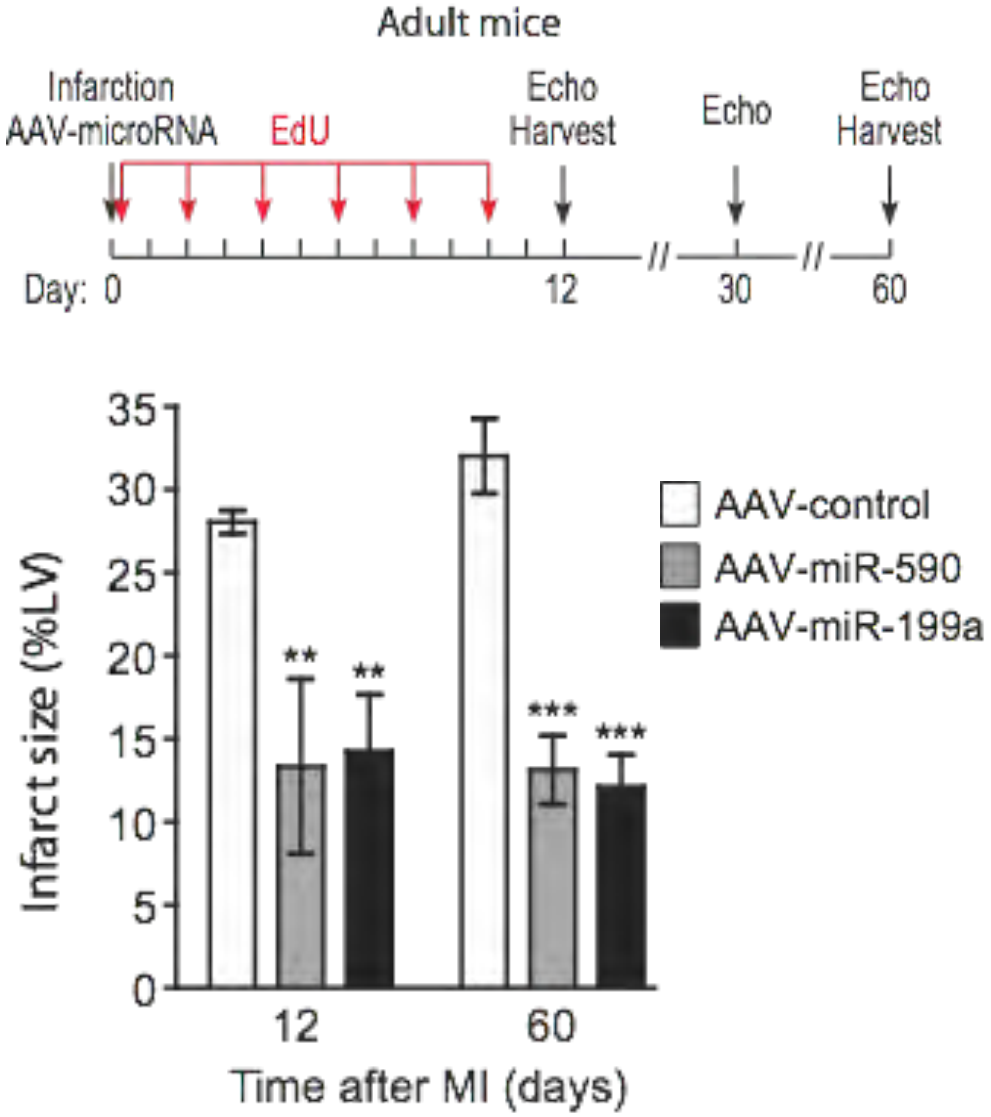

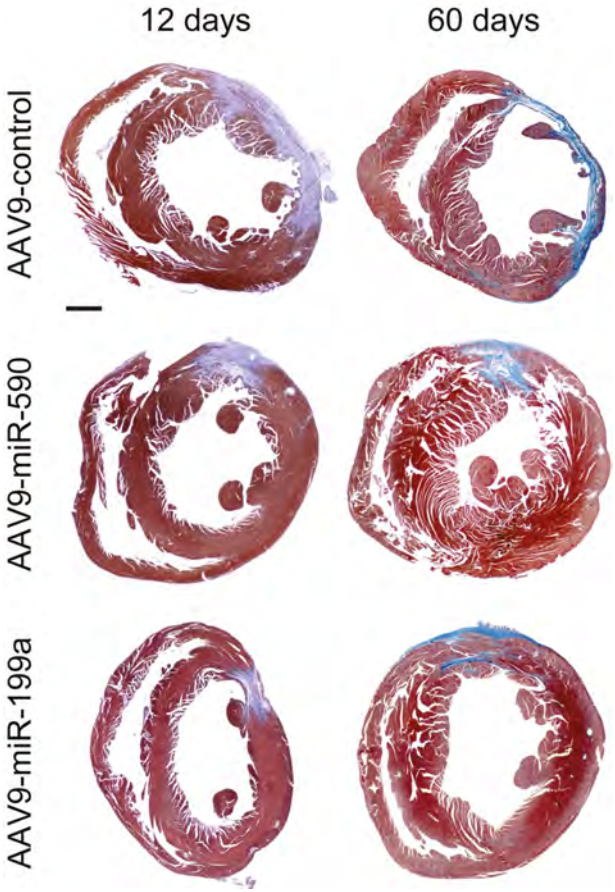

Masson Trichrome staining

Mechanism?

Identification of miR-590 and miR-199a target genes

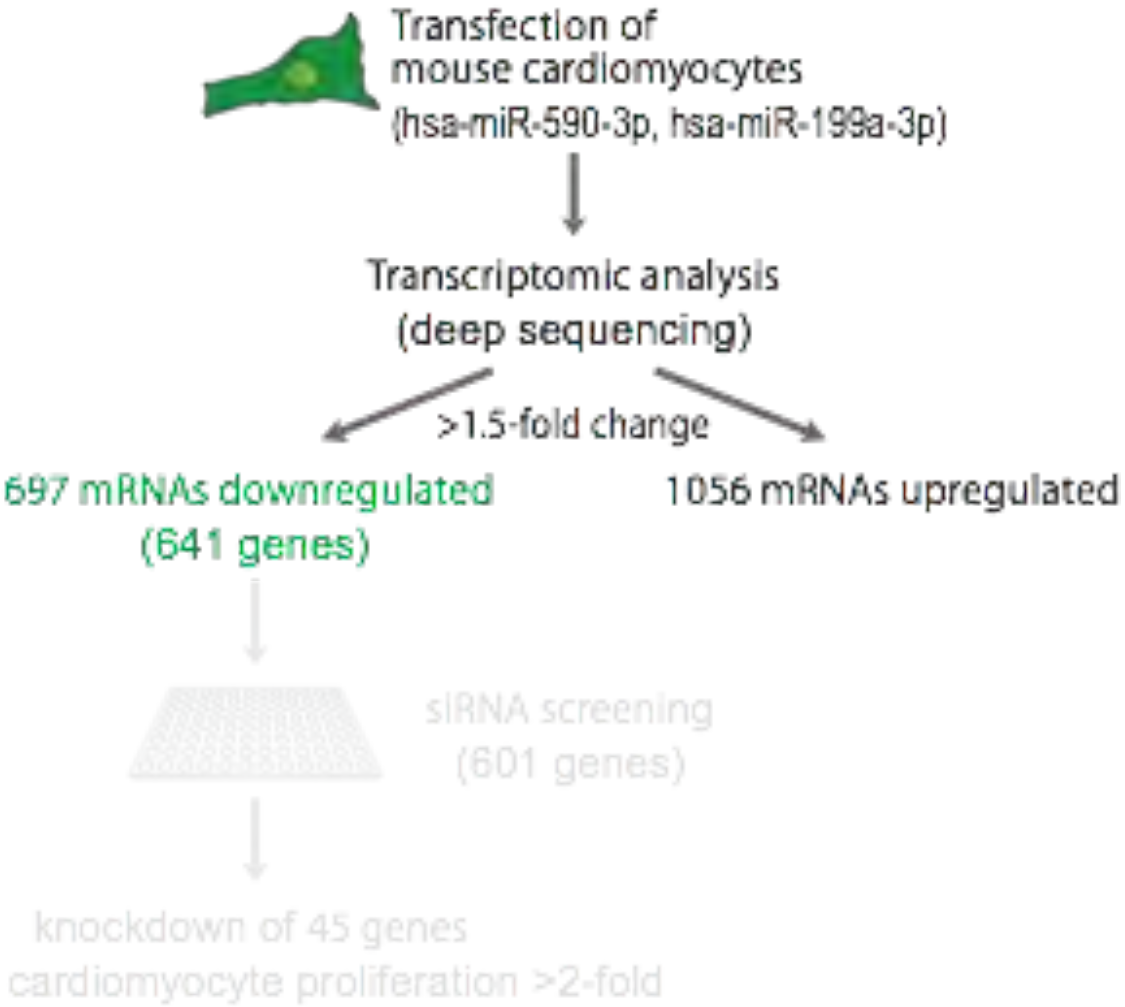

Functional analysis (IPA) of transcripts up- and down-regulated by hsa-miR-590-3p and hsa-miR-199a-3p

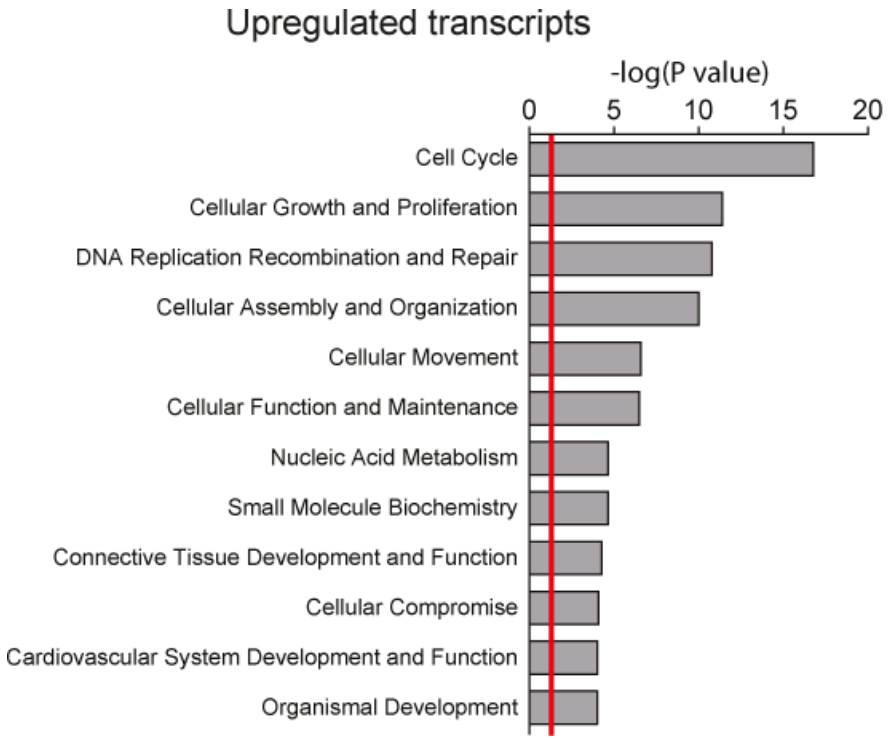

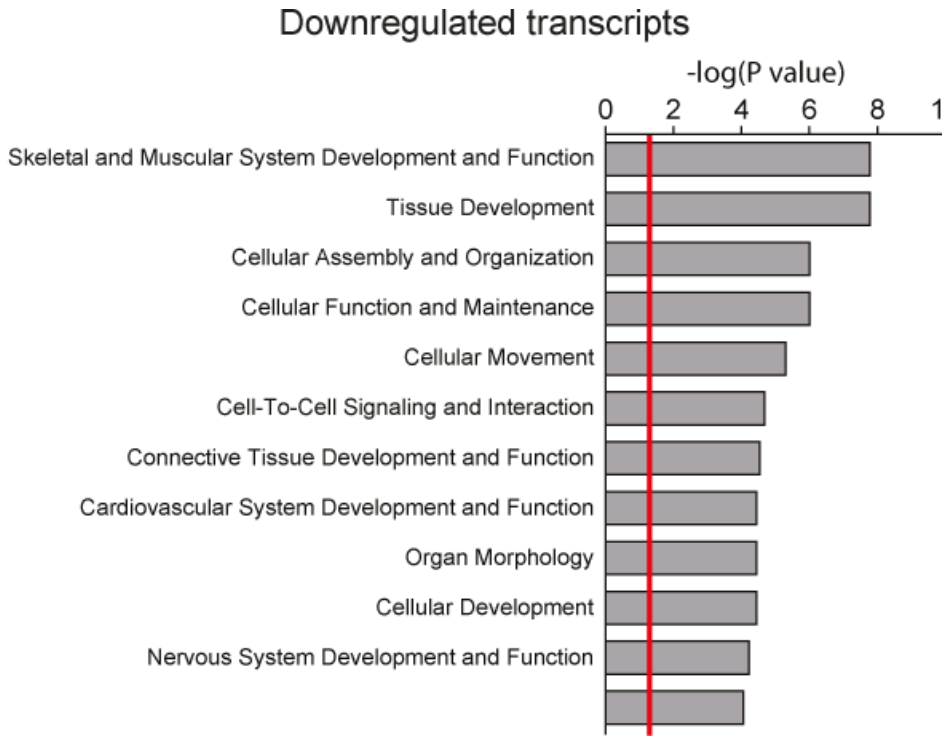

Among the 641 genes downregulated by miR-590-3p and miR-199a-3p are:

Myomesin 1 (Myom1)
Myomesin 2 (Myom2)
Myosin light polypeptide 4 (Myl4)
Nebulin-related anchoring protein (Nrap)
Myosin IB (Myo1b)
Titin (Ttn)
Troponin T1, skeletal slow (Tnnt1)
Troponin T2 cardiac (Tnnt2)
Cofilin2 (Cofilin2)
Dynamin1-like (Dnm1l)
Ankyrin repeat domain 52 (Ankrd52)
Nebulette (Nbl)

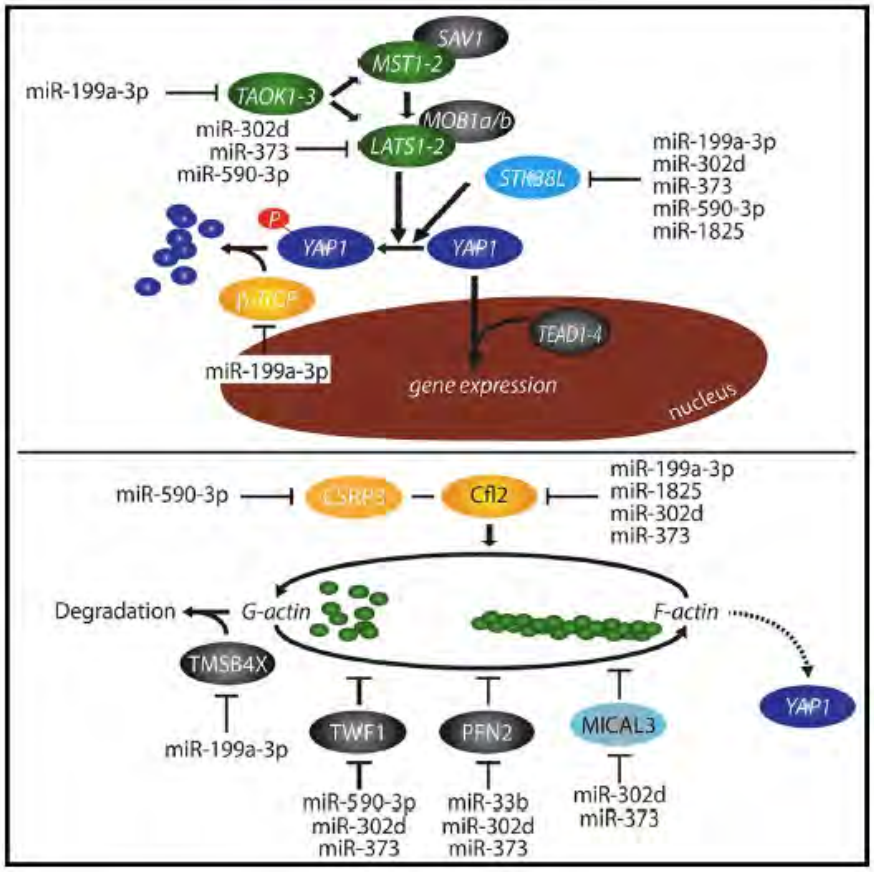

Highlights

- A few microRNAs can stimulate cardiac myocyte proliferation
- The most effective of these microRNAs activate YAP
- Several pro-proliferative microRNAs also inhibit actin depolymerization
- miR-199a-3p directly targets TAOK1, b-TrCP, and Cofilin2 to achieve its effects

What about large animal models?

AAV6-miR-199a reduces infarct size after MI

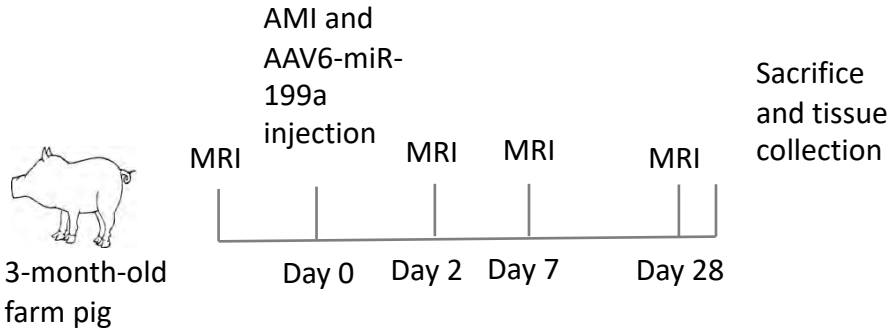

AAV6 empty

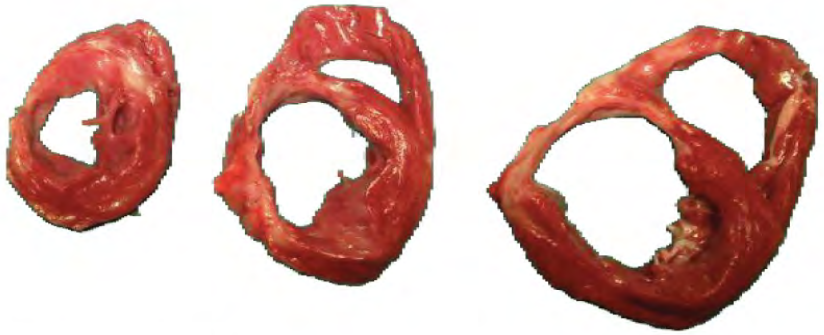

AAV6 miR-199a

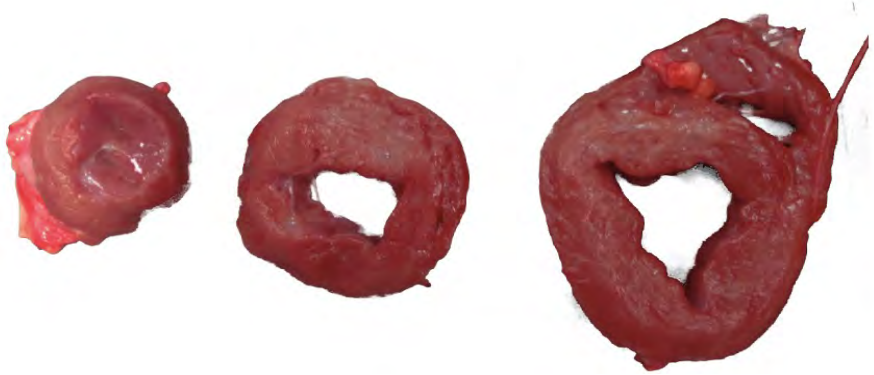

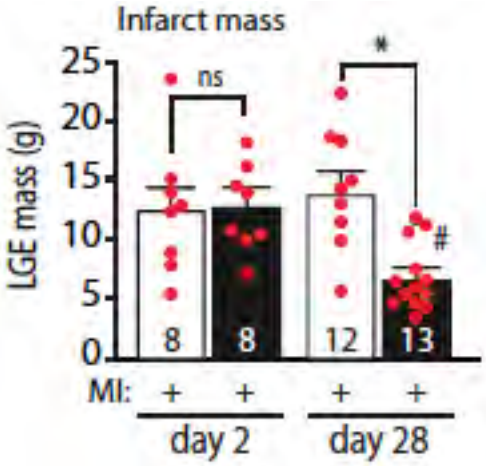

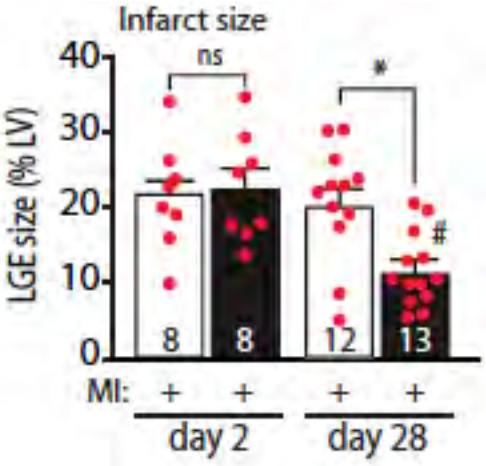

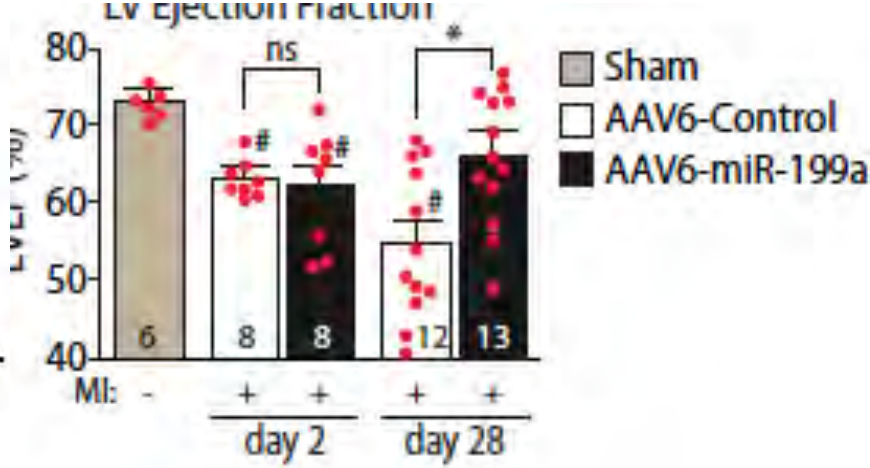

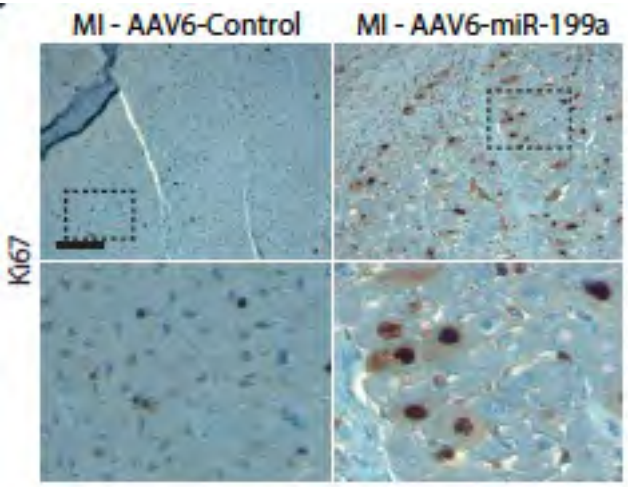

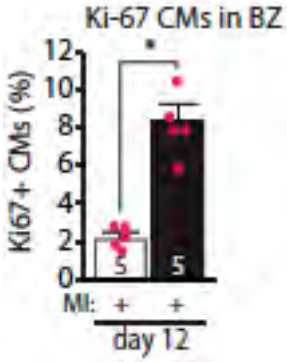

Common markers of cell cycle progression

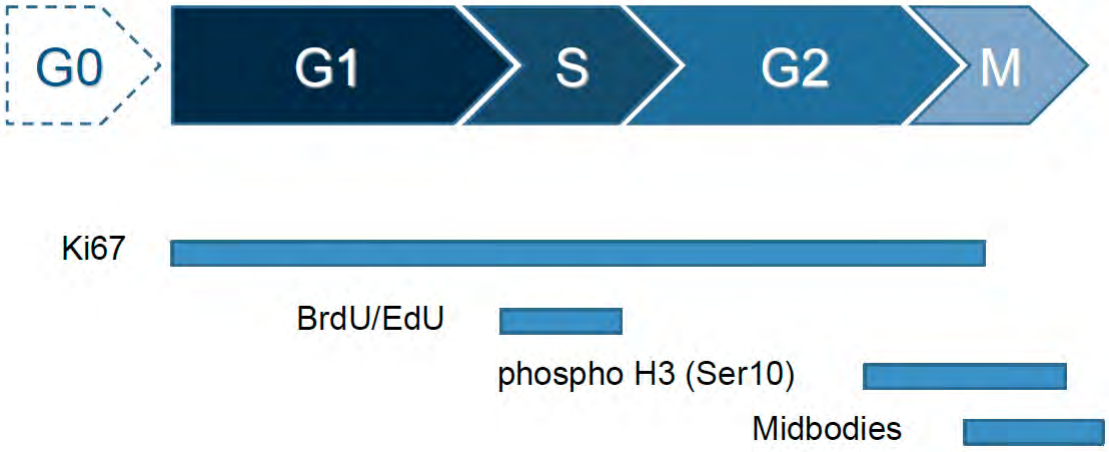

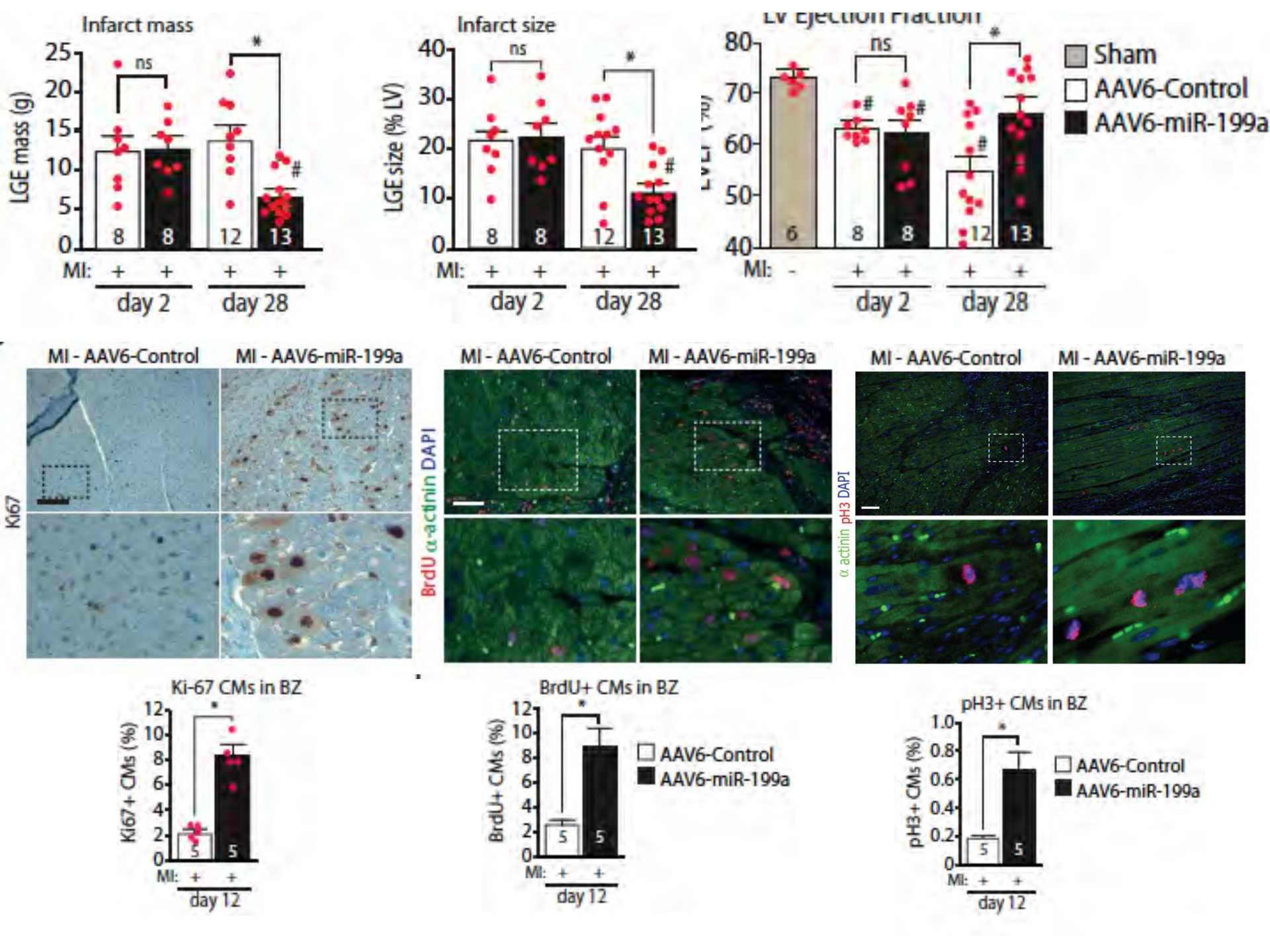
Infarct mass
LGE mass (g)
ns
*
#
8
8
12
13
MI: + + + +
day 2
day 28
Infarct size
LGE size (% LV)
LV Ejection Fraction
6
Sham
AAV6-Control
AAV6-miR-199a
MI: - + + + +
MI - AAV6-Control
MI - AAV6-miR-199a
Ki67
BrdU α-actinin DAPI
α actinin pH3 DAPI
Ki-67 CMs in BZ
Ki67+ CMs (%)
BrdU+ CMs in BZ
BrdU+ CMs (%)
pH3+ CMs in BZ
pH3+ CMs (%)
day 12

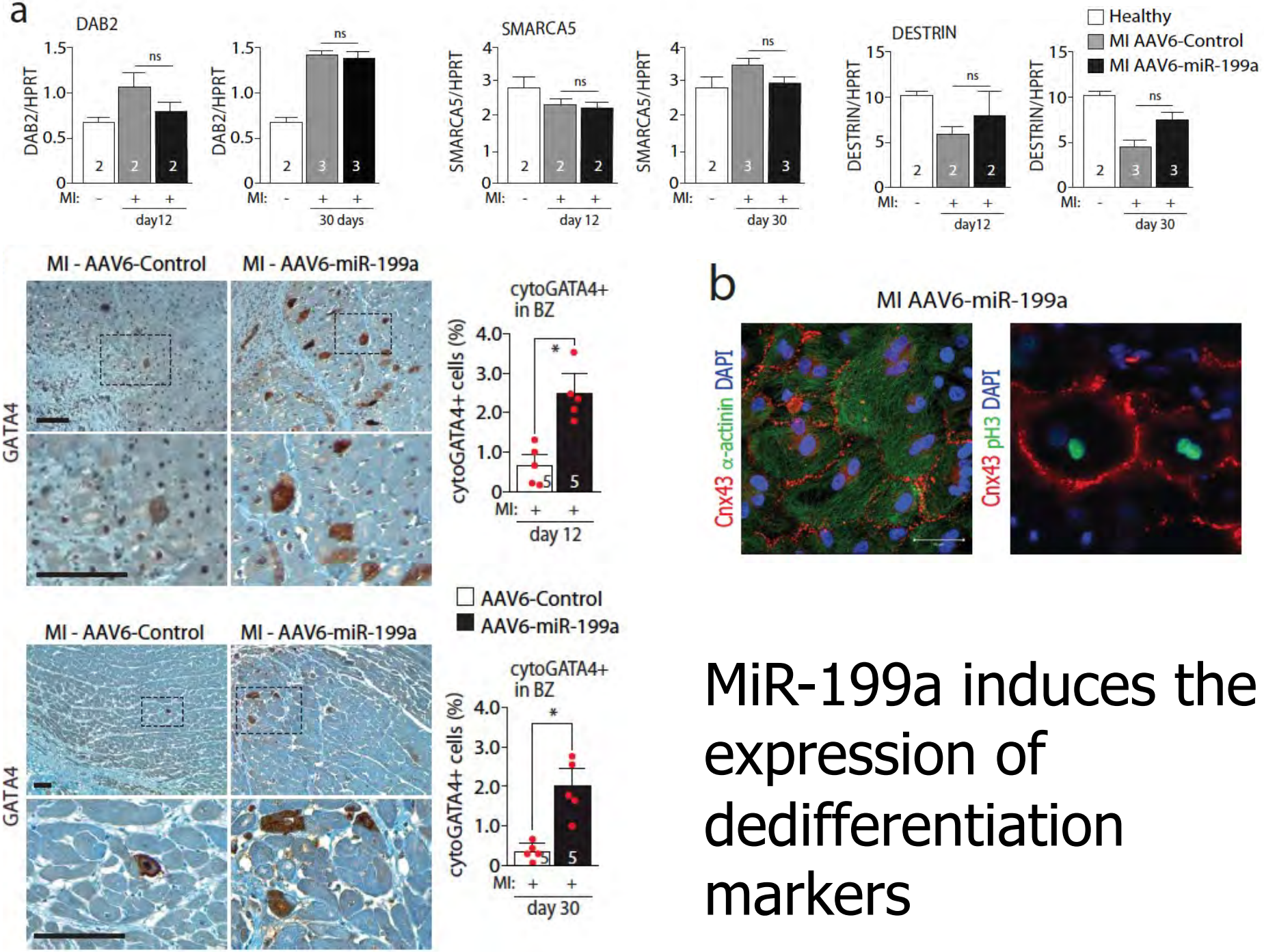

MiR-199a induces the expression of dedifferentiation markers

AMERICAN JOURNAL OF PATHOLOGY. VOL. XIII

HYPERPLASIA AND REGENERATION OF THE MYOCARDIUM IN INFANTS AND IN CHILDREN *

H. EDWARD MACMAHON, M.D.

(*From the Department of Pathology, Tufts College Medical School, Boston, Mass.*)

* Received for publication May 26, 1937.